CHARACTERIZATION OF THE *ASPERGILLUS NIDULANS* SEPTIN ASPB AND ITS INTERACTIONS

by

YAINITZA HERNÁNDEZ RODRÍGUEZ

(Under the Direction of Michelle Momany)

ABSTRACT

Septins are evolutionarily conserved GTP binding proteins that form heteroligomeric complexes, are considered novel cytoskeletal elements and control diverse cellular functions and processes. Septins are found in some protists, fungi and animals, and though present in some algae they are absent in higher plants. Septins have been shown to interact with and organize actin and tubulin and have been suggested to bridge interactions between both cytoskeleton systems. We explored these connections by characterizing the septin AspB and its interaction with actin and microtubules in the filamentous fungus *Aspergillus nidulans*. AspB is key for conidiophore morphology and sporulation as Δ*aspB* shows conidiophores with fused abnormal layers, very few attached conidia and poor conidiation. *ΔaspB* also shows early germination, multiple emergence of polarity axes during germ tube and branch formation and delayed septation. AspB localizes to sites of germ tube emergence, septation and branching and emerging layers of the conidiophore. AspB forms filaments and bars that are lost in the absence of septins AspA and AspC, suggesting that septin-septin interactions are necessary for filament formation. AspB filaments are extremely reduced in hyphae of *ΔaspE*, a septin exclusive to filamentous fungi. AspB seems to influence polarity by interacting with microtubules as they colocalize, Δ*aspB*

hyperemergence of growth can be reduced by depolymerization of microtubules, fewer microtubule bundles were observed in newly formed branches of Δ*aspB* and depolymerization of microtubules results in abnormal AspB filaments. AspB might also influence polarity by interacting with actin as they colocalize, polarity defects were observed in Δ*aspB* after depolymerization of actin, tropomyosin TpmA was lost from actin filaments and depolymerization of actin resulted in abnormal AspB cytoplasmic ring localization. AspB might play roles in endocytosis as AspB colocalized with endocytic vesicles and the endocytic zone is absent or of abnormal length and abnormally positioned in Δ*aspB*. We show that AspB is essential for normal growth, development and conidiation, it localizes throughout fungal growth and development, it may play roles in nuclear dynamics and might control polar growth by its interactions with the endocytic machinery, actin and microtubules and/or their associated proteins.

INDEX WORDS: *Aspergillus nidulans*, septins, AspB, polar growth, actin, microtubules, endocytosis, cytoskeleton, growth emergence, branching, germtube, septa, conidiophores, filaments, bars.

CHARACTERIZATION OF THE *ASPERGILLUS NIDULANS* SEPTIN ASPB AND ITS INTERACTIONS

by

YAINITZA HERNÁNDEZ RODRÍGUEZ

B.S., University of Puerto Rico-Mayagüez Campus, Puerto Rico, 2004

A Dissertation Submitted to the Graduate Faculty of The University of Georgia in Partial Fulfillment of the Requirements for the Degree

DOCTOR OF PHILOSOPHY

ATHENS, GEORGIA

2011

CHARACTERIZATION OF THE *ASPERGILLUS NIDULANS* SEPTIN ASPB AND ITS INTERACTIONS

by

YAINITZA HERNÁNDEZ RODRÍGUEZ

Major Professor: Michelle Momany

Committee: Sarah Covert
Claiborne Glover
Michael McEachern
Mark Farmer

Electronic Version Approved:

Maureen Grasso
Dean of the Graduate School
The University of Georgia
August 2011

DEDICATION

I want to dedicate this work to many important people in my life throughout these years. To my first advisor Dr. Carlos Betancourt, from the University of Puerto Rico-Mayagüez Campus, for introducing me to the wonderful world of mycology and for guiding me to obtain my PhD at the University of Georgia. To my current advisor Dr. Michelle Momany, who has provided unconditional support and has been an outstanding advisor and guide throughout these years. I want to dedicate this work to my mother Sophia, who taught me to persevere and made me promise, before passing, that one day she could call me “Dr”. To my father Fernando, who moved in with me to raise my baby and to help me finish my degree. I also want to dedicate this to my husband Jaime, for all his support throughout my illness and my career. To my daughter Eva Sophia, who came unexpectedly to my life and cured my disease, allowing me to finish my career. Finally, I want to dedicate this work to family, friends, professors and staff that by one way or another encouraged, helped and supported me throughout this journey to obtain my career. Thank you!

ACKNOWLEDGMENTS

This work was supported by the UGA Graduate Recruitment Opportunity Fellowship (GRO), Robert Watkins American Society of Microbiology Fellowship, Plant Biology Palfrey Grant, Howard Hughes Support and Dissertation Completion Grant to Yainitza Rodriguez; and by the NSF grant MCB 0211787 and NSF grant DevMech 1051730 to Dr. Michelle Momany. I want to thank my major advisor Michelle Momany, and my committee members: Sarah Covert, Claiborne Glover, Michael McEachern, and Mark Farmer for all their input and support. I also want to thank previous and current Momany lab and Fungal Molecular Biology Group members for their help, input and/or advice in my project.

TABLE OF CONTENTS

Page

ACKNOWLEDGEMENTS v

LIST OF TABLES viii

LIST OF FIGURES ix

CHAPTER

1 INTRODUCTION 1

References 15

2 THE SEPTIN ASPB IN *ASPERGILLUS NIDULANS* FORMS BARS AND FILAMENTS AND PLAYS ROLES IN GROWTH EMERGENCE AND CONIDIATION 22

Abstract 23

Introduction 24

Materials and Methods 28

Results 31

Discussion 37

Acknowledgements 41

Tables and Figures 42

References 62

3 INTERACTIONS OF THE *ASPERGILLUS NIDULANS* SEPTIN ASPB WITH OTHER CYTOSKELETAL ELEMENTS 68

Abstract 69

Introduction 70

Materials and Methods 73

Results 76

Discussion 84

Acknowledgements 89

Tables and Figures 90

References 125

4 CONCLUSIONS AND FUTURE EXPERIMENTS 130

References 143

5 APPENDICES 146

GROWTH POLARITY 147

SEPTINS ASPA AND ASPC ARE IMPORTANT FOR NORMAL DEVELOPMENT AND LIMIT THE EMERGENCE OF NEW GROWTH FOCI IN THE MULTICELLULAR FUNGUS *ASPERGILLUS NIDULANS* 153

ASPERGILLUS TERREUS ACCESSORY CONIDIA ARE MULTINUCLEATED, HYPERPOLARIZING STRUCTURES THAT DISPLAY DIFFERENTIAL DECTIN STAINING AND CAN INDUCE HEIGHTENED INFLAMMATORY RESPONSES IN A PULMONARY MODEL OF ASPERGILLOSIS 162

LIST OF TABLES

Page

Table 2.1. Strains used and plasmids 42

Table 2.2. Primers for constructing *aspB-gfp* and *ΔaspB* 43

Table 3.1. Strains used 90

LIST OF FIGURES

Page

Figure 1.1. *Aspergillus nidulans* life cycle 12

Figure 1.2. Septin domains and filaments....13

Figure 2.1. *aspB* is required for normal growth and morphology 44

Figure 2.2. *ΔaspB* shows hyperemergence of growth and abnormal conidiophores 46

Figure 2.3. *ΔaspB* shows clumped nuclei 48

Figure 2.4. AspB forms bars and filaments 50

Figure 2.5. AspB forms bars, filaments, caps and rings during conidiophore formation 52

Figure 2.6. AspB bars and filaments move....54

Figure 2.7. AspB structures are lost in the absence of AspA and AspC and filaments and bars are lost in hyphae in the absence of AspE 56

Figure 2.8. AspB bars are lost in conidiophores in the absence of AspA and AspC....58

Supplemental Figure 2.1. *ΔaspA* and *ΔaspC* show multinucleated conidia and nuclear abnormalities....60

Figure 3.1. AspB-GFP partially colocalizes with α-TubA labeled microtubules....91

Figure 3.2. Depolymerization of microtubules results in AspB-GFP star filaments 93

Figure 3.3. AspB-GFP partially colocalizes with α-Tyrosinolated TubA labeled microtubules...95

Figure 3.4. AspB-GFP partially colocalizes with mRFP-UncA^{rigor} 97

Figure 3.5. *ΔaspB* showed less microtubule filaments in branches 99

Figure 3.6. Depolymerization of actin results in many AspB-GFP free-floating cytoplasmic rings 101

Figure 3.7. TpmA-GFP localization to actin filaments and tips are lost in *ΔaspB* 103

Figure 3.8. Depolymerization of microtubules, but not actin, reduced hypergermtube and hyperbranch emergence in *ΔaspB* 105

Figure 3.9. Depolymerization of actin results in polarity defects during hyperbranch emergence in *ΔaspB* 107

Figure 3.10. AspB-GFP partially colocalizes with AbpA 109

Figure 3.11. SlaB-GFP showed less exclusion distance from tips and smaller zone lengths in *ΔaspB*. 111

Figure 3.12. SlaB-GFP showed smaller zone lengths and localized at or very close to the tip apex in *ΔaspB* 113

Supplemental Figure 3.1. AspB-GFP filaments and bars localize near nuclei 115

Supplemental Figure 3.2. Microtubule depolymerization results in AspB-GFP star filament formation 117

Supplemental Figure 3.3. Actin filaments are present in *ΔaspB* 119

Supplemental Figure 3.4. TubA-GFP and TpmA-GFP localizations under Benomyl and Cytochalasin A treatments respectively are reversible and not affected by DMSO 121

Supplemental Figure 3.5. Wild type hardly shows swelling during branch emergence after recovery from Cytochalsin A treatment 123

CHAPTER 1

INTRODUCTION

The septin cytoskeleton is made of different septin proteins that interact to form non-polar heteroligomeric filaments. This novel cytoskeleton is found in some lower eukaryotes such as algae, as well as in fungi and animals, but not in higher plants (ESTEY *et al.* 2011). As cytoskeletal elements, septins play roles as diverse as those of actin and microtubules (Field 1999, Mitchison and Field 2002). Septins are part of the P-loop GTPase family that includes kinesins, myosins and ras proteins, and its GTP binding capacity seems to be important for structure stability and subunit interaction, but its ability to hydrolize GTP is not clearly understood. Electron microcopy studies have shown that septin basic rods are usually composed of two members of each septin which interact through the N-C interface (N-terminal and C-terminal) and their GTP binding domains, which leaves the coiled-coil extensions free from the structure and available to interact with other proteins (BERTIN *et al.* 2008b; ESTEY *et al.* 2011; MCMURRAY and THORNER 2009; VERSELE *et al.* 2004; VERSELE and THORNER 2004; VERSELE and THORNER 2005). Basic rods can interact, through septin-septin N-C or GTP binding domains, with other basic rods to form longer filaments and through coiled-coil extensions to form paired filaments (BERTIN *et al.* 2008b; ESTEY *et al.* 2011). Fluorescent tagging has shown that *in vivo* septins form higher order structures such as bundled filaments, bars, dots, rings, caps that can form scaffolds, diffusion barriers, filamentous arrays and gausses. These structures recruit and interact with a huge array of proteins and the cell membrane. Their ability to form different structures and interact with such a large variety of proteins seems to be dependent to the

developmental stage, cell type and mode of growth of the organism and it might explain how septins are involved in so many different cell processes. For instance, septins are involved in cytokinesis, vesicle trafficking, nuclear division coordination, cytoskeleton organization and polarity maintenance, and compartmentalization of pre-existing cellular material and formation of diffusion barriers (KINOSHITA 2006; LINDSEY and MOMANY 2006; MCMURRAY and THORNER 2008b; RUSSELL and HALL 2005; VERSELE and THORNER 2005). In addition, septin defects have been associated with diseases such as leukemia and many other types of cancer, Parkinson's, Alzheimer's, Down's syndrome, schizophrenia, bipolar disorder, mesial temporal lobe epilepsy, systematic lung erythematosus, Listeria infection, human herpes virus 8 and hepatitis C (Hall and Finger 2008). All these characteristics make septins a very important and exciting group of proteins to study.

Septins were first discovered by Lee Hartwell in the early 1970's in a screen for temperature-sensitive cell cycle mutants in *Saccharomyces cerevisiae* and named "septins" for their roles in septum formation in yeast (HARTWELL 1971b). The first septins discovered were named *cdc3*, *cdc10*, *cdc11* and *cdc12* for being cell cycle mutants defective in cytokinesis. Still today we don't completely comprehend septins essential roles in cytokinesis in all cell types (Pringle 2008).

Septins have now been identified and described in other fungal and animal systems and quite recently in lower eukaryotes. The number of septin genes can vary among organisms. For instance the worm *C. elegans* has 2, fungi have 4-7 septins, the fly *D. melanogaster* has 5 septins, and humans have 14. In humans the number of septin proteins is even higher as splice variants can add up to 30 different septin proteins (Hall et al, 2005). Phylogenetic studies, from different model systems, have suitably grouped septins into: septins found only in fungi, only in

animals and in both fungi and animals (PAN *et al.* 2007). This study also revealed septin protein motifs which allow for further identification of additional septins in other model systems. In different model systems septins from similar representative groups polymerize into heteroligomeric filaments (VERSELE *et al.* 2004).

Septins display three basic patterns of localization within cells and localization seems to be correlated to septin function (Lindsey and Momany 2006). In general, fungal septins localize to bases or tips of newly forming growth areas such as buds or germ tubes. In general, animal septins localize to membranes as punctae or to the cytoplasm as cytoskeletal filaments. In both animals and fungi septins localize to partitions as cells divide; in fungi to septum or areas of cell division and in animals to the cleavage furrow. Here, I will review septins in some fungi and animals.

Septins in Fungi

Septins were first discovered in *S. cerevisiae* through a cell cycle temperature-sensitive mutation screen and named CDC as cell division cycle genes (HARTWELL 1971a; LONGTINE *et al.* 1996). At restrictive temperature Cdc3, 10, 11, and 12 mutants result in multibuded elongated cells that do not complete cytokinesis. These septins localize to the mother-bud neck (area of division after formation of the daughter cell) and mutations in one septin result in loss of localization of the others. Septins recruit and interact with many proteins involved in cell cycle regulation and help coordinate nuclear and cell division with morphology to ensure normal bud formation via the morphogenesis checkpoint (GLADFELTER *et al.* 2001a; GLADFELTER *et al.* 2002; GLADFELTER *et al.* 2001c; LEW 2003; LEW and REED 1995). If bud formation is disrupted, the nuclear cycle is paused by the morphogenesis checkpoint. This ensures that only one nucleus is present in each cell. Septins localize to the prebud emergence site where they form caps that

help recruit the bud emergence machinery, form a ring at the mother bud neck as the bud emerges, and form an hourglass structure as the bud develops. The hourglass breakes into two rings as septins help coordinate cytokinesis (GLADFELTER *et al.* 2001b; GLADFELTER *et al.* 2005; LEW 2003). Septin hourglass, scaffolds and rings at the neck form diffusion barriers that keep the machinery necessary for growth and cytokinesis localized and concentrated to this area (BARRAL 2009; BARRAL *et al.* 2000; DOBBELAERE and BARRAL 2004; DOUGLAS *et al.* 2005; FINGER 2005; TAKIZAWA *et al.* 2000). After cytokinesis, a ring remains that marks the position of the division event and determines the position for the emergence of the next bud (CHANT 1996; CHANT and PRINGLE 1995; FLESCHER *et al.* 1993). They are also likely involved in the response to mating pheromone (FORD and PRINGLE 1991; KIM 1991; KONOPKA *et al.* 1995). During spore formation two additional septins, Spr3 and Spr28, play roles during spore wall formation and localize with other septins to the developing prospore wall in sporulating cells and their deletions can cause mislocalization of the other septins (DE VIRGILIO *et al.* 1996; FARES *et al.* 1996; LONGTINE *et al.* 1996).

S. cerevisiae has been a great model system for studying septin complexes and dynamics. Here, septins organize into heteroligomeric filamentous octamers that give rise to septin rings and filaments (BERTIN *et al.* 2008a; MCMURRAY *et al.* 2011). These nonpolar hetero-octamers are composed of two representatives of each septin molecule organized as: Cdc11-Cdc12-Cdc3-Cdc10-Cdc10-Cdc3-Cdc12-Cdc11 (BERTIN *et al.* 2008a). In addition, EM studies have shown that long filaments can align in pairs forming higher order structures after the initial filament is formed. Removal of septin members from the complex can result in abnormalities whose severity depends on the member that is removed (MCMURRAY *et al.* 2011). FRAP experiments showed that septin turnover occurs prior to bud emergence, hourglass splitting and ring

disassembly, while there is no turnover during bud formation and cytokinesis in *S. cerevisiae* (BARRAL 2009; CAVISTON *et al.* 2003; DOBBELAERE *et al.* 2003). In addition, within a complex, septin monomers can be old or new, so that certain septins can be recycled from complex to complex throughout development (MCMURRAY and THORNER 2008a). This provides more evidence of the large dynamics of septin complexes not only by the changes of structure dynamics throughout development, but also within the complex itself.

Schizosaccharomyces pombe also has seven septins (Spn1, Spn2, Spn3, Spn4, Spn5, Spn6 and Spn7) and ring formation only requires a minimum of three septins in a complex (Spn3-Spn4-Spn1 or Spn4-Spn1-Spn2) (AN *et al.* 2004b). Here, septins are involved in, but not essential for, cytokinesis. Septin defects are associated with abnormal septin localization and septin deletion mutants show only a delay in breakdown of the septum before cell separation (AN *et al.* 2004a). Septins Spn1, 2, 3 and 4 form a complex that is diffusely localized throughout interphase (AN *et al.* 2004b). Septins are recruited to the division site after the cytokinesis machinery is assembled, unlike septins in *S. cerevisiae*, but they also form a ring that splits and encloses the actin-myosin ring for cytokinesis (BERLIN *et al.* 2003; TASTO *et al.* 2003; WU *et al.* 2003)

In the pathogenic yeast *Candida albicans*, septin defects impair cell separation and cells are linked together forming chains. Here, septins localize very similarly to *S. cerevisiae* during budding. During hyphal growth septins assemble and disassemble as septin bands at the base of emerging germ tubes and septation sites, and form collars at hyphal tips (BERMAN and SUDBERY 2002; GLADFELTER and SUDBERY 2008; SUDBERY 2001; WARENDA and KONOPKA 2002a). A cap of septins localizes to tips and an unknown signal makes a cloud of septins anchor to the wall staying behind from the polarizing tip and marking future septation sites. Septins remain

localized to pre-septation sites until the septum is formed. Interestingly, there are septin dynamics differences in *C. albicans* which affects if the fungus displays budding or hyphal growth. In the yeast form, the collar is frozen as in *S. cerevisiae*. After transition to hyphal growth, Cdc11 is phosphorylated and the Cdc10 subunit, assisted by Shs1, is dynamically exchanged with the cytoplasmic pool (GONZALEZ-NOVO *et al.* 2008; SINHA *et al.* 2007; WARENDA and KONOPKA 2002b). These dynamics prevent cell separation and allow for hyphal growth. In contrast to bud and hyphal morphogenesis, septins form long filamentous structures during chlamydospore morphogenesis (MARTIN *et al.* 2005).

In *Cryptococcus neoformans* Cdc3 and Cdc12 are essential for growth at body temperature (37°C) and their deletion results in reduced virulence (Kozubowski and Heitman 2009). Septin mutants also display abnormal nuclear distribution. In *C. neoformans* septins localize to emerging spores, septa and clamp connections and are involved in morphology, sporulation, clamp cell fusion, nuclear dynamics and contribute to virulence (Kozubowski and Heitman 2009).

Ashbya gossypii has five septin proteins (Cdc3, Cdc10, Cdc11, Cdc12, Shs1/Sep7), septin mutants shift mitosis sites and it has been suggested that septin rings promote mitosis near new branches (Helfer and Gladfelter 2006). *A. gossypii*, septins also form a cap at the hyphal tip and septins then become anchored to the membrane, forming a band as seen in *C. albicans.* In *A. gossypii* septins form various rings in the hyphae and their morphological and behavioral differences are regulated by Elm1p and Gin4p kinases (DEMAY *et al.* 2009; HELFER and GLADFELTER 2006).

In the plant pathogen *Ustilago maydis*, a normal contractile actomyosin ring is necessary for septin ring formation. Sep3 is required for normal cellular morphology and division during

budding and lipid-induced filamentous growth in culture. Sep3 defects showed reduced symptoms in maize due to morphological defects in filamentous cells *in planta*. Sep3 is also involved in the differentiation of hyphae into teliospores and their germination, and forms multiple buds in strains carrying a mutation in the regulatory subunit of the protein kinase A, suggesting connections between Sep3 and cAMP signaling during morphogenesis (BOYCE *et al.* 2005). *U. maydis* septins undergo dynamic rearrangements from hourglass collars into ring structures during septation (Böhmer et al., 2009, (Cánovas and Pérez-Martín 2009). The Don3 kinase initiates septin reorganization during secondary septum formation (BÖHMER *et al.* 2009). In *U. maydis*, Sep1 and sterol-rich domains show interdependent partial colocalization and seem to maintain and stabilize polarity (Cánovas and Pérez-Martín 2009), and Sep4 localizes as cortical fibers (Alvarez-Tabares and Perez-Martin 2010).

In another plant pathogen *Magneporthe oryzae*, if the septation location is disturbed, the fungus does not cause rice blast disease (SAUNDERS *et al.* 2010). Septins form a pre-mitotic ring during appressorium morphogenesis, containing Sep4 and 5, which defines the position of the appressorium septum. After mitosis, nuclei migrate and the actomyosin ring forms in the forming appresorium for septation. SEP1 is a spatial regulator for cytokinesis and is therefore required for appressorium-mediated infection (SAUNDERS *et al.* 2010).

In *Aspergillus nidulans* there are five septins (AspA, AspB, AspC, AspD and AspE) (Momany et al., 2001). AspB temperature sensitive mutants displayed irregular septa, high numbers of branches, and immature asexual reproductive structures (Westfall and Momany 2002). AspA and AspC deletions showed increased germ tube and branch emergence, abnormal septation, and abnormal conidiophores (LINDSEY *et al.* 2010). Polyclonal antibodies against the most-highly expressed septin AspB showed that it localizes to septa, emerging secondary germ

tubes and branches, and developing conidiophores (Westfall and Momany 2002). Similar to budding yeast, AspB forms a ring at septa that eventually splits into two rings. Similar to *C. albicans* and *A. gossypii*, AspB forms a ring or collar at emerging secondary germ tubes and branches. AspB also forms rings that circumscribe the emerging budding layers of conidiophores (asexual reproductive structure). AspA-GFP and AspC-GFP localize as discrete spots or bars in dormant and expanding conidia, as rings at forming septa and at the bases of emerging germ tubes and branches, and as spots and filaments in the cytoplasm and near the cell cortex. In conidiophores, AspA-GFP and AspC-GFP also localize as rings at the bases of emerging layers. AspA and AspC display abnormal localization in each other's deletion backgrounds suggesting that they interact. (LINDSEY *et al.* 2010).

Septins in animals

Septins in animals are also key for cytokinesis and localization to the cleaveage furrow has been shown in *C. elegans* and *D. melanogaster* (FARES *et al.* 1995; NGUYEN 2000). In mammals septins are involved in a variety of processes. One of its roles is the organization and coordination of the actin and microtubule cytoskeletons. Septin filaments colocalize to actin and microtubule fibers. Moreover, different septins preferentially bind certain modified cytoskeletal elements. For example, SEPT2 is not associated to actin that is rapidly turned over, but it is to polyglutamylated microtubules; while SEPT4 binds stress fibers and cortical actin (KINOSHITA 2006; KINOSHITA *et al.* 2002; KINOSHITA *et al.* 1997; SCHMIDT and NICHOLS 2004a; SPILIOTIS and NELSON 2006; SPILIOTIS 2010; SPILIOTIS *et al.* 2008b; SPILIOTIS *et al.* 2005; SURKA *et al.* 2002; XIE *et al.* 1999).

Septins have also been shown to associate to membranes and have been suggested to provide shape and control growth emergence by its interactions with the membrane, cytoskeleton

and their associated proteins (GILDEN and KRUMMEL 2010; TANAKA-TAKIGUCHI *et al.* 2009). Actin and septins colocalize and are codependent. Upon treatment with actin depolymerizing agents septin filaments form arc-shaped structures (KINOSHITA *et al.* 2002). Therefore, septin filament integrity is dependent on F-actin integrity and adaptor proteins seem to help bridge actin-septin interactions, making their structures interdependent (Spiliotis and Nelson 2008). Septins have also been shown to regulate microtubule stability and treatment with microtubule depolymerizing agents causes septin mislocalization (KREMER *et al.* 2005; SPILIOTIS *et al.* 2005). Microtubule modifications can regulate microtubule binding partners which can modulate cellular processes. Microtubules directly interact with septins in mammals and also show preferential binding. The SEPT 2/6/7 complex binds both free tubulin as well as polymerized microtubules (NAGATA *et al.* 2003; SPILIOTIS and NELSON 2008). Septins have been reported to localize with centromeres, kinetochore, spindles and microtubule organizing centers (GROMLEY *et al.* 2003; QI *et al.* 2005; SHU *et al.* 1995; SPILIOTIS and NELSON 2008 ; VEGA and HSU 2003). In mammals, SEPT2 associates with polyglutamylated microtubules facilitating vesicle transport by maintaining this microtubule modification and hindering MAP4 binding (microtubule associated protein 4) (SPILIOTIS *et al.* 2008).

Septins in mammals are also involved in morphogenesis and form diffusion barriers. For instance, in developing polar neuron cells, septins are involved in the morphogenesis of normal mature spines and interestingly septin knockdown defects vary from septin to septin (TADA *et al.* 2007). Particularly, SEPT7 localizes at the base of dendritic protrusions similar to septin localization at the bud neck in *S. cerevisiae*. SEPT7 overexpression increased dendrite branching and the density of dendritic protrusions, while its knockdown resulted in reduced dendrite arborization and increased proportion of immature protrusions. Also, SEPT4 and SEPT14 are

involved in neuron formation and cell polarity maintenance during brain development (SHINODA *et al.* 2010). Septins are also involved in the formation of diffusion barriers (Schmidt and Nichols 2004b). SEPT2 is essential for retaining receptor-signaling pathways in the primary cilium and is also key for diffusion in the cleavage furrow of dividing cells (HU *et al.* 2010; SCHMIDT and NICHOLS 2004b). The annulus (composed of septins) of the mouse sperm tail is also key in the formation of diffusion barriers and proper function of the sperm (IHARA *et al.* 2005; KWITNY *et al.* 2010).

Contributions of this dissertation to the septin field

Though septin studies in yeast have been very useful; unicellular cells cannot address how septins coordinate cell division across compartments in multicellular organisms or how they function in highly polar cells such as neurons. Septins in animals show differential splicing making their studies more challenging. Filamentous fungi, being highly polarized multicellular organisms, are a more tractable model system to study septin biology in multicellular systems. Here we present a continuation on the characterization of AspB, which is the most highly expressed septin during asexual reproduction in *A. nidulans* (Momany *et al.*, 2001). AspB is closely related to Cdc3 in *S. cerevisiae* and *C. albicans*, Spn1 in *S. pombe*, and Sep1 in *C. neoformans* and *U. maydis* (PAN *et al.* 2007a). *aspB* was previously reported to be essential (Momany and Hamer 1996). *aspB* temperature sensitive mutants displayed irregular septa, high numbers of branches, and immature asexual reproductive structures (Westfall and Momany 2002). Immunofluorescence with polyclonal antibodies showed that AspB localizes to septation and branching sites, and conidiophore interface layers (Westfall and Momany 2002). Here we show that deletion of *aspB* is not lethal, but causes aberrant morphology in several developmental stages and severe defects in asexual reproduction. AspB is key for conidiophore

morphology and sporulation as Δ*aspB* showed conidiophores with fused abnormal layers, very few conidia attached to conidiophores and poor conidiation, which explains why this mutant was not recovered in the first study. AspB-GFP *in vivo* fluorescence studies showed that AspB localizes not only as dots, rings and caps but also as filaments and bars throughout vegetative growth and asexual reproduction. AspB localizes to areas of emerging growth and AspB filaments are lost in the absence of septins AspA and AspC, suggesting that septin-septin interactions are necessary for filament formation. AspB filaments are present in dormant and early germinating conidia, but are extremely reduced in hyphae of *ΔaspE*. This suggests that AspE, which belongs to a septin family only found in filamentous fungi, has evolved to maintain septin filament stability in highly polar growing cells. AspB seems to control emergence of growth in conjunction with its interactions with microtubules as Δ*aspB* results in hyperemergence of germtubes and branches that can be reduced by depolymerization of microtubules. In addition AspB might be involved in nuclear migration as AspB colocalizes with microtubules and near nuclei and Δ*aspB* results in binucleated conidia and clumped nuclei. Furthermore, less microtubule bundles were observed in newly formed branches of Δ*aspB* and depolymerization of microtubules resulted in abnormal AspB filaments. AspB might also control polarity in conjuction with its interactions with actin as polarity defects, such as swelling and lysis, were observed in Δ*aspB* after depolymerization of actin. In addition tropomyosin TpmA, which blocks myosin access to actin for active trafficking, was lost from actin filaments and localization to septa was very faint in Δ*aspB*. Still, actin filaments labeled with *lifeact-egfp* were visible in Δ*aspB*. AspB colocalized with actin vesicles and depolymerization of actin resulted in abnormal AspB cytoplasmic ring localizations. AspB might also be involved in growth by playing roles in endocytosis as AspB colocalized with endocytic vesicles and the endocytic zone

is absent or of abnormal length and abnormally positioned in Δ*aspB*. In summary, AspB plays roles in fungal morphology, growth, nuclear dynamics and asexual reproduction and its filamentous localization throughout fungal growth and development might control polar growth by its interactions with the endocytic machinery, actin and microtubules and/or their associated proteins.

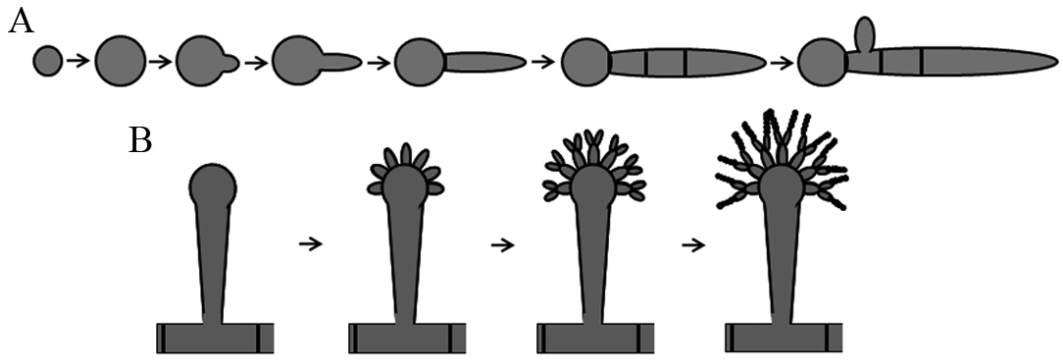

Figure 1.1. *Aspergillus nidulans* life cycle. (A) *A. nidulans* asexual dormant conidia (stage 1) initiate growth in the presence of a carbon source and grow isotropically (stages 2). Conidia switch from isotropic to polar growth with the emergence of a germ tube (stage 3). This germ tube continues to extend in a polar manner (stage 4). Growth is then divided by the formation of a septum (stage 5). Septa are crosswalls that divide the growth in an apical growing tip compartment and subapical non growing compartments (stage 6). Growth is initiated in nongrowing compartments with the emergence of a lateral branch (stage 7). (B) *A. nidulans* forms conidia from a conidiophore structure. This structure is made from a specialized hypha that swells at the tip (stage 1) from which layers bud: metulae (stage 2) and phialides (stage 3). Conidia continuously bud from the phialide layers and form conidial chains (stage 4). Adapted from (MOMANY 2002)

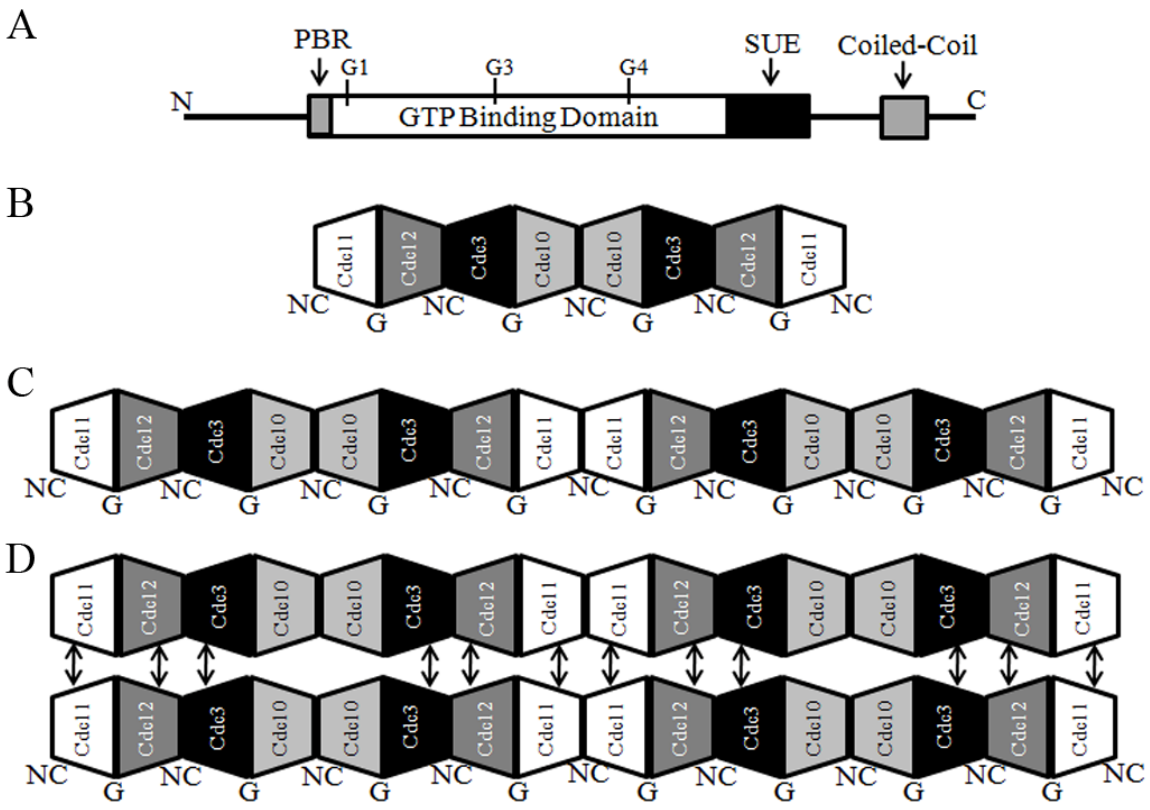

Figure 1.2. Septin domains and filaments. (A) Septins belong to the P-loop NTPase Family that includes the myosin/kinesin and Ras Superfamily of GTPases (SPILIOTIS 2010). Septins have a N-terminus of variable length followed by a Polybasic Region (PBR) (PAN *et al.* 2007). The PBR is the region next to the GTP binding domain and it seems to be important for membrane interactions through Phosphatidylinositol binding (BERTIN *et al.* 2008; BERTIN *et al.* 2010; TANAKA-TAKIGUCHI *et al.* 2009). There are six key amino acids in this region where a basic residue (Histidine, Lysine, Arginine) can be found in positions 1, 2, 5, and 6 in 60-78% of septins and a Glycine follows the PBR in 90% of septins (PAN *et al.* 2007). Septins have a GTP binding domain with the G1, G3 and G4 motifs found in the Ras superfamily. G1 seems to form a loose loop for GTP binding, G3 interacts with Mg^{+2} and the β and γ phosphates of GTP and G4

seems to provide GTP specificity (PAN *et al.* 2007). Septins belong to a class of G proteins activated by nucleotide-dependent dimerization (GADs) and its ability to hydrolyze GTP is not clearly understood (SPILIOTIS 2010). Septins have a unique element region (SUE) made of 53 amino acids, where half of the residues are conserved in 50-90% of septins (PAN *et al.* 2007). Most septins (except for the CDC10 group) have a coiled-coil region near the C-terminus that is key for septin-septin and septin-protein interactions and for septin bundling which form the different septin structures seen in Fluorescence microscopy. Coiled coils usually contain a repeated heptad pattern of hydrophobic (h) and charged (c) amino-acid residues (hxxhcxc) (PAN *et al.* 2007). Adapted from (PAN *et al.* 2007). (B) GTP-binding drives the formation of hetero-oligomeric complexes, which assemble into higher-order nonpolar filaments (BERTIN *et al.* 2008). In *S. cerevisiae* septins assemble as non polar filaments made of basic heteroctameric rods composed of two monomers of four different septins: Cdc3, Cdc10, Cdc11 and Cdc12. Septins interact through their N and C-terminal called the NC-dimer and their GTP binding domain called the G-dimer to form the basic octameric rod. (C) Octameric rods can interact with other rods to form long filaments. (D) Septin filaments can also form paired filaments by interactions through the coiled coil domains (double arrow) for septin bundling which form the different septin structures seen in Fluorescence microscopy. Adapted from (BERTIN *et al.* 2008).

References

ALVAREZ-TABARES, I., and J. PEREZ-MARTIN, 2010 Septins from the phytopathogenic fungus Ustilago maydis are required for proper morphogenesis but dispensable for virulence. PLoS ONE **5:** e12933.

AN, H., J. MORRELL, J. JENNINGS, A. LINK and K. GOULD, 2004a Requirements of fission yeast septins for complex formation, localization, and function. Molecular biology of the cell **15:** 5551-5564.

AN, H., J. L. MORRELL, J. L. JENNINGS, A. J. LINK and K. L. GOULD, 2004b Requirements of fission yeast septins for complex formation, localization, and function. Mol Biol Cell **15:** 5551-5564.

BARRAL, Y., 2009 Yeast septins: a cortical organizer. The Septins**:** 101.

BARRAL, Y., V. MERMALL, M. S. MOOSEKER and M. SNYDER, 2000 Compartmentalization of the cell cortex by septins is required for maintenance of cell polarity in yeast. Mol Cell **5:** 841-851.

BERLIN, A., A. PAOLETTI and F. CHANG, 2003 Mid2p stabilizes septin rings during cytokinesis in fission yeast. J Cell Biol **160:** 1083-1092.

BERMAN, J., and P. SUDBERY, 2002 Candida albicans: a molecular revolution built on lessons from budding yeast. Nature Reviews Genetics **3:** 918-932.

BERTIN, A., M. MCMURRAY, P. GROB, S. PARK, G. GARCIA *et al.*, 2008a Saccharomyces cerevisiae septins: Supramolecular organization of heterooligomers and the mechanism of filament assembly. Proceedings of the National Academy of Sciences **105:** 8274.

BERTIN, A., M. A. MCMURRAY, P. GROB, S. S. PARK, G. GARCIA, 3RD *et al.*, 2008b Saccharomyces cerevisiae septins: supramolecular organization of heterooligomers and the mechanism of filament assembly. Proc Natl Acad Sci U S A **105:** 8274-8279.

BÖHMER, C., C. RIPP and M. BÖLKER, 2009 The germinal centre kinase Don3 triggers the dynamic rearrangement of higher-order septin structures during cytokinesis in Ustilago maydis. Molecular microbiology **74:** 1484-1496.

BOYCE, K., H. CHANG, C. D'SOUZA and J. KRONSTAD, 2005 An Ustilago maydis septin is required for filamentous growth in culture and for full symptom development on maize. Eukaryotic Cell **4:** 2044.

CÁNOVAS, D., and J. PÉREZ-MARTÍN, 2009 Sphingolipid biosynthesis is required for polar growth in the dimorphic phytopathogen Ustilago maydis. Fungal genetics and biology **46:** 190-200.

CAVISTON, J. P., M. LONGTINE, J. R. PRINGLE and E. BI, 2003 The role of Cdc42p GTPase-activating proteins in assembly of the septin ring in yeast. Mol Biol Cell **14:** 4051-4066.

CHANT, J., 1996 Septin scaffolds and cleavage planes in Saccharomyces. Cell **84:** 187-190.

CHANT, J., and J. R. PRINGLE, 1995 Patterns of bud-site selection in the yeast Saccharomyces cerevisiae. J Cell Biol **129:** 751-765.

DE VIRGILIO, C., D. J. DEMARINI and J. R. PRINGLE, 1996 SPR28, a sixth member of the septin gene family in Saccharomyces cerevisiae that is expressed specifically in sporulating cells. Microbiology **142 (Pt 10):** 2897-2905.

DEMAY, B., R. MESEROLL, P. OCCHIPINTI and A. GLADFELTER, 2009 Regulation of distinct septin rings in a single cell by Elm1p and Gin4p kinases. Molecular Biology of the Cell **20:** 2311.

DOBBELAERE, J., and Y. BARRAL, 2004 Spatial coordination of cytokinetic events by compartmentalization of the cell cortex. Science **305:** 393-396.

DOBBELAERE, J., M. S. GENTRY, R. L. HALLBERG and Y. BARRAL, 2003 Phosphorylation-dependent regulation of septin dynamics during the cell cycle. Dev Cell **4:** 345-357.

DOUGLAS, L. M., F. J. ALVAREZ, C. MCCREARY and J. B. KONOPKA, 2005 Septin function in yeast model systems and pathogenic fungi. Eukaryot Cell **4:** 1503-1512.

ESTEY, M. P., M. S. KIM and W. S. TRIMBLE, 2011 Septins. Curr Biol **21:** R384-387.

FARES, H., L. GOETSCH and J. R. PRINGLE, 1996 Identification of a developmentally regulated septin and involvement of the septins in spore formation in Saccharomyces cerevisiae. J Cell Biol **132:** 399-411.

FARES, H., M. PEIFER and J. R. PRINGLE, 1995 Localization and possible functions of Drosophila septins. Mol Biol Cell **6:** 1843-1859.

FINGER, F., 2005 Reining in cytokinesis with a septin corral. Bioessays **27:** 5-8.

FLESCHER, E. G., K. MADDEN and M. SNYDER, 1993 Components required for cytokinesis are important for bud site selection in yeast. J Cell Biol **122:** 373-386.

FORD, S. K., and J. R. PRINGLE, 1991 Cellular morphogenesis in the Saccharomyces cerevisiae cell cycle: localization of the CDC11 gene product and the timing of events at the budding site. Dev Genet **12:** 281-292.

GILDEN, J., and M. F. KRUMMEL, 2010 Control of cortical rigidity by the cytoskeleton: emerging roles for septins. Cytoskeleton (Hoboken) **67:** 477-486.

GLADFELTER, A., J. PRINGLE and D. LEW, 2001a The septin cortex at the yeast mother–bud neck. Curr Opin Microbiol **4:** 681-689.

GLADFELTER, A., J. PRINGLE and D. LEW, 2001b The septin cortex at the yeast mother–bud neck. Current Opinion in Microbiology **4:** 681-689.

GLADFELTER, A. S., I. BOSE, T. R. ZYLA, E. S. BARDES and D. J. LEW, 2002 Septin ring assembly involves cycles of GTP loading and hydrolysis by Cdc42p. J Cell Biol **156:** 315-326.

GLADFELTER, A. S., L. KOZUBOWSKI, T. R. ZYLA and D. J. LEW, 2005 Interplay between septin organization, cell cycle and cell shape in yeast. J Cell Sci **118:** 1617-1628.

GLADFELTER, A. S., J. R. PRINGLE and D. J. LEW, 2001c The septin cortex at the yeast mother-bud neck. Curr Opin Microbiol **4:** 681-689.

GLADFELTER, A. S., and P. SUDBERY, 2008 Septins in four model fungal systems: diversity in form amd function, pp. 125-146 in *The Septins*, edited by P. A. HALL, S. E. H. RUSSELL and J. R. PRINGLE. Wiley-Blackwell.

GONZALEZ-NOVO, A., J. CORREA-BORDES, L. LABRADOR, M. SANCHEZ, C. R. VAZQUEZ DE ALDANA *et al.*, 2008 Sep7 is essential to modify septin ring dynamics and inhibit cell separation during Candida albicans hyphal growth. Mol Biol Cell **19:** 1509-1518.

GROMLEY, A., A. JURCZYK, J. SILLIBOURNE, E. HALILOVIC, M. MOGENSEN *et al.*, 2003 A novel human protein of the maternal centriole is required for the final stages of cytokinesis and entry into S phase A. Gromley and A. Jurczyk contributed equally to this work. The online version of this article includes supplemental material. Journal of Cell Biology **161:** 535-545.

HALL, P. A., and F. P. FINGER, 2008 Septin and human disease, pp. 295-317 in *The Septins*, edited by P. A. HALL, H. RUSSELL, S.E. and J. R. PRINGLE. John Wiley & Sons, Ltd, UK.

HARTWELL, L., 1971a Genetic control of the cell division cycle in yeast. IV. Genes controlling bud emergence and cytokinesis. Exp Cell Res **69:** 265-276.

HARTWELL, L. H., 1971b Genetic control of the cell division cycle in yeast. IV. Genes controlling bud emergence and cytokinesis, pp. 265-276.

HELFER, H., and A. S. GLADFELTER, 2006 AgSwe1p regulates mitosis in response to morphogenesis and nutrients in multinucleated Ashbya gossypii cells. Mol Biol Cell **17:** 4494-4512.

HU, Q., L. MILENKOVIC, H. JIN, M. P. SCOTT, M. V. NACHURY *et al.*, 2010 A septin diffusion barrier at the base of the primary cilium maintains ciliary membrane protein distribution. Science **329:** 436-439.

IHARA, M., A. KINOSHITA, S. YAMADA, H. TANAKA, A. TANIGAKI *et al.*, 2005 Cortical organization by the septin cytoskeleton is essential for structural and mechanical integrity of mammalian spermatozoa, pp. 343-352.

KIM, H., 1991 Cellular morphogenesis in the Saccharomyces cerevisiae cell cycle: localization of the CDC3 gene product and the timing of events at the budding site. J Cell Biol **112:** 535-544.

KINOSHITA, M., 2006 Diversity of septin scaffolds. Curr Opin Cell Biol **18:** 54-60.

KINOSHITA, M., C. M. FIELD, M. L. COUGHLIN, A. F. STRAIGHT and T. J. MITCHISON, 2002 Self- and actin-templated assembly of mammalian septins, pp. 791-802.

KINOSHITA, M., S. KUMAR, A. MIZOGUCHI, C. IDE, A. KINOSHITA *et al.*, 1997 Nedd5, a mammalian septin, is a novel cytoskeletal component interacting with actin-based structures. Genes & development **11:** 1535-1547.

KONOPKA, J. B., C. DEMATTEI and C. DAVIS, 1995 AFR1 promotes polarized apical morphogenesis in Saccharomyces cerevisiae. Mol Cell Biol **15:** 723-730.

KOZUBOWSKI, L., and J. HEITMAN, 2009 Septins enforce morphogenetic events during sexual reproduction and contribute to virulence of Cryptococcus neoformans. Molecular microbiology **75:** 658-675.

KREMER, B., T. HAYSTEAD and I. MACARA, 2005 Mammalian septins regulate microtubule stability through interaction with the microtubule-binding protein MAP4. Molecular Biology of the Cell **16:** 4648.

KWITNY, S., A. V. KLAUS and G. R. HUNNICUTT, 2010 The annulus of the mouse sperm tail is required to establish a membrane diffusion barrier that is engaged during the late steps of spermiogenesis. Biol Reprod **82:** 669-678.

LEW, D. J., 2003 The morphogenesis checkpoint: how yeast cells watch their figures. Curr Opin Cell Biol **15:** 648-653.

LEW, D. J., and S. I. REED, 1995 A cell cycle checkpoint monitors cell morphogenesis in budding yeast. J Cell Biol **129:** 739-749.

LINDSEY, R., S. COWDEN, Y. HERNANDEZ-RODRIGUEZ and M. MOMANY, 2010 Septins AspA and AspC are important for normal development and limit the emergence of new growth foci in the multicellular fungus Aspergillus nidulans. Eukaryot Cell **9:** 155-163.

LINDSEY, R., and M. MOMANY, 2006 Septin localization across kingdoms: three themes with variations. Curr Opin Microbiol **9:** 559-565.

LONGTINE, M., D. DEMARINI, M. VALENCIK, O. AL-AWAR, H. FARES *et al.*, 1996 The septins: roles in cytokinesis and other processes. Curr Opin Cell Biol **8:** 106-119.

MARTIN, S., L. DOUGLAS and J. KONOPKA, 2005 Cell cycle dynamics and quorum sensing in Candida albicans chlamydospores are distinct from budding and hyphal growth. Eukaryotic Cell **4:** 1191.

MCMURRAY, M., and J. THORNER, 2008a Septin stability and recycling during dynamic structural transitions in cell division and development. Current Biology **18:** 1203-1208.

MCMURRAY, M., and J. THORNER, 2009 Biochemical properties and supramolecular architecture of septin hetero-oligomers and septin laments. The Septins**:** 49.

MCMURRAY, M. A., A. BERTIN, G. GARCIA, 3RD, L. LAM, E. NOGALES *et al.*, 2011 Septin filament formation is essential in budding yeast. Dev Cell **20:** 540-549.

MCMURRAY, M. A., and J. THORNER, 2008b Biochemical properties and supramolecular architecture of septin hetero-oligomers and septin filaments, pp. 49-100 in *The Septins*, edited by P. A. HALL, H. S. E. RUSSELL and J. R. PRINGLE. John Wiley & Sons, Ltd., UK.

MOMANY, M., and J. E. HAMER, 1996 The Aspergillus nidulans septin encoding gene, aspB, is essential for growth. Fungal Genet Biol **21:** 92-100.

MOMANY, M., and J. E. HAMER, 1997 The Aspergillus nidulans Septin Encoding Gene, aspB, Is Essential for Growth. Fungal Genet Biol **21:** 92-100.

NAGATA, K., A. KAWAJIRI, S. MATSUI, M. TAKAGISHI, T. SHIROMIZU *et al.*, 2003 Filament formation of MSF-A, a mammalian septin, in human mammary epithelial cells depends on interactions with microtubules. Journal of Biological Chemistry **278:** 18538-18543.

NGUYEN, T. Q., 2000 The C. elegans septin genes, unc-59 and unc-61, are required for normal postembryonic cytokineses and morphogenesis but have no essential function in embryogenesis, pp. 3825-3837.

PAN, F., R. MALMBERG and M. MOMANY, 2007a Analysis of septins across kingdoms reveals orthology and new motifs. BMC Evolutionary Biology **7:** 103.

PAN, F., R. L. MALMBERG and M. MOMANY, 2007b Analysis of septins across kingdoms reveals orthology and new motifs. BMC Evol Biol **7:** 103.

PRINGLE, J. R., 2008 Origins and development of te septin field, pp. 7-34 in *The Septins*, edited by P. A. HALL, S. E. H. RUSSELL and J. R. PRINGLE. Wiley-Blackwell John Wiley & Sons, Ltd., UK.

QI, M., W. YU, S. LIU, H. JIA, L. TANG *et al.*, 2005 Septin1, a new interaction partner for human serine/threonine kinase aurora-B. Biochemical and Biophysical Research Communications **336:** 994-1000.

RUSSELL, S. E. H., and P. A. HALL, 2005 Do septins have a role in cancer?, pp. 499-503.

SAUNDERS, D. G., Y. F. DAGDAS and N. J. TALBOT, 2010 Spatial uncoupling of mitosis and cytokinesis during appressorium-mediated plant infection by the rice blast fungus Magnaporthe oryzae. Plant Cell **22:** 2417-2428.

SCHMIDT, K., and B. NICHOLS, 2004a Functional interdependence between septin and actin cytoskeleton. BMC Cell Biology **5:** 43.

SCHMIDT, K., and B. J. NICHOLS, 2004b A barrier to lateral diffusion in the cleavage furrow of dividing mammalian cells. Curr Biol **14:** 1002-1006.

SHINODA, T., H. ITO, K. SUDO, I. IWAMOTO, R. MORISHITA *et al.*, 2010 Septin 14 Is Involved in Cortical Neuronal Migration via Interaction with Septin 4. Molecular Biology of the Cell**:** E09.

SHU, H., Z. LI, M. PALACIOS, Q. LI and H. JOSHI, 1995 A transient association of gamma-tubulin at the midbody is required for the completion of cytokinesis during the mammalian cell division, pp. 2955-2962.

SINHA, I., Y. M. WANG, R. PHILP, C. R. LI, W. H. YAP *et al.*, 2007 Cyclin-dependent kinases control septin phosphorylation in Candida albicans hyphal development. Dev Cell **13:** 421-432.

SPILIOTIS, E., S. HUNT, Q. HU, M. KINOSHITA and W. NELSON, 2008a Epithelial polarity requires septin coupling of vesicle transport to polyglutamylated microtubules. Journal of Cell Biology **180:** 295.

SPILIOTIS, E., and W. NELSON, 2006 Here come the septins: novel polymers that coordinate intracellular functions and organization. Journal of Cell Science **119:** 4.

SPILIOTIS, E. T., 2010 Regulation of microtubule organization and functions by septin GTPases. Cytoskeleton **67:** 339-345.

SPILIOTIS, E. T., S. J. HUNT, Q. HU, M. KINOSHITA and W. J. NELSON, 2008b Epithelial polarity requires septin coupling of vesicle transport to polyglutamylated microtubules. J Cell Biol **180:** 295-303.

SPILIOTIS, E. T., M. KINOSHITA and W. J. NELSON, 2005 A mitotic septin scaffold required for Mammalian chromosome congression and segregation. Science **307:** 1781-1785.

SPILIOTIS, E. T., and W. J. NELSON, 2008 Septin Functions in the mammalian cytoskeleton, pp. 229-246 in *The Septins*, edited by P. A. HALL, S. E. H. RUSSELL and J. R. PRINGLE. Wiley-Blackwell.

SUDBERY, P., 2001 The germ tubes of Candida albicans hyphae and pseudohyphae show different patterns of septin ring localization. Molecular Microbiology **41:** 19-31.

SURKA, M., C. TSANG and W. TRIMBLE, 2002 The mammalian septin MSF localizes with microtubules and is required for completion of cytokinesis. Molecular Biology of the Cell **13:** 3532.

TADA, T., A. SIMONETTA, M. BATTERTON, M. KINOSHITA, D. EDBAUER *et al.*, 2007 Role of Septin cytoskeleton in spine morphogenesis and dendrite development in neurons. Current Biology **17:** 1752-1758.

TAKIZAWA, P. A., J. L. DERISI, J. E. WILHELM and R. D. VALE, 2000 Plasma membrane compartmentalization in yeast by messenger RNA transport and a septin diffusion barrier. Science **290:** 341-344.

TANAKA-TAKIGUCHI, Y., M. KINOSHITA and K. TAKIGUCHI, 2009 Septin-mediated uniform bracing of phospholipid membranes. Curr Biol **19:** 140-145.

TASTO, J. J., J. L. MORRELL and K. L. GOULD, 2003 An anillin homologue, Mid2p, acts during fission yeast cytokinesis to organize the septin ring and promote cell separation. J Cell Biol **160:** 1093-1103.

VEGA, I., and S. HSU, 2003 The septin protein Nedd5 associates with both the exocyst complex and microtubules and disruption of its GTPase activity promotes aberrant neurite sprouting in PC12 cells. Neuroreport **14:** 31.

VERSELE, M., B. GULLBRAND, M. J. SHULEWITZ, V. J. CID, S. BAHMANYAR *et al.*, 2004 Protein-protein interactions governing septin heteropentamer assembly and septin filament organization in Saccharomyces cerevisiae. Mol Biol Cell **15:** 4568-4583.

VERSELE, M., and J. THORNER, 2004 Septin collar formation in budding yeast requires GTP binding and direct phosphorylation by the PAK, Cla4. J Cell Biol **164:** 701-715.

VERSELE, M., and J. THORNER, 2005 Some assembly required: yeast septins provide the instruction manual. Trends Cell Biol **15:** 414-424.

WARENDA, A., and J. KONOPKA, 2002a Septin function in Candida albicans morphogenesis. Molecular biology of the cell **13:** 2732.

WARENDA, A. J., and J. B. KONOPKA, 2002b Septin function in Candida albicans morphogenesis. Mol Biol Cell **13:** 2732-2746.

WESTFALL, P. J., and M. MOMANY, 2002 Aspergillus nidulans septin AspB plays pre- and postmitotic roles in septum, branch, and conidiophore development. Mol Biol Cell **13:** 110-118.

WU, J. Q., J. R. KUHN, D. R. KOVAR and T. D. POLLARD, 2003 Spatial and temporal pathway for assembly and constriction of the contractile ring in fission yeast cytokinesis. Dev Cell **5:** 723-734.

XIE, H., M. SURKA, J. HOWARD and W. TRIMBLE, 1999 Characterization of the mammalian septin H5: distinct patterns of cytoskeletal and membrane association from other septin proteins. Cell motility and the cytoskeleton **43**.

CHAPTER 2

THE SEPTIN ASPB IN *ASPERGILLUS NIDULANS* FORMS BARS AND FILAMENTS AND PLAYS ROLES IN GROWTH EMERGENCE AND CONIDIATION[1]

[1]Hernández-Rodríguez, Y., Cowden, S., and Momany, M. 2011. Submitted to Eukaryotic Cell, 7/4/2011.

Abstract

Septins are found in fungi and animals, but not in plants. In yeast, septins form rings at the mother-bud neck. In animals, septins form filaments that colocalize with cytoskeletal elements. In the filamentous fungus *Aspergillus nidulans* there are five septins, *aspA/cdc11*, *aspB/cdc3*, *aspC/cdc12*, *aspD/cdc10*, and *aspE*. *AspB/cdc3* was previously reported to be the most highly expressed septin and to be essential. Using improved gene deletion techniques, we found that deletion of *aspB/cdc3* is not lethal, but results in aberrant germ tube emergence, branching and asexual development (conidiation). Deletion of the *aspB* gene results in hypergermtube and hyperbranch emergence and thin, hooked abortive branches. Conidiophore layers are abnormal and conidiation is extremely poor. AspB-GFP localizes to sites of septation and branching and emerging layers of the conidiophore. AspB also localizes to sites of germ tube and branch emergence and forms filamentous arrangements, bars and filaments, whose localization varies with developmental and morphological changes. Bars are found in dormant and early germinating spores, remain in subapical nongrowing compartments and display fast movements. Filaments form as the germ tube emerges, localize to the hyphal and branch tips and display slower movements within compartments and near nuclei. AspB filaments are lost in the absence of septins AspA and AspC, suggesting that septin interactions are necessary for filament formation. AspB filaments are extremely reduced in hyphae of *ΔaspE*. This suggests that AspE, which belongs to a septin family only found in filamentous fungi, has evolved to maintain septin filament stability in highly polar growing cells.

Introduction

Septins are evolutionarily conserved GTP binding proteins that form filamentous complexes (VERSELE and THORNER 2005).These cytoskeletal elements are found in all eukaryotes except higher plants (ESTEY *et al.* 2011; PAN *et al.* 2007b). Septins are involved in numerous events such as cytokinesis, vesicle trafficking, nuclear division, cytoskeleton organization, polarity maintenance, compartmentalization of pre-existing cellular material and formation of diffusion barriers (KINOSHITA 2006; LINDSEY and MOMANY 2006; MCMURRAY and THORNER 2008b; RUSSELL and HALL 2005; VERSELE and THORNER 2005). In addition, septin defects have been associated with diseases such as leukemia and many other types of cancer, Parkinson's, Alzheimer's, Down's syndrome and schizophrenia (HALL and FINGER 2008).

Septins *cdc3*, *cdc10, cdc11*and *cdc12* were first discovered in a screen for temperature-sensitive cell cycle mutants in *Saccharomyces cerevisiae* by Hartwell and named "septins" for their roles in septum formation (HARTWELL 1971b). Septin mutations in *S. cerevisiae* result in multibuded cells defective in cytokinesis (HARTWELL 1971a; LONGTINE *et al.* 1996). Early in the cell cycle, septins localize as a cap at the future site of bud emergence. As the bud emerges, septins localize first as a ring at the mother/bud neck and later as an hourglass structure as the bud develops (GLADFELTER *et al.* 2001a; GLADFELTER *et al.* 2005b; LEW 2003). These septin structures form diffusion barriers that keep the polarity machinery and key proteins for growth localize to the daughter cell (ORLANDO *et al.* 2011). At cytokinesis, the hourglass structure converts into two rings. Septin scaffolds at the neck form diffusion barriers that keep the machinery necessary for growth and cytokinesis localized and concentrated to this area (DOBBELAERE and BARRAL 2004; DOUGLAS *et al.* 2005; FINGER 2005; OH and BI 2011; TAKIZAWA *et al.* 2000). In addition, septins are part of the morphogenesis checkpoint that

controls and coordinates bud formation and nuclear division. If bud formation is disrupted, the nuclear cycle is paused by the morphogenesis checkpoint. This ensures that only one nucleus is present in each cell (LEW 2003).

In *S. cerevisiae* septins organize into hetero-oligomeric filamentous octamers that give rise to septin rings (BERTIN *et al.* 2008). These nonpolar hetero-octamers are composed of two monomers of each septin molecule. Individual septins can be recycled from complex to complex throughout development (MCMURRAY and THORNER 2008a). FRAP experiments showed that septin turnover occurs prior to bud emergence, hourglass splitting and ring disassembly, while there is no turnover during bud formation and cytokinesis in *S. cerevisiae* (BARRAL 2009; BARRAL *et al.* 2000; CAVISTON *et al.* 2003; DOBBELAERE *et al.* 2003). In addition, EM studies have shown that long filaments can align in pairs forming higher order structures after the initial filament is formed. Removal of septin members from the complex can result in abnormalities whose severity depends on which member is removed (MCMURRAY *et al.* 2011).

Septins have also been studied in other fungal systems. In *Schizosaccharomyces pombe*, septins are mainly involved, but not essential, in cytokinesis. Septins assemble into a ring that splits and encloses the actin-myosin ring for cytokinesis (AN *et al.* 2004). In *Candida albicans*, septin mutations result in defects in cell separation forming cell chains. During budding, septins localize very similarly to *S. cerevisiae*. During hyphal growth, septins assemble and disassemble forming septin bands at the base of emerging germ tubes and septation sites, and collars at hyphal tips (BERMAN and SUDBERY 2002; GLADFELTER and SUDBERY 2008; SUDBERY 2001; WARENDA and KONOPKA 2002). Unlike bud and hyphal development, septins form long filamentous structures during chlamydospore morphogenesis (MARTIN *et al.* 2005). In *Cryptococcus neoformans* septins are involved in morphology, sporulation, clamp cell fusion and

nuclear dynamics (KOZUBOWSKI and HEITMAN 2009). Here septins localize to emerging spores, septa and clamp connections. *A. gossypii*, has five septin proteins (Cdc3p, Cdc10p, Cdc11p, Cdc12p, Shs1/Sep7p) that form various rings in the hyphae and their morphological and behavioral differences are regulated by Elm1p and Gin4p kinases (DEMAY *et al.* 2009; HELFER and GLADFELTER 2006). In *A. gossypii*, septin mutants shift mitoses from the normal site and it has been suggested that septin rings promote mitosis near new branches (HELFER and GLADFELTER 2006). In *Ustilago maydis*, septins undergo dynamic rearrangements from hourglass collars into ring structures during septation (BÖHMER *et al.* 2009; CÁNOVAS and PÉREZ-MARTÍN 2009). Sep3 is required for normal cellular morphology and division during budding and filamentous growth. Sep3 is also involved in the germination and differentiation of hyphae into teliospores and may be connected to cAMP signaling during morphogenesis (BOYCE *et al.* 2005).

In mammals, septins are involved in a variety of processes. In developing polar neuron cells, septins are involved in the morphogenesis of normal mature dendritic spines (TADA *et al.* 2007). Sept7 localizes at the base of dendritic protrusions and its overexpression increases dendrite branching and density of dendritic protrusions, while its knockdown results in reduced dendrite arborization and increased proportion of immature protrusions. In mammals, septins are also involved in the formation of diffusion barriers (SCHMIDT and NICHOLS 2004). SEPT2 is essential for retaining receptor-signaling pathways in the primary cilium and is also key for diffusion in the cleavage furrow of dividing cells (HU *et al.* 2010; SCHMIDT and NICHOLS 2004). The annulus (composed of septins) of the mouse sperm tail is also key in the formation of diffusion barriers and proper function of the sperm (IHARA *et al.* 2005; KWITNY *et al.* 2010).

Though septin studies in yeast have been very useful; studies of unicellular cells cannot address how septins coordinate cell division across compartments in multicellular organisms or how they function in highly polar cells such as neurons. Filamentous fungi, being highly polarized multicellular organisms, in addition to their different cell geometries, make them suitable model systems to answer these questions. *Aspergillus nidulans* has 5 septins: AspA, AspB, AspC, AspD and AspE. We previously showed that deletions of *aspA*, *aspC*, or both *aspA* and *aspC* result in early and increased germ tube and branch emergence, abnormal septation, and disorganized conidiophores and their normal localization is codependent; suggesting that AspA and AspC interact (LINDSEY *et al.* 2010b). *aspB* was previously reported to be essential and immunofluorescence showed that AspB localizes pre- and postmitotically to septation, branching sites, and conidiophore interface layers (MOMANY and HAMER 1997b; WESTFALL and MOMANY 2002). Here we show that *aspB* deletion is not lethal, but causes aberrant morphology in several developmental stages and severe defects in asexual reproduction. AspB-GFP localizes not only as dots, rings and caps but also as bars and filaments throughout vegetative growth and asexual reproduction. We observed rapid large scale movements of AspB bars in cells with young germ tubes and more restricted movement of AspB filaments in longer hyphae. AspB-GFP structures are lost in the absence of AspA, AspC and at times in the absence of AspE. AspB seems to play roles in fungal growth and asexual reproduction and its filamentous localization throughout fungal growth and development requires certain septin partners and resembles other cell cytoskeleton.

Materials and Methods

Strains and growth conditions

Experiments were carried out using A. nidulans strains presented in Table 2.1. Fungal cultures for microscopy, crosses, DNA isolation and strain purification studies were grown in minimal medium (MM) (1 % glucose, nitrate salts, biotin, trace elements and 1% thiamine, pH 6.5) or with complete medium (CM) (1% glucose, 2% peptone, 1% yeast extract, 1% casamino acids, 0.01% vitamins and supplements, nitrate salts solution and trace elements, pH 6.5, 1.8% agar was added for solid medium.) (Kafer 1977). Additional supplements were added depending on strains auxotrophic markers (i.e. pyridoxine HCl, p-aminobenzoate, riboflavin HCl, arginine and uridine and uracyl (Kaminskyj 2001). Strains were cultured at 30°C.

Gene targeting and tagging

Septin deletions with *AfpyrG* and tagging with *gfp* were constructed as described by Yang et al. (YANG *et al.* 2004). We amplified around 2kb upstream and downstream of *aspB* from *A. nidulans* genomic DNA strain A850 (Table 2.1), and amplified the *AfpyrG* marker from the plasmid pFNO3 as explained in the above reference and using primers listed in Table 2.2. AccuPrime *Pfx* DNA Polymerase was used to amplify and fuse DNA fragments with annealing temperatures as described by Szewczyk et al. (SZEWCZYK *et al.* 2007). PCR products were separated on 1% agarose gel and purified using the QIA quick gel extraction kit (QIAGEN Inc., Valencia, CA). Typical *Aspergillus nidulans* protoplast transformation was used in combination with strains and new techniques modified in the nonhomologous DNA repair pathway (Table 2.1) (SZEWCZYK *et al.* 2007; YANG *et al.* 2004; YELTON *et al.* 1984). We verified that the native *aspB* gene was tagged with C terminal *gfp* at the native locus, driven by the native promoter by PCR and confirmed that only the single tagged copy of *aspB* was present in the strain and that it

was integrated at the native *aspB* locus by Southern Blot. Transformants were selected by auxotrophic markers of preference (considering future analysis and crosses) and verified by PCR (as described in Yang et al. (YANG *et al.* 2004) and confirmed by Southern Blot (BROWN 2001). All PCRs and Southern Blot primers were designed to amplify or detect a product of different sizes for both positive and negative results, and the untagged wild type strain A850 was used as a control. Genetic crosses were used to recover *nkuA* in strains of interest as previously described (HARRIS 2001); strains were crossed to wild type strains A773 and A850. Strains with preferred auxotrophic markers were selected and PCR verified for recovery of *nkuA*. *aspB/aspB-gfp* heterozygous diploids were constructed as previously described by Harris (HARRIS 2001) using AYR6 (haploid *aspB-gfp*) and wild type A850 as parents.

Microscopy

Culture preparation: Conidia were harvested from agar plates with sterile water. For fungal observation and characterization, 1 x 10^4 or 1 x 10^7 spores were grown in 10 ml of MM or CM liquid in a Petri dish containing a glass cover slip, and incubated at 30°C. To examine conidiophores, a flame-sterile coverslip was put over a water agar plate, followed by a block of MM or CM plus supplements. The block was inoculated with fungal spores in water and a flame-sterile coverslip was placed on top. Unsealed plates were incubated for 1, 2 and 3 days at 30°C. To stain cell wall and septa, we followed protocols previously published by Momany (MOMANY 2001). Calcoflour Blankophour BDH was used to stain septa and Hoechst 33342 (for dormant conidia) and Hoechst 33258 bis-benzimide were used to stain nuclei. Photoshop CS3 was used to combine DIC or light images with fluorescence images and for micrograph organization, improve contrast and brightness and/or Hue saturation coloration. Microsoft Excel was used to make graphs.

Fluorescence microscopy: For *in vivo* GFP observations strains were incubated as described above until the appropriate time point at 30°C, and coverslips with attached fungus were not fixed, but mounted in 8-10µls of liquid medium onto slides. Incubation time points for examining fungal development at 30°C were as follow: isotropic growth (4-5 hrs), germ tube emergence (6-7 hrs), hyphal elongation and septation (9-11hrs), branching (12-16hrs). Fungal hyphae were viewed using a Zeiss Axioplan microscope with a Plan –NEOFLUAR 100X/1.30 NA oil immersion objective lens, X-cite Fluorescence Illumination System (EXFO), and were digitally photographed using Zeiss Axiocam MRc CCD (charge-coupled device) camera and software.

Confocal microscopy: Strains were prepared as for fluorescence microscopy. A Leica SP2 Spectral Confocal Scanning Laser Microscope was used with the 63X HCX PL APO 1.20 W CORR water immersion objective lens. The Ar/HeNe laser was used for GFP excitation with a wavelength of 488nm (20%) and filter RT 30/70. Images were acquired with the AxioCam CCD (Zeiss) camera and the Leica Confocal LCS Lite software. Image collection and Z-stacks were calculated by the software based on the observed fluorescence of each sample and consequently the amount Z-stack sections varied for each samples and the program adjusted X/Y settings to avoid distortion of the data. Beam expander was set to 3 and scanning setting was 1024 x 1024. Reference images were taken with white light microscopy not DIC. Line and frame average varied on the GFP background, but in general we used a line average of 1-4 and a frame average 2-6, and Q-Lut was used as a reference to avoid collection of saturated pixels. Maximum Projection was used in the LS software to combine Z-stack images and brightness and contrast were adjusted to enhance image presentation.

Time lapse microscopy: For *in vivo gfp* examination, strains were prepared as described above, but a Gene Frame® (Thermo Scientific) adhesive was used prior to mounting. This adhesive was mounted onto slides making a small well to which 100µls of MM liquid medium were added, and coverslips with adhering fungus were floated on top. An Olympus IX-71 inverted fluorescence microscope with the Olympus 100X/1.35 NA U Plan Apo objective lens was used and a mercury light source. Images were acquired with the Photometrix Cool Snap HQ CCD camera and the Delta Vision Experiment Designer software was used to collect time lapse data and movies. Time lapse was set for collection of GFP and DIC simultaneously with a time frame of 5 sec, but due to the exposure and dual image collection time lapse in between frames varied from 5-10 seconds. We used flat-field calibration and when focus was lost it was adjusted manually. Data was analyzed using DIC movies as reference and movies were edited with Windows Movie Maker to show data from the same focal plane.

Results

aspB is nonessential, but required for normal growth and morphology

The *Aspergillus nidulans aspB* septin was previously reported to be essential (MOMANY and HAMER 1996). To further characterize septins in *A. nidulans*, we used improved gene targeting techniques using fusion PCR and *ΔnkuA* strains with reduced nonhomologous recombination (YANG *et al.* 2004) to create strains in which septin genes *aspA, aspC*, *aspD* and *aspE* were replaced with *pyrG* from *A. fumigatus (AfpyrG)* (LINDSEY *et al.* 2010a). In order to verify that *aspB* was an essential gene, we included it in the analysis. Surprisingly, *ΔaspB::AfpyrG* transformants were recovered. We verified that the *aspB* gene was replaced with the *AfpyrG* marker by PCR and DNA hybridization (data not shown). We crossed the resulting

ΔaspB ΔnkuA strain to wild type, selected for *ΔaspB nkuA*$^{+}$ progeny and verified them by PCR. All strains used in this study are described in Table 2.1.

We examined freshly harvested wild type and *ΔaspB* conidia by differential interference contrast microscopy (DIC) and scored relevant phenotypes. Freshly harvested wild type conidia were of uniform size measuring ~3µm (MIMS *et al.* 1988; TRINCI 1969). In contrast, *ΔaspB* conidia ranged from ~3 to ~5µm (data not shown). To determine whether conidial size might be related to nuclear number, we used Hoechst 33342 to stain nuclei of dormant conidia. As expected, wild type (wt) conida were all uninucleate (n=200) (ROSENBERGER and KESSEL 1967). However, *ΔaspB* conidia were both uninucleate (61%) and binucleate (39%), and the binucleate conidia were generally larger (n=200) (Figure 2.1A). Binucleate conidia were also observed in *ΔaspA* (30%) and *ΔaspC* (38% 2) (Supplemental Figure 2.1). In wild type, nuclei are uniformly distributed along the hypha (XIANG and FISCHER 2004). In *ΔaspB* hyphae, nuclei appeared smaller and clumped relative to wild type (Figure 2.3).

In *S. cerevisiae*, septins are important in determining when and where buds will emerge (CARROLL *et al.* 1998; CID *et al.* 2001; FORD and PRINGLE 1991; HAARER and PRINGLE 1987; KIM 1991; MINO *et al.* 1998). To determine whether *aspB* affects when and where germ tubes will emerge, we compared wild type and *ΔaspB* after incubation at 30°C. After 4hrs of incubation at 30°C, wt cells were not yet polar (0%, n=300) while in *ΔaspB* cells polarization was visible in 20% of cells (n=300) (Figure 2.1B). After 6hrs of incubation, few wild type cells formed more than 1 germ tube (10%, n=200) while many more *ΔaspB* cells formed more than 1 germ tube per cell (34%) (Figure 2.1C and Figure 2.2A).

In *S. cerevisiae* septins are required for septation (HARTWELL 1971a; LONGTINE *et al.* 1996). To determine whether *aspB* is necessary for septation, we compared wild type and *ΔaspB*

strains after 11-14 hrs of incubation at 30°C. In *A. nidulans*, compartmentalization of growth by septation gives rise to an actively growing tip compartment and inactive subapical compartments that later initiate polar growth by forming one branch per compartment (DYNESEN and NIELSEN 2003; FIDDY and TRINCI 1976). At 11hrs most wild type hyphae had 1-2 septa (71 %, n=200) while a minority of *ΔaspB* germlings had septa (12%) (Figure 2.1D). However, when *ΔaspB* cells were examined at 14hrs, virtually all had formed septa indicating that septation was delayed, but not absent in *ΔaspB*. Septa in *ΔaspB* strains appeared to be morphologically normal by DIC microscopy, but Calcofluor staining of chitin faded much more quickly under UV light in *ΔaspB* cells compared to wild type (data not shown) suggesting that there might be abnormalities in septum organization.

As expected, in wild type, branches were fairly uniform tubes of 5μm in diameter with a single branch formed in most compartments (69%, n=200). In the *ΔaspB* strain, branches were often stunted, thin (2-2.5 μm in diameter) and hooked (67%) with 2 or more branches per compartment (13%) (Figure 2.1E and Figure 2.2B). To determine if these abnormal branches might be branch initials which later elongated into normal branches, we observed *ΔaspB* after 16-18 hours of incubation at 30°C. Even at this later time point branches remained thin, short and hooked indicating they were abortive branch initials (data not shown).

A. nidulans produces asexual spores (conidia) on specialized structures (conidiophores) in a process that has been compared to *S. cerevisiae* budding (MIMS *et al.* 1988). During conidiophore development, a specialized foot cell is delineated by septa, an aerial hypha emerges from the foot cell, the tip of the aerial hypha swells to form a vesicle from which two specialized layers bud: metulae and phialides. Conidia bud from phialides forming a conidial chain that can be many units long (MIMS *et al.* 1988). When isolating *ΔaspB*, we observed very poor

conidiation. To determine whether *aspB* plays a role in asexual reproduction, we examined conidiophore development. As expected, after 2 days of incubation wild type conidiophores were morphologically normal with discrete, organized layers (97%, n=200). In contrast, conidiophores in the *ΔaspB* strain were morphologically abnormal with disorganized layers (100%, n=200) that formed many fewer conidia, with only 1-2 conidia visible on most phialides (Figure 2.1F and Figure 2.2C).

AspB forms bars and filaments throughout vegetative growth and conidiophore production

Using polyclonal antibodies, we previously reported AspB localization to forming septa, branches and conidiophore layers in *A. nidulans* (WESTFALL and MOMANY 2002). Immunofluorescence of cytoplasmic proteins in fungi requires fixation and digestion of the fungal cell wall in order for the antibodies to reach their target epitopes. To characterize AspB localization in live cells we used fusion PCR in a *ΔnkuA* strain as previously described to construct a strain carrying a single copy of *aspB-gfp*, replacing the native *aspB* gene (LINDSEY *et al.* 2010a; YANG *et al.* 2004). To ensure that localization was not affected by deletion of *nkuA*, we crossed *aspB-gfp ΔnkuA* to wild type, selected for *aspB-gfp nkuA*$^{+}$ progeny and verified them by PCR. Because diploid cells are larger and better for microscopy, and to further reduce the concentration of GFP- tagged AspB in the cell, we constructed a heterozygous diploid strain carrying a single copy of wild type *aspB* and a single copy of *aspB-gfp* (HARRIS 2001). In the haploid *aspB-gfp* and heterozygous diploid *aspB-gfp/ aspB* strain, conidial nuclear number, polarity establishment, germ tube emergence, septation, branching and conidiophore formation were nearly identical to wild type, showing that the GFP tag does not interfere with normal function (Figure 2.1, A-F).

We visualized AspB-GFP localization in live cells throughout development using fluorescence microscopy. In freshly harvested conidia AspB-GFP localized as rings, dots and ~1μm thick bars of variable lengths (Figure 2.4A). As the spores began to swell, we also observed AspB-GFP localized as small X-shaped structures (Figure 2.4B inset). AspB-GFP localized as a cap in emerging germ tubes and as a collar at the base of germ tubes (Figure 2.4B). Bars were also seen in newly formed germ tubes (Figure 2.4B). As germ tubes continued to extend AspB-GFP filaments which appeared thinner and longer than bars were also observed (Figure 2.4C-H). In older hyphae, tip localization was mostly as filaments and subapical localization was mostly as bars (Figure 2.4F-G). AspB-GFP localized as a ring at septa as previously shown by immunofluorescence (Figure 2.4H) (WESTFALL and MOMANY 2002). During branch emergence AspB-GFP localized as filaments perpendicular to and just below the nascent branches of less than 2.5μm in length (Figure 2.4I and 2.4K). As branches extended to ~3μm in length, the perpendicular filaments disappeared and AspB-GFP filaments were seen within branches (Figure 2.4M-N, 2.4P, 2.4R). In newly formed branches AspB-GFP localized as a cap (Figure 2.4J, 2.4L, 2.4M, 2.4O, 2.4Q and 2.4T) or single bright dot at branch tips (Figure 2.4L). AspB-GFP bars and/or filaments were also seen in mature branches. A low level of cytoplasmic AspB-GFP was also seen in all developmental stages. This cytoplasmic signal was excluded from nuclei and the extreme apices (~0.5μm) of hyphae and branches.

During conidiogenesis, we observed AspB-GFP localization to several conidiophore layers by confocal microscopy (Figure 2.5). Figure 2.5A shows a single hypha with several intermediates in conidiophore development. AspB bars and filaments were observed in the main hypha and in foot cells at the base of the aerial hypha. In aerial hyphae with developing vesicles at the tips AspB-GFP localized as a cap. In swollen vesicles AspB-GFP localized as a diffuse

cap. In budding layers AspB-GFP localized as rings at the base of emerging layers and disappeared once the layer was complete (Figure 2.5B). AspB-GFP remained localized to the phialide-conidium interface where there is constant nuclear division as conidia are continuously made (reviewed by (TIMBERLAKE 1990)). AspB-GFP bars were observed in conidia both on the conidial chain and free (Figure 2.5C-D). In free conidia, the ends of some AspB-GFP bars appeared to be frayed, giving the impression of unraveling (Figure 2.5D).

AspB-GFP bars and filaments show dynamic movement

Septins have been reported to be dynamic, changing conformational arrangements, with subunits being recycled from one structure to another through development (CID *et al.* 2001; GLADFELTER *et al.* 2001b; KINOSHITA 2006; LONGTINE and BI 2003). To determine whether AspB-GFP bars show dynamic movement in *A. nidulans*, we used time lapse fluorescence microscopy. During isotropic growth and early germ tube emergence, AspB-GFP bars moved freely throughout the conidium and/or bounced back and forth from the tip of germ tubes. In addition, many bars seemed to have one end anchored in the region of the membrane, while the other end moved in and out of the plane of focus. For example, Figure 2.6A shows a bar that appeared to have one end anchored and one end oscillating back and forth (Figure 2.6A, time frames 2-7). Eventually, both ends began to move freely followed by an apparent break into two pieces that moved independently in and out of the plane of focus (Figure 2.6A, time frames 10-27). In contrast to the rapid large scale movements of AspB bars in cells with young germ tubes, AspB filaments in longer hyphae showed more restricted movement. Figure 2.6B shows the slower gradual movement in and out of the plane of focus of a long filament that extends through the hypha into the branch tip (Figure 2.6B).

AspB rings, bars and filaments are lost in the absence of other septins

We recently showed that in *Aspergillus nidulans* septins AspA and AspC interact as AspA-GFP forms abnormal structures in *ΔaspC* strains, while AspC-GFP does not localize in *ΔaspA* strains (LINDSEY *et al.* 2010a). To determine whether AspB interacts with other septins we crossed the *aspB-gfp* strain to *ΔaspA*, *ΔaspC*, *ΔaspA ΔaspC*, *ΔaspD* and *ΔaspE* strains and selected progeny carrying *aspB-gfp* and the appropriate septin deletion. Progeny were checked by PCR to verify the *aspB-gfp* cassette was present and the appropriate septin was deleted. Strains were characterized throughout vegetative growth and asexual reproduction. AspB-GFP rings, bars and filaments were lost in all stages of development and reproduction in *ΔaspA*, *ΔaspC* and *ΔaspA ΔaspC* strains with only cytoplasmic localization in 100% of the population (Figure 2.7IB-II, Figure2. 8B, and data not shown). In the *ΔaspD* strain AspB-GFP bars were present only half as often as in wild type, while filaments were only slightly reduced (Figure 2.7IC-II). AspB-GFP localization to septa and conidiophores seemed normal in *ΔaspD* (Figure 2.7IC and Figure 2.8C). Interestingly, AspB-GFP bars, rings and filaments were present through early germ tube emergence of *ΔaspE*, but localization was mostly as dots and/or X's in older hyphae (Figure2. 7ID-II). AspB-GFP localization to septa and conidiophores appeared to be normal in *ΔaspE* (Figure 2.7ID and Figure 2.8D).

Discussion

***aspB* affects the emergence of new growth foci**

Septins display a variety of functions and their essentiality varies (CAO *et al.* 2009; GILDEN and KRUMMEL 2010; GLADFELTER 2010; OH and BI 2011). *Aspergillus nidulans* has 5 septins (AspA-E) and we have previously shown that septins *aspA* and *aspC* are not essential (LINDSEY *et al.* 2010a). We also previously reported that *aspB* was essential (MOMANY and HAMER 1996),

but using new gene deletion techniques we isolated viable *ΔaspB* mutants. A possible reason that *ΔaspB* was not recovered from our initial screen is that our strategy for isolation depended on conidiating colony sectors and, as we show here, *ΔaspB* strains make few conidia.

In *S. cerevisiae*, septins are required for proper bud emergence and morphology and septin mutants fail to complete cytokinesis (HARTWELL *et al.* 1974). In *A. nidulans,* cells do not separate at cytokinesis, but septa partition the organism into unique compartments and septation is coordinated with nuclear division (CLUTTERBUCK 1970; HARRIS *et al.* 1994; MOMANY and HAMER 1997a; WOLKOW *et al.* 1996). Septation gives rise to actively growing tips and non growing subapical compartments. These compartments remain arrested in interphase until branch initiation (DYNESEN and NIELSEN 2003; FIDDY and TRINCI 1976). Surprisingly, *ΔaspB* did not abolish septation but delayed it. Therefore, AspB might play a role in septation timing rather than septum formation. The more rapid loss of Calcoflour label in Δ*aspB* septa versus wild type septa suggests that AspB might be important for septum organization, though careful ultrastructural studies will be needed to clarify this point.

In *S. cerevisiae*, septins have been shown to be regulated by the cell cycle (GLADFELTER *et al.* 2005b; LEW 2003). In addition, septin interactions with microtubules and kinetochore proteins in mammals suggest roles in nuclear division (SPILIOTIS and NELSON 2006; SURKA *et al.* 2002). In *S. cerevisiae* septin mutants continue nuclear division forming multinucleated buds. Interestingly, *ΔaspA*, *ΔaspB* and *ΔaspC* showed both normal uninucleate conidia and abnormal binucleate conidia (Figure 2.1 and Supp. Figure 2.1), suggesting that loss of these septins might cause defects in nuclear division and/or migration at the conidium-phialide interface. In addition, *ΔaspB* and *ΔaspC* might also cause defects in nuclear migration in hyphae as clustered nuclei

were sometimes observed at later stages of growth (Figure 2.3 and Supp. Figure 2.1) (SPILIOTIS *et al.* 2005; XIANG *et al.* 1994).

In *S. cerevisiae,* septin mutations result in an aberrant bud emergence pattern and chains of elongated buds, but multiple buds do not emerge simultaneously (GLADFELTER *et al.* 2005b; HARTWELL 1971a). Upon deletion of *aspB* in *A. nidulans*, we observed the emergence of extra growth foci in the form of germ tubes and branches suggesting a role in selecting new growth sites similar to septin involvement in bud site selection in *S. cerevisiae* (Figures 2.1 and 2.2) (GLADFELTER *et al.* 2005a). However since yeast septin mutants don't display the simultaneous emergence of multiple buds, AspB appears to have a role in suppressing new growth foci not seen in *S. cerevisiae*. Alternatively, AspB may be involved in selecting the emergence of a single growth zone and/or might work with the polarity machinery to control growth emergence.

AspB forms bars and filaments throughout vegetative growth and sporulation

Septins in vegetatively growing fungi have been shown to mainly form dots, rings, collars or caps. More recently septin bars and filaments that resemble animal septins have been reported in limited developmental stages of some fungi (DEMAY *et al.* 2009; GLADFELTER 2010; JUVVADI *et al.* 2011; KOZUBOWSKI and HEITMAN 2009; LINDSEY *et al.* 2010a; LINDSEY *et al.* 2010c; MARTIN *et al.* 2005; PABLO-HERNANDO *et al.* 2008). Here we report that the *A. nidulans* AspB septin localizes as rings, bars and filaments throughout vegetative growth.

Septins in a variety of systems have been shown to be dynamic (CID *et al.* 2001; GLADFELTER *et al.* 2001b; KINOSHITA 2006; LONGTINE and BI 2003). In *S. cerevisiae*, septins at the mother bud neck change conformation throughout budding, shifting from a ring to a collar and then dividing at cytokinesis (CID *et al.* 2001; GLADFELTER *et al.* 2001b; KINOSHITA 2006; LONGTINE and BI 2003). In this study we observed that *A. nidulans* new growth emerged through

AspB collars during the formation of germ tubes, branches and conidiophore layers, processes that are morphologically quite similar to budding in yeast. An AspB ring that divided into two rings was seen at forming septa, a process that is morphologically similar to cytokinesis in yeast.

In addition to the yeast-like collars and rings, we also observed AspB rods and filaments, structures that are much more like septins in animal cells. In freshly harvested dormant conidia of *A. nidulans* we observed AspB bars mostly in the center of the cell and/or near the cell periphery. The presence of this bar in dormant spores shows that the septin filament is assembled before breaking of dormancy and growth initiation. The deletion of *aspB* resulted in the emergence of multiple germ tubes suggesting that in wildtype conidia, the AspB bar might suppress the emergence of extra growth foci.

In *A. nidulans*, as germ tubes emerged and hyphal tips elongated, AspB localized as caps to polar tips and formed thick bars and thinner filaments within the hyphae. Bars showed rapid oscillating movements and filaments showed slow waving movements. AspB bars and filaments were frequently found in the same compartment before septation, and occasionally before branch initiation and in mature branches. Interestingly, in older hyphae AspB bars mainly remained in quiescent subapical regions while AspB filaments were observed in actively growing areas including branching compartments and emerging branches. We only rarely observed bars and filaments within the same compartment of older hyphae. Similarly during conidiophore formation, AspB bars were only seen in the quiescent regions where layers were not actively budding. The presence of septin bars in dormant conidia and quiescent regions of hyphae and conidiophores is consistent with bars playing a role in suppressing emergence of new growth foci.

AspB interacts with AspA and AspC throughout vegetative growth and sporulation and with AspE in extending hyphae

Septins have been shown to interact and colocalize forming complexes and heteropolymers that regulate different aspects of cell dynamics, which can be abolished or perturbed in the absence of one or more of the septin members (CAO *et al.* 2009; LONGTINE *et al.* 1996; MCMURRAY *et al.* 2011). Generally, septin-septin interactions are key for function and septin heteroligomers are seen in all models studied to date (CAO *et al.* 2009; KREMER 2008; MCMURRAY 2008). AspB rings, bars and filaments were lost in the absence of AspA or AspC suggesting that these three septins interact in a variety of septin morphologies. In contrast, AspB localization was only slightly affected by the loss of AspD, suggesting that either AspD does not interact directly with AspB or that, if these interactions exist, they are not necessary for the formation of rings, bars and filaments. In the absence of AspE, AspB localization was similar to wild type in dormant conidia, early germ tubes and conidiophores. Interestingly in elongating hyphae, AspB bars and filaments were lost suggesting that AspE might maintain septin bar and filament stability in highly polar cells (PAN *et al.* 2007a). This is especially interesting because AspE belongs to a septin family found exclusively in fungi that grow by highly polar tip extension, the filamentous fungi.

Acknowledgments

This work was supported by the UGA Graduate Recruitment Opportunity Fellowship (GRO), Robert Watkins American Society of Microbiology Fellowship, Plant Biology Palfrey Grant, and Dissertation Completion Grant from the University of Georgia to Yainitza Rodriguez; by the NSF grant MCB 0211787 to Michelle Momany and the Office of the Vice President for

Research at the University of Georgia. We thank Rebecca Lindsey for the construction of the *aspB::aspB-gfp* and *aspB:AfpyrG* strains.

Tables and Figures

Table 2.1: Strains and plasmids used

Strain/plasmid	Genotype	Reference
pFNO3	*ga5-gfp, AfpyrG, kan*	(YANG *et al.* 2004)
A1145 (TN02A7)	*pyrG89; pyroA4;nkuA::argB; riboB2*	(YANG *et al.* 2004)
A1147 (TNO2A25)	*pyrG89; argB2; pabaB22nku::argB; riboB2*	(YANG *et al.* 2004)
A850	*biA1;_argB::trpC_B;methG1; veA1; trpC801*	FGSC
A773	*pyrG89;wA3;pyroA4*	FGSC
ARL115	*pyrG89, aspB::aspB-gfp- AfpyrG; argB2; pabaB22; nku::argB; riboB2*	This study
ARL144	*pyrG89, aspB:AfpyrG; pyroA4;nkuA::argB; riboB2*	This study
ARL157	*aspC::AfpyrG; pyrG89; pyroA4*	(LINDSEY *et al.* 2010b)
ARL162	*aspC::AfpyrG; aspA::argB2; pyrG89; pyroA4; biA1_argB::trpC_B; veA1; trpC801*	(LINDSEY *et al.* 2010b)
AYR1	*pyrG89, aspB:: AfpyrG; pyroA4; riboB2*	This study
AYR6	*pyrG89, aspB::aspB-gfp- AfpyrG; argB2*	This study
AYR10	*aspB::aspB-gfp- AfpyrG*\\	This study
AYR20	*aspB::aspB-gfp- AfpyrG; aspA:: argB2*	This study
AYR21	*aspB::aspB-gfp- AfpyrG; aspA:: argB2*	This study
AYR22	*aspB::aspB-gfp- AfpyrG; aspA:: argB2*	This study
AYR23	*aspB::aspB-gfp- AfpyrG; aspC::AfpyrG*	This study
AYR24	*aspB::aspB-gfp- AfpyrG; aspC::AfpyrG*	This study
AYR25	*aspB::aspB-gfp- AfpyrG ; aspC::AfpyrG*; *aspA:: argB2*	This study
AYR26	*aspB::aspB-gfp- AfpyrG; aspE::AfpyrG*	This study
AYR27	*aspB::aspB-gfp- AfpyrG; aspE::AfpyrG*	This study
AYR32	*aspB:: AfpyrG; pyroA4; argB2*	This study
AYR35	*aspB::aspB-gfp- AfpyrG; pyroA4*	This study
AYR45	*aspB::aspB-gfp- AfpyrG; nkuA::argB; aspD::Afpyr*	This study
AYR50	*An-H1-chRFP::pyroAAf; aspB::aspB-gfp- AfpyrG*	This study
AYR64	*aspB::aspB-gfp- AfpyrG; pyroA4; aspD::pyrGAf*	This study
AYR65	*aspB::aspB-gfp- AfpyrG; pyroA4; aspD::pyrGAf*	This study
ASH26	*aspA::argB2, pyrG89, wa3,* argB::*trpC_B methG1, pyroA4*	(LINDSEY *et al.* 2010b)
ASH41	*aspE::AfpyrG; riboB2*	This study

[a] The symbol \\ indicates haploids fused to make diploid strain.

Table 2.2: Primers for constructing *aspB-gfp* and *ΔaspB*

Primers for GFP Tag	**Sequence**
AspB-GSP1	CAGAAGGTGCAACCTGTTCAGGGGAACTTAC
AspB-GSP2	ACGAAGAGAGAATCCCTTCCTCTTTCCCTTTTC
AspB-GFP1	GGAAAGAGGAAGGGATTCTCTCTTCGTGGAGCTGGTGCAGGCG CTG
AspB-GFP2	CGGGGTTTCCGACTAAGCGTCTGTCTGTCTGAGAGGAGGCACTG ATGCG
AspB-GSP3	ACAGACGCTTAGTCGGAAACCCCGACGGTC
AspB-GSP4	GATACTGAACGTTCTCATCGCCCGCAAGC
AspB-SSP3	GCGTCGATGCTAAGAATTAGCTTCCC
AspB-SSP4	CGAGATCCATGCTAGCGTCATAGTAC
Primers for aspB deletion	**Sequence**
AspB-Up-F	CTGTTCAATTGGATACTGCCGAG
AspB-Up-R	GAAGATGGAGTCAGCAGCTGTATAGG
AspB pyrG1	GCCTATACAGCTGCTGACTCCATCTTCTGCCTCAAACAATGCTCT TCACCCTC
AspB pyrG2	GTGGAGAATCAAACGTAGAAGTTCCAATAAGTGTCTGAGAGGA GGCACTGATGCG
AspB-Down-F	CTTCTACGTTTGATTCTCCACG
AspB-Down-R	CTACAGGATGACACCCAGTCAG
AspBKOck-up	GGTCATTCCTGGTGTGACAGTACC
pyrgAFcheck Rv	CAGAGCCCACAGAGCGCCTTGAG

Figure 2.1. *aspB* is required for normal growth and morphology. (A) *ΔaspB* forms uninucleate and binucleate spores. Dormant spores from wt, *aspB-gfp* and *ΔaspB* were stained with Hoescht 33342 and the number of nuclei were counted. n=200. (B) *ΔaspB* breaks dormancy earlier than wild type. Spores were incubated for 4hrs at 30°C and categorized as dormant (~2.5µm), isotropic (~5µm) and polar (presence of a germ tube). n=200. (C) *ΔaspB* forms multiple germ tubes. Spores were incubated for 6hrs at 30°C and the number of germ tubes were counted. n=300. (D) *ΔaspB* delays septation. Spores were incubated for 11hrs at 30°C and the number of septa were counted. n=200. (E) *ΔaspB* hyperbranches. Spores were incubated for 14hrs at 30°C and the number of branches per compartment delineated by 2 septa were counted. n=200. (F) *ΔaspB* forms abnormal coniodiophores. Spores were incubated in agar between coverslips for 2 days at 30°C. Conidiophores were categorized as normal if all layers were present and abnormal if layers were absent or aberrant. n=200.

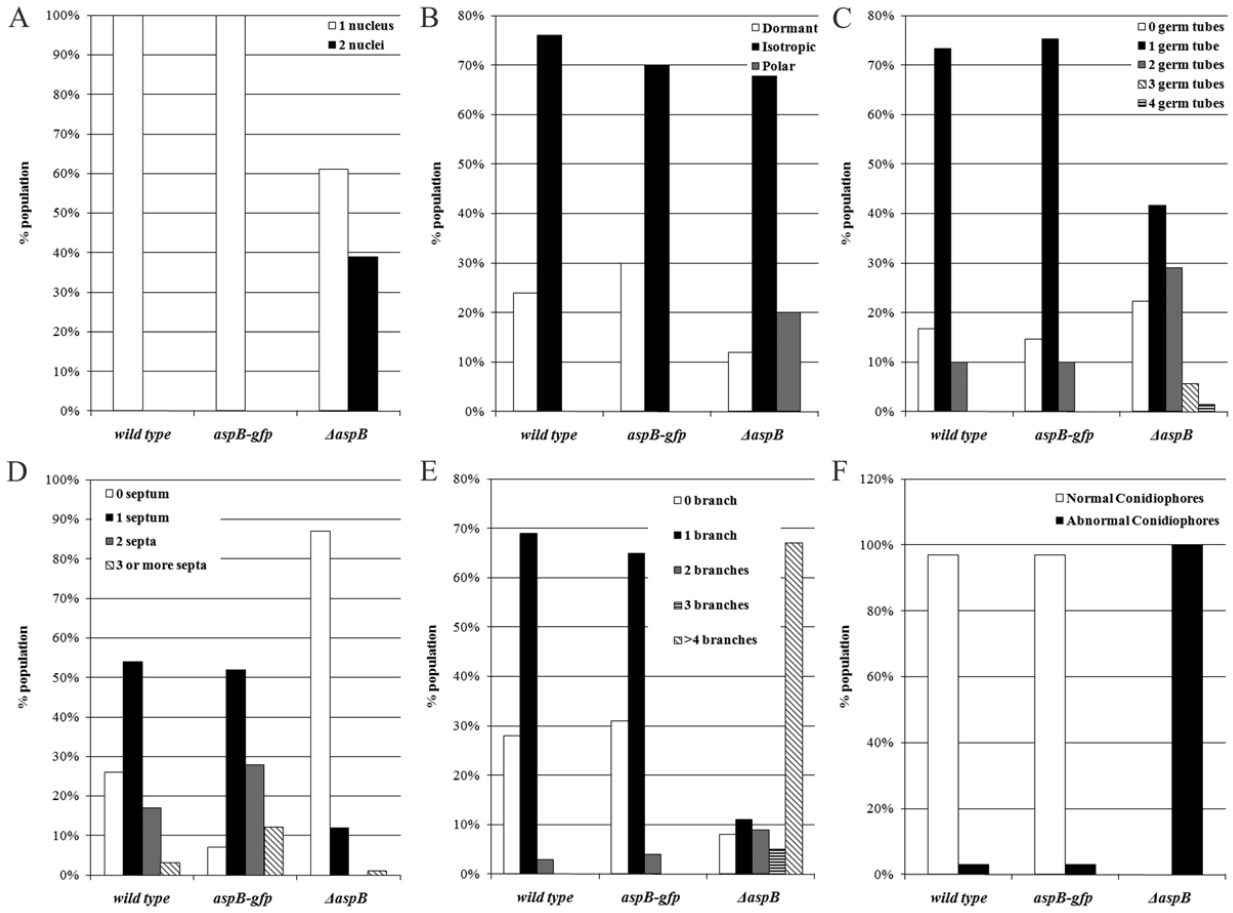
A
100%
90%
80%
70%
60%
50%
40%
30%
20%
10%
0%
% population
1 nucleus
2 nuclei
wild type
aspB-gfp
ΔaspB
B
80%
70%
60%
50%
40%
30%
20%
10%
0%
% population
Dormant
Isotropic
Polar
wild type
aspB-gfp
ΔaspB
C
80%
70%
60%
50%
40%
30%
20%
10%
0%
% population
0 germ tubes
1 germ tube
2 germ tubes
3 germ tubes
4 germ tubes
wild type
aspB-gfp
ΔaspB
D
100%
90%
80%
70%
60%
50%
40%
30%
20%
10%
0%
% population
0 septum
1 septum
2 septa
3 or more septa
wild type
aspB-gfp
ΔaspB
E
80%
70%
60%
50%
40%
30%
20%
10%
0%
% population
0 branch
1 branch
2 branches
3 branches
>4 branches
wild type
aspB-gfp
ΔaspB
F
120%
100%
80%
60%
40%
20%
0%
% population
Normal Conidiophores
Abnormal Conidiophores
wild type
aspB-gfp
ΔaspB

Figure 2.2. *ΔaspB* shows hyperemergence of growth and abnormal conidiophores. (A) *ΔaspB* forms multiple germ tubes, while wild type forms 1 germ tube. (B) *ΔaspB* forms multiple abnormal and stunted branches per compartment, while wild type forms 1 branch per compartment. (C) *ΔaspB* forms disorganized conidiophores. Arrow denotes new aerial hypha arising from vesicle. Wild type forms many conidia and conidiophores are organized with different layers (V-vesicle, P-phialide, M-metulae, Cc-conidia chain). Conditions for growth as in Figure 2.1. Scale bar is 5μm.

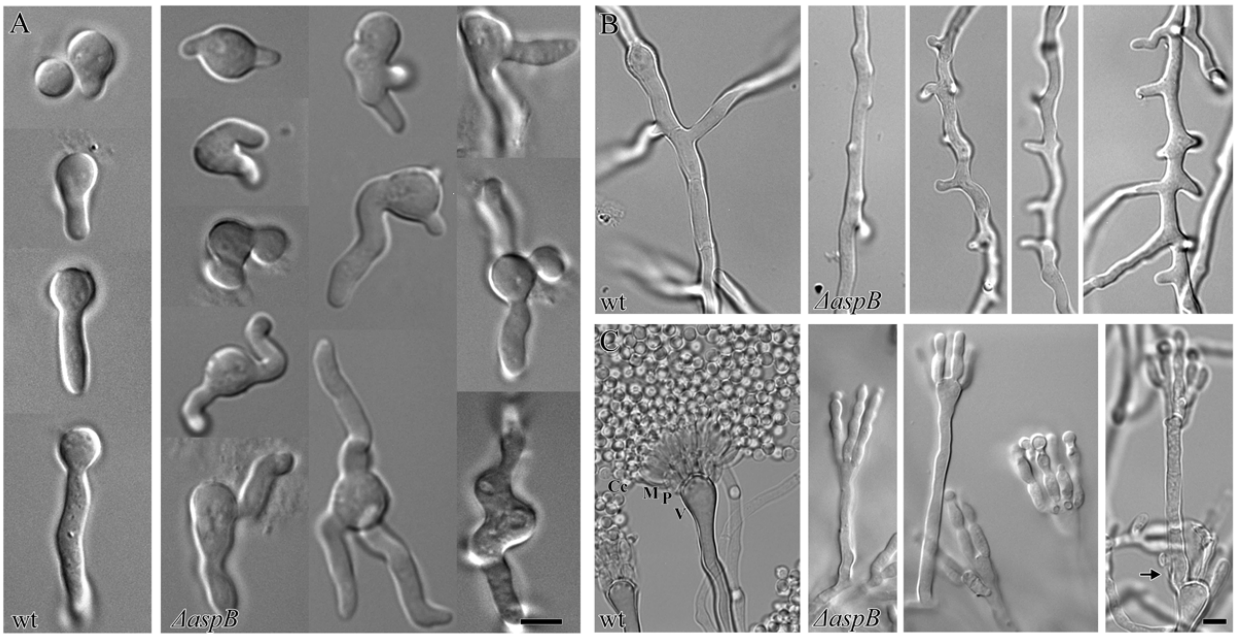
A
wt
ΔaspB
B
wt
ΔaspB
C
Ce
M
P
wt
ΔaspB

Figure 2.3. *ΔaspB* shows clumped nuclei. (A) Wild type nuclei positioned along hyphae. (B) *ΔaspB* results in clumped nuclei, particularly near branches. (C) *ΔaspB* shows clumped nuclei: *ΔaspB* showed more nuclei in 15µm around the most basal branch than wild type. To delineate the area for nuclear counts, the most basal branch was identified, 7.5µm from the center of the branch to the left and right of the branch was measured (total area = 15µm). n=200. Spores were incubated for 14-16hrs at 30°C and nuclei were stained with Hoechst 33258. Scale bar 5µm.

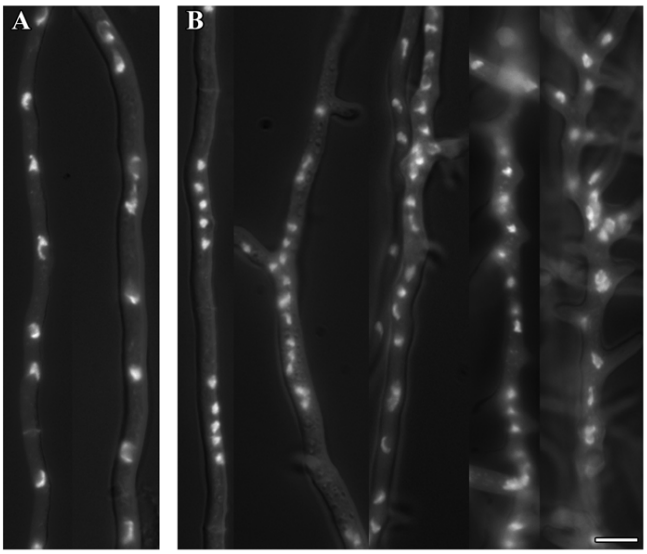
A
B

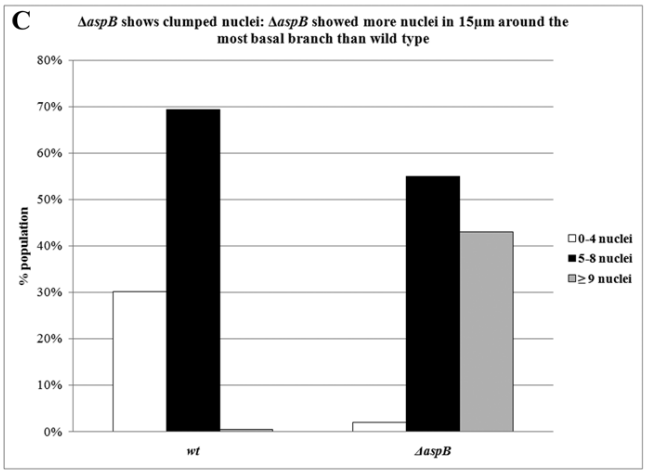
C
ΔaspB shows clumped nuclei: ΔaspB showed more nuclei in 15µm around the most basal branch than wild type
80%
70%
60%
50%
40%
30%
20%
10%
0%
% population
wt
ΔaspB
0-4 nuclei
5-8 nuclei
≥ 9 nuclei

Figure 2.4. AspB forms bars and filaments. (A) AspB forms bars (*), rings (^) and dots (arrow head) in dormant and germinating spores. Inset shows enlarged view of a ring, scale bar is 0.5µm. (B-D) AspB forms "X's" (#) in addition to bars, rings and dots as conidia swell. Inset shows enlarged view of an "X", scale bar is 0.75µm. AspB forms caps and collars as the germtube emerges, bars that localize to conidia and filaments (arrows) that localize to tips. (E-G) AspB forms bars that localize subapically and filaments that localize to tips as the hypha extends. Cytoplasmic gfp fluorescence is excluded from nuclei (N). (H) AspB forms rings at septa. (I-R) AspB forms filaments in branching compartments, caps as the branch emerges and dots at the tip of branches. Filaments localize to newly formed branches. (S) Filaments and bars localize to longer branches. (T) Top view of a branch cap. Incubation time points for following AspB-GFP structures at 30°C were as follow: isotropic growth (4-5 hrs), germ tube emergence (6-7 hrs), hyphal elongation and septation (9-11hrs), branching (12-16hrs). Scale bar is 5µm.

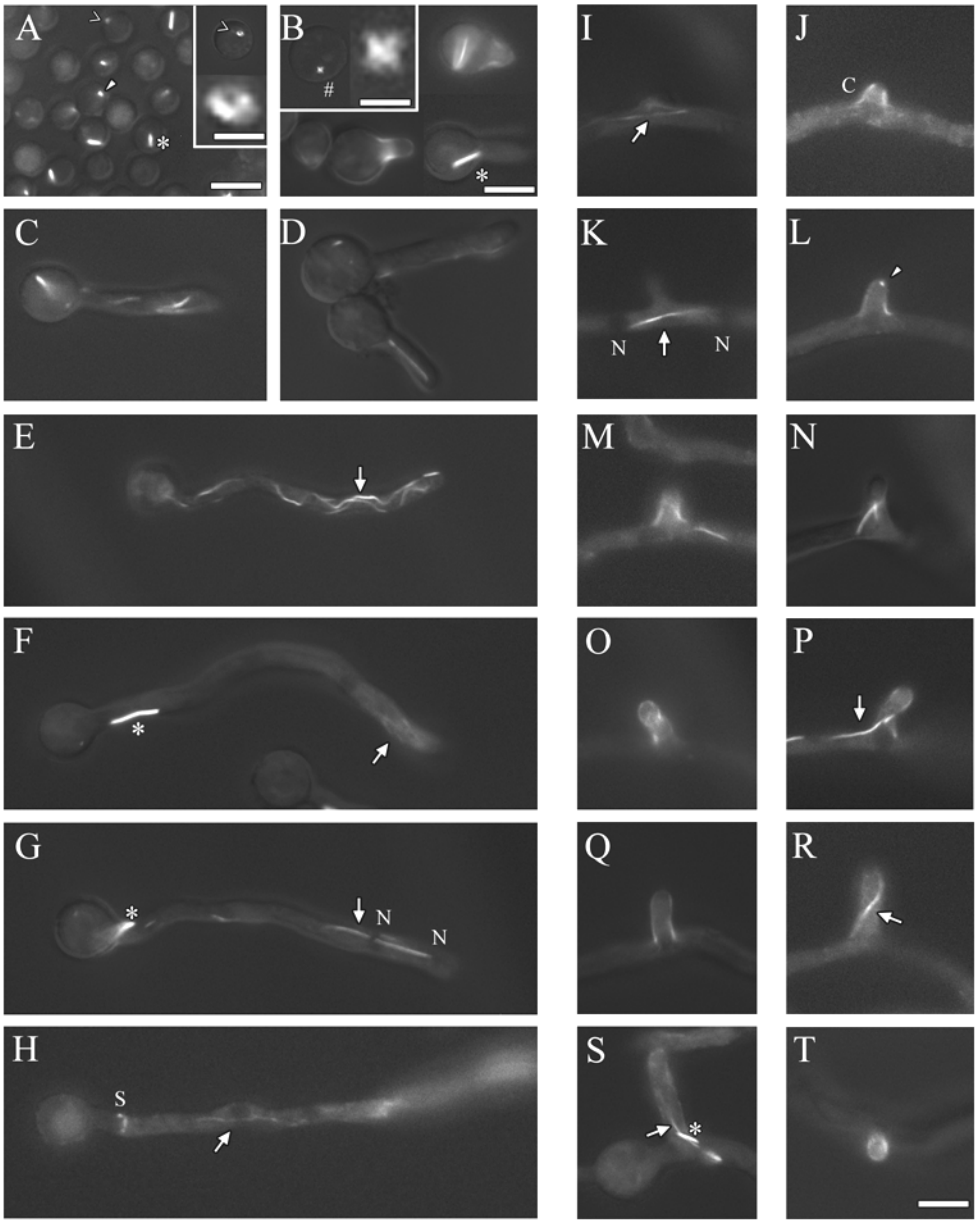
A
B
#
*
I
J
C
D
K
N
N
L
E
M
N
F
*
O
P
G
*
N
N
Q
R
H
S
S
*
T

Figure 2.5. AspB forms bars, filaments, caps and rings during conidiophore formation. (A) AspB-GFP localization at several stages of early conidiophore development. AspB-GFP forms bars (*) and filaments (arrow) in conidiophores stalks. AspB-GFP forms caps (C) in aerial hyphae. AspB-GFP caps are diffuse in swollen vesicles. AspB-GFP forms rings (^) at the base of budding layers. (B) AspB-GFP remains localized at the phialide-conidium interface as conidia form. (C) Conidial chains attached to conidiophores show AspB-GFP localization as dots and bars. (D) AspB-GFP forms bars on conidia freshly detached from conidiophores. Some bars looked "frayed" (X) at the ends. Spores were incubated in agar between coverslips for 1, 2 and 3 days at 30°C. Confocal Microscopy was used. Scale bar is 5μm.

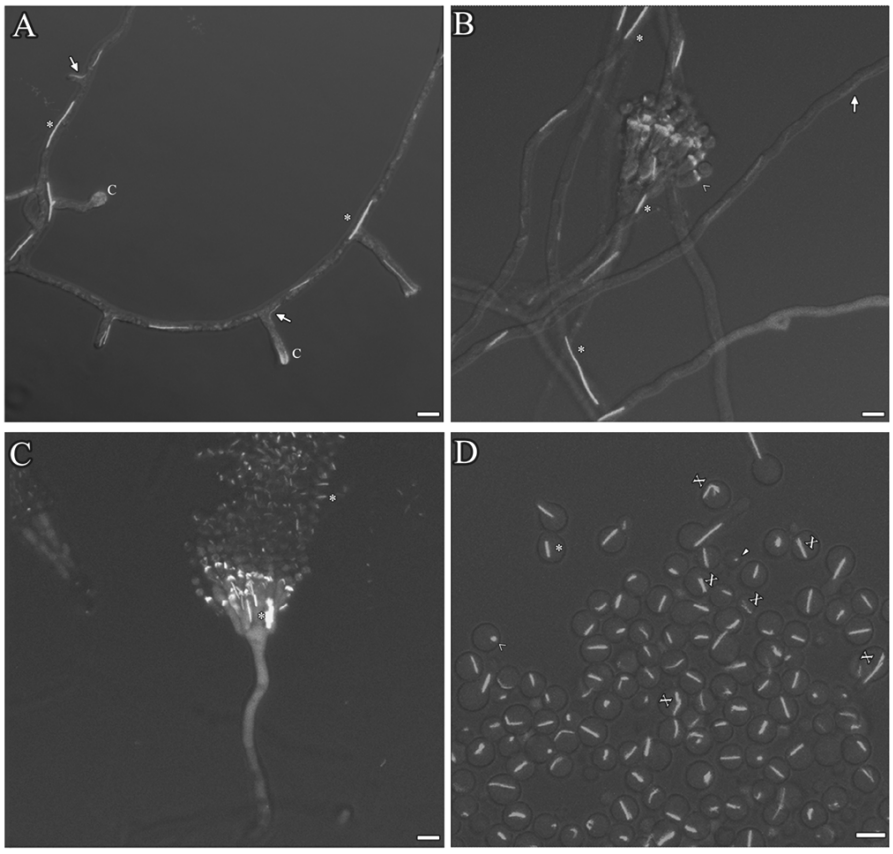
A
B
C
D

Figure 2.6. AspB bars and filaments move. (A) AspB-GFP bar (*) in a germinating conidium moves away from the cell periphery, oscillates in and out of the plane of focus and breaks in two. “Frayed” ends (X) can be observed. (B) AspB-GFP filaments (arrow) show slower movement than bars at hyphal tips. Cytoplasmic gfp fluorescence is excluded from nuclei. Filaments move near nuclei and tips. Time lapse fluorescence microscopy was used. Numbers represents time lapse frame. Frames are 5-10 seconds apart. Conditions for growth as in Figure 2.4. Scale bar is 5μm.

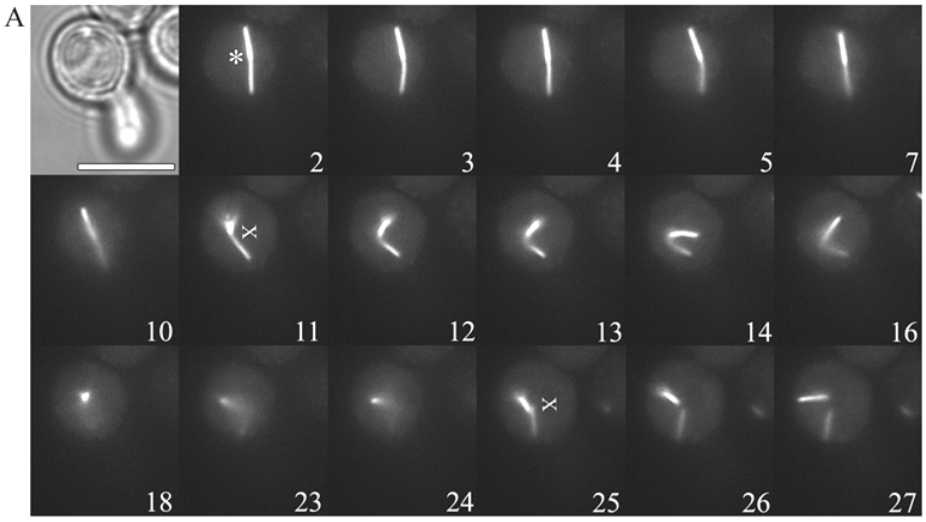
A
*
2
3
4
5
7
10
11
12
13
14
16
18
23
24
25
26
27

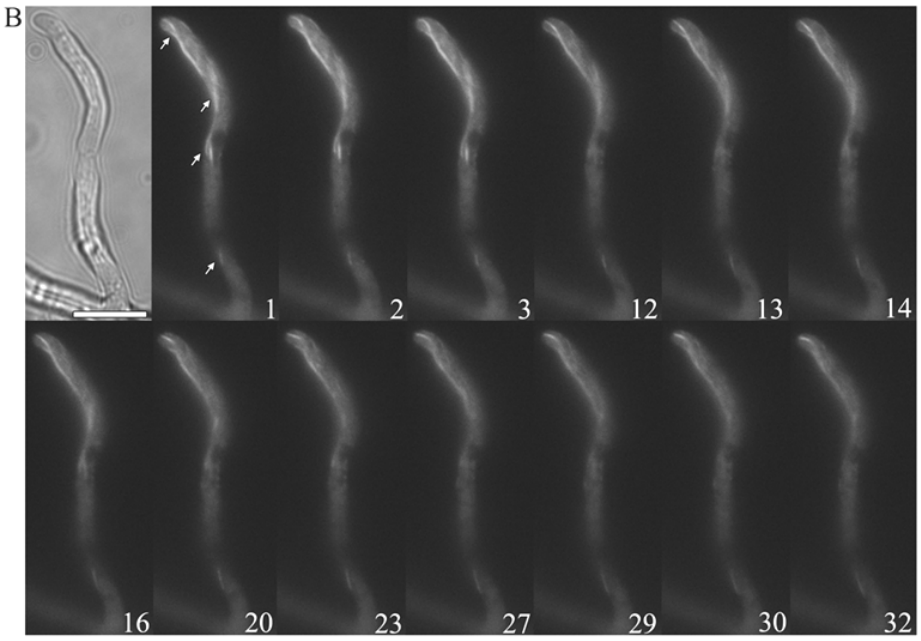
B
1
2
3
12
13
14
16
20
23
27
29
30
32

Figure 2.7. AspB structures are lost in the absence of AspA and AspC and filaments and bars are lost in hyphae in the absence of AspE. (I.) AspB-GFP structures in septin deletion backgrounds. (A) AspB-GFP structures: rings (^), dots (arrow head), bars (*) filaments (arrow) and at septa (S). (B) All AspB-GFP structures are lost in *ΔaspA ΔaspC*. (C) All AspB-GFP structures are found in *ΔaspD* strains. (D) All AspB-GFP structures are found in early *ΔaspE*, but was mostly as dots and/or "X's" in hyphae. Conditions for growth as in Figure 2.4. (II.) AspB-GFP structures found in septin deletion backgrounds. Spores were incubated for 10hrs at 30°C and AspB structures were classified by filament, bar, spots (rings, dots, X's) and cytoplasmic. n=100. In *ΔaspA ΔaspC* AspB-GFP was only found in the cytoplasm and structures as spots, bars and filaments were lost. In *ΔaspD* there was a slight reduction of AspB-GFP bars and filaments. In *ΔaspE* AspB-GFP was mostly localized to spots and the cytoplasm and very few bars and filaments were observed. Scale bar is 5µm.

I.

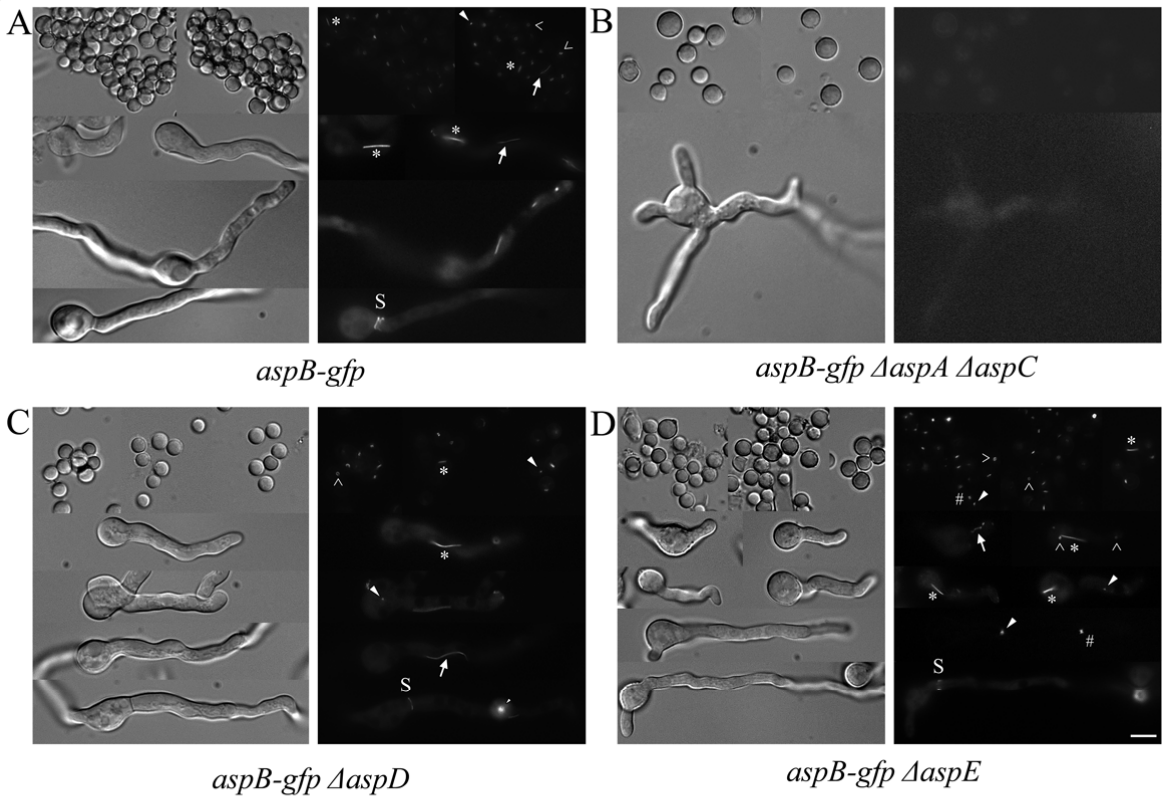
A
B
C
D
S
aspB-gfp
aspB-gfp ΔaspA ΔaspC
aspB-gfp ΔaspD
aspB-gfp ΔaspE

II.

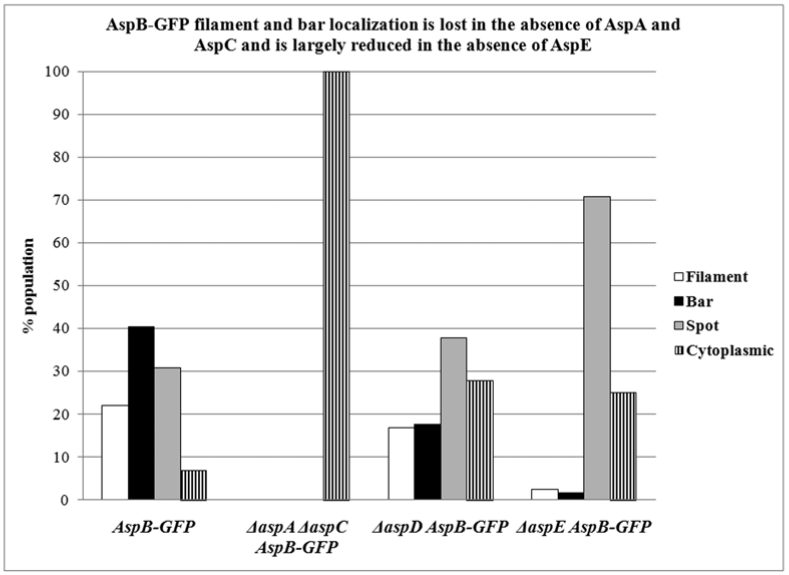
AspB-GFP filament and bar localization is lost in the absence of AspA and AspC and is largely reduced in the absence of AspE
% population
100
90
80
70
60
50
40
30
20
10
0
Filament
Bar
Spot
Cytoplasmic
AspB-GFP
ΔaspA ΔaspC AspB-GFP
ΔaspD AspB-GFP
ΔaspE AspB-GFP

Figure 2.8. AspB bars are lost in conidiophores in the absence of AspA and AspC. (A) AspB-GFP bars (*) in conidiophores. (B) AspB-GFP bars are lost in conidiophores in *ΔaspA ΔaspC*. (C) AspB-GFP bars and dots (arrow head) in *ΔaspD*. (D) AspB-GFP bars and dots in *ΔaspE*. Conditions for growth as in Figure 2.5. Scale bar is 5μm.

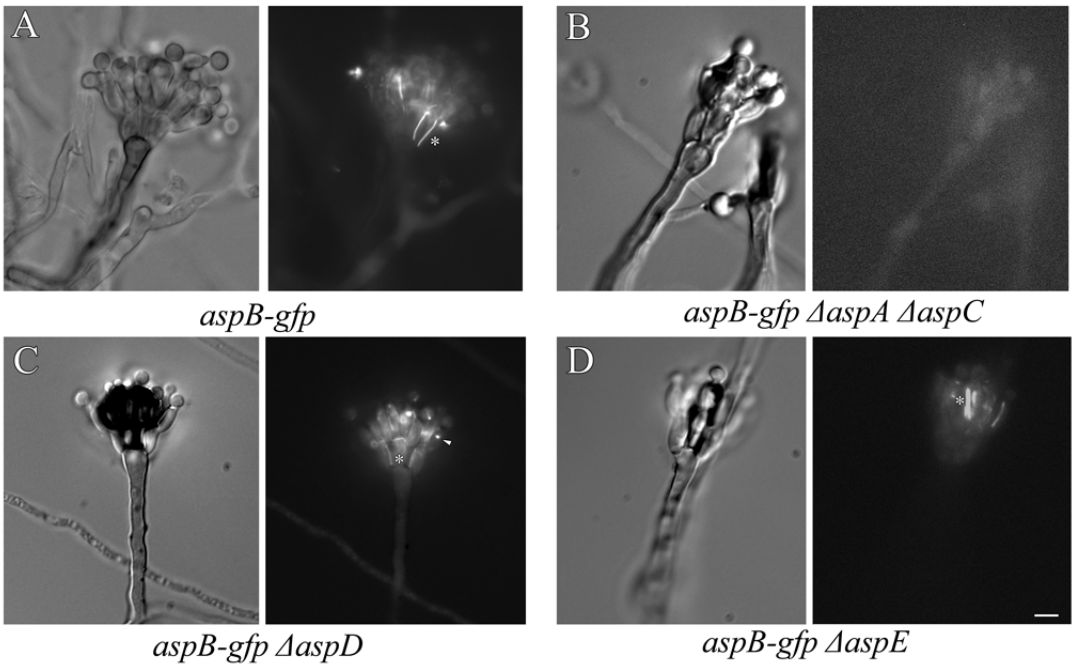

aspB-gfp

aspB-gfp ΔaspA ΔaspC

aspB-gfp ΔaspD

aspB-gfp ΔaspE

Supplemental Figure 2.1. *ΔaspA* and *ΔaspC* show multinucleated conidia and nuclear abnormalities. (I.) *ΔaspA* and *ΔaspC* show multinucleated conidia. Dormant spores from wt, *ΔaspA* and *ΔaspC* where stained with Hoescht 33342 and the number of nuclei were counted. n=100. (II.) *ΔaspA* and *ΔaspC* show nuclear abnormalities. (A) Wild type nuclei positioned along hypha. (B) *ΔaspA* nuclei show a "tail" (arrow). (C) *ΔaspC* shows clumped nuclei. Spores were incubated for 14-16hrs at 30°C and nuclei were stained with Hoechst. Scale bar 5μm.

I.

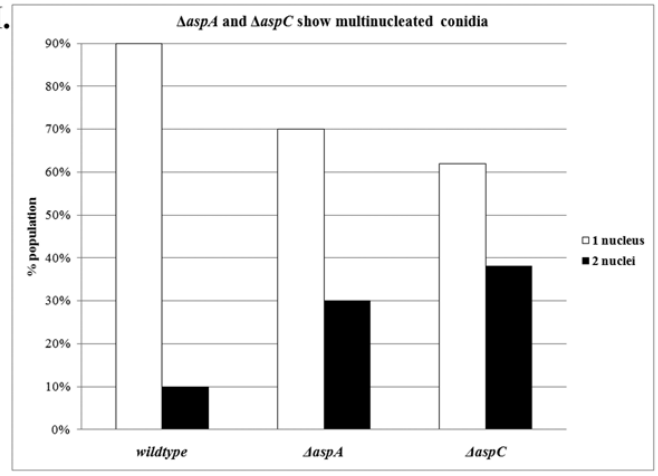
ΔaspA and ΔaspC show multinucleated conidia
90%
80%
70%
60%
50%
40%
30%
20%
10%
0%
% population
1 nucleus
2 nuclei
wildtype
ΔaspA
ΔaspC

II.

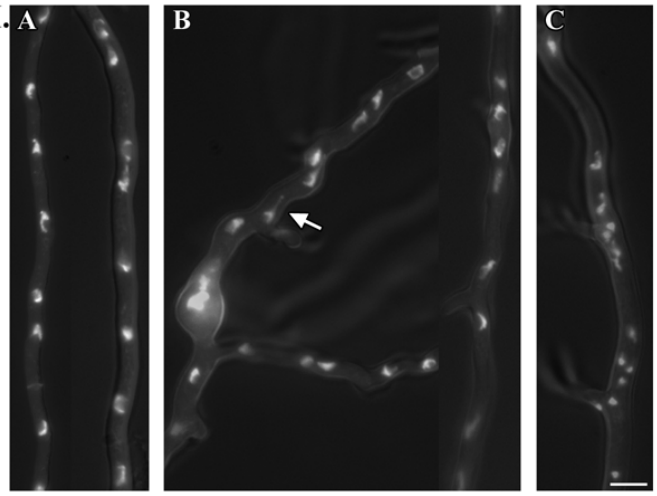
A
B
C

References

AN, H., J. MORRELL, J. JENNINGS, A. LINK and K. GOULD, 2004 Requirements of fission yeast septins for complex formation, localization, and function. Molecular biology of the cell **15:** 5551-5564.

BARRAL, Y., 2009 Yeast septins: a cortical organizer. The Septins**:** 101.

BARRAL, Y., V. MERMALL, M. S. MOOSEKER and M. SNYDER, 2000 Compartmentalization of the cell cortex by septins is required for maintenance of cell polarity in yeast. Mol Cell **5:** 841-851.

BERMAN, J., and P. SUDBERY, 2002 Candida albicans: a molecular revolution built on lessons from budding yeast. Nature Reviews Genetics **3:** 918-932.

BERTIN, A., M. MCMURRAY, P. GROB, S. PARK, G. GARCIA *et al.*, 2008 Saccharomyces cerevisiae septins: Supramolecular organization of heterooligomers and the mechanism of filament assembly. Proceedings of the National Academy of Sciences **105:** 8274.

BÖHMER, C., C. RIPP and M. BÖLKER, 2009 The germinal centre kinase Don3 triggers the dynamic rearrangement of higher-order septin structures during cytokinesis in Ustilago maydis. Molecular microbiology **74:** 1484-1496.

BOYCE, K., H. CHANG, C. D'SOUZA and J. KRONSTAD, 2005 An Ustilago maydis septin is required for filamentous growth in culture and for full symptom development on maize. Eukaryotic Cell **4:** 2044.

BROWN, T., 2001 Analysis of DNA sequences by blotting and hybridization in *Current protocols in molecular biology* Edited by R. B. FREDERICK M. AUSUBEL, ROBERT E. KINGSTON, DAVID D. MOORE, J.G. SEIDMAN, JOHN A SMITH, KEVIN STRUHL. J. Wiley, New York.

CÁNOVAS, D., and J. PÉREZ-MARTÍN, 2009 Sphingolipid biosynthesis is required for polar growth in the dimorphic phytopathogen Ustilago maydis. Fungal genetics and biology **46:** 190-200.

CAO, L., W. YU, Y. WU and L. YU, 2009 The evolution, complex structures and function of septin proteins. Cell Mol Life Sci **66:** 3309-3323.

CARROLL, C., R. ALTMAN, D. SCHIELTZ, J. YATES and D. KELLOGG, 1998 The Septins Are Required for the Mitosis-specific Activation of the Gin4 Kinase, pp. 709-717. Rockefeller Univ Press.

CAVISTON, J. P., M. LONGTINE, J. R. PRINGLE and E. BI, 2003 The role of Cdc42p GTPase-activating proteins in assembly of the septin ring in yeast. Mol Biol Cell **14:** 4051-4066.

CID, V., L. ADAMIKOVA, M. SANCHEZ, M. MOLINA and C. NOMBELA, 2001 Cell cycle control of septin ring dynamics in the budding yeast, pp. 1437-1450. Soc General Microbiol.

CLUTTERBUCK, A., 1970 Synchronous nuclear division and septation in Aspergillus nidulans. Microbiology **60:** 133.

DEMAY, B., R. MESEROLL, P. OCCHIPINTI and A. GLADFELTER, 2009 Regulation of distinct septin rings in a single cell by Elm1p and Gin4p kinases. Molecular Biology of the Cell **20:** 2311.

DOBBELAERE, J., and Y. BARRAL, 2004 Spatial coordination of cytokinetic events by compartmentalization of the cell cortex. Science **305:** 393-396.

DOBBELAERE, J., M. S. GENTRY, R. L. HALLBERG and Y. BARRAL, 2003 Phosphorylation-dependent regulation of septin dynamics during the cell cycle. Dev Cell **4:** 345-357.

DOUGLAS, L. M., F. J. ALVAREZ, C. MCCREARY and J. B. KONOPKA, 2005 Septin function in yeast model systems and pathogenic fungi. Eukaryot Cell **4:** 1503-1512.

DYNESEN, J., and J. NIELSEN, 2003 Branching is coordinated with mitosis in growing hyphae of Aspergillus nidulans. Fungal Genetics and Biology **40:** 15-24.

ESTEY, M. P., M. S. KIM and W. S. TRIMBLE, 2011 Septins. Curr Biol **21:** R384-387.

FIDDY, C., and A. TRINCI, 1976 Mitosis, septation, branching and the duplication cycle in Aspergillus nidulans. J Gen Microbiol **97:** 169-184.

FINGER, F., 2005 Reining in cytokinesis with a septin corral. Bioessays **27:** 5-8.

FORD, S., and J. PRINGLE, 1991 Cellular morphogenesis in the Saccharomyces cerevisiae cell cycle: localization of the CDC11 gene product and the timing of events at the budding site. Dev. Genet **12:** 281-292.

GILDEN, J., and M. F. KRUMMEL, 2010 Control of cortical rigidity by the cytoskeleton: emerging roles for septins. Cytoskeleton (Hoboken) **67:** 477-486.

GLADFELTER, A., 2010 Guides to the final frontier of the cytoskeleton: septins in filamentous fungi. Current Opinion in Microbiology.

GLADFELTER, A., L. KOZUBOWSKI, T. ZYLA and D. LEW, 2005 Interplay between septin organization, cell cycle and cell shape in yeast. Journal of cell science **118:** 1617-1628.

GLADFELTER, A., J. PRINGLE and D. LEW, 2001 The septin cortex at the yeast mother–bud neck. Current Opinion in Microbiology **4:** 681-689.

GLADFELTER, A. S., and P. SUDBERY, 2008 Septins in four model fungal systems: diversity in form amd function, pp. 125-146 in *The Septins*, edited by P. A. HALL, S. E. H. RUSSELL and J. R. PRINGLE. Wiley-Blackwell.

HAARER, B., and J. PRINGLE, 1987 Immunofluorescence localization of the Saccharomyces cerevisiae CDC12 gene product to the vicinity of the 10-nm filaments in the mother-bud neck. Mol Cell Biol **7:** 3678-3687.

HALL, P. A., and F. P. FINGER, 2008 Septin and human disease, pp. 295-317 in *The Septins*, edited by P. A. HALL, H. RUSSELL, S.E. and J. R. PRINGLE. John Wiley & Sons, Ltd, UK.

HARRIS, S., 2001 Genetic analysis of ascomycete fungi, pp. 47-58 in *Molecular and Cellular Biology of Filamentous Fungi*, edited by N. TALBOT. Oxford University press, New York.

HARRIS, S., J. MORRELL and J. HAMER, 1994 Identification and characterization of Aspergillus nidulans mutants defective in cytokinesis. Genetics **136:** 517.

HARTWELL, L., 1971 Genetic control of the cell division cycle in yeast. IV. Genes controlling bud emergence and cytokinesis. Exp Cell Res **69:** 265-276.

HARTWELL, L., J. CULOTTI, J. PRINGLE and B. REID, 1974 Genetic Control of the Cell Division Cycle in Yeast A model to account for the order of cell cycle events is deduced from the phenotypes of yeast mutants. Science **183:** 46-51.

HELFER, H., and A. S. GLADFELTER, 2006 AgSwe1p regulates mitosis in response to morphogenesis and nutrients in multinucleated Ashbya gossypii cells. Mol Biol Cell **17:** 4494-4512.

HU, Q., L. MILENKOVIC, H. JIN, M. P. SCOTT, M. V. NACHURY *et al.*, 2010 A septin diffusion barrier at the base of the primary cilium maintains ciliary membrane protein distribution. Science **329:** 436-439.

IHARA, M., A. KINOSHITA, S. YAMADA, H. TANAKA, A. TANIGAKI *et al.*, 2005 Cortical organization by the septin cytoskeleton is essential for structural and mechanical integrity of mammalian spermatozoa, pp. 343-352.

JUVVADI, P. R., J. R. FORTWENDEL, L. E. ROGG and W. J. STEINBACH, 2011 Differential localization patterns of septins during growth of the human fungal pathogen Aspergillus fumigatus reveal novel functions. Biochem Biophys Res Commun **405:** 238-243.

KAFER, E., 1977 Meiotic and mitotic recombination in Aspergillus and its chromosomal aberrations. Adv Genet **19:** 33-131.

KAMINSKYJ, S. G. W., 2001 Fundamentals of growth, storage, genetics and microscopy of Aspergillus nidulans, pp. in *FUNGAL GENETICS NEWSLETTER #48*. Fungal Genetic Stock Center.

KIM, H., 1991 Cellular morphogenesis in the Saccharomyces cerevisiae cell cycle: localization of the CDC3 gene product and the timing of events at the budding site. J Cell Biol **112:** 535-544.

KINOSHITA, M., 2006 Diversity of septin scaffolds. Curr Opin Cell Biol **18:** 54-60.

KOZUBOWSKI, L., and J. HEITMAN, 2009 Septins enforce morphogenetic events during sexual reproduction and contribute to virulence of Cryptococcus neoformans. Molecular microbiology **75:** 658-675.

KREMER, B. A. M. I. G., 2008 Septin-interacting proteins in mammals, pp. 211-228 in *The Septins*, edited by P. A. HALL, RUSSELL, S.E.H., PRINGLE, J.R. . John Wiley & Sons,Ltd., UK.

KWITNY, S., A. V. KLAUS and G. R. HUNNICUTT, 2010 The annulus of the mouse sperm tail is required to establish a membrane diffusion barrier that is engaged during the late steps of spermiogenesis. Biol Reprod **82:** 669-678.

LEW, D. J., 2003 The morphogenesis checkpoint: how yeast cells watch their figures. Curr Opin Cell Biol **15:** 648-653.

LINDSEY, R., S. COWDEN, Y. HERNANDEZ-RODRIGUEZ and M. MOMANY, 2010 Septins AspA and AspC are important for normal development and limit the emergence of new growth foci in the multicellular fungus Aspergillus nidulans. Eukaryotic Cell **9:** 155.

LINDSEY, R., Y. HA and M. MOMANY, 2010b A septin from the filamentous fungus A. nidulans induces atypical pseudohyphae in the budding yeast S. cerevisiae. PLoS ONE **5:** e9858.

LINDSEY, R., and M. MOMANY, 2006 Septin localization across kingdoms: three themes with variations. Curr Opin Microbiol **9:** 559-565.

LONGTINE, M., and E. BI, 2003 Regulation of septin organization and function in yeast. Trends Cell Biol **13:** 403-409.

LONGTINE, M., D. DEMARINI, M. VALENCIK, O. AL-AWAR, H. FARES *et al.*, 1996 The septins: roles in cytokinesis and other processes. Curr Opin Cell Biol **8:** 106-119.

MARTIN, S., L. DOUGLAS and J. KONOPKA, 2005 Cell cycle dynamics and quorum sensing in Candida albicans chlamydospores are distinct from budding and hyphal growth. Eukaryotic Cell **4:** 1191.

MCMURRAY, M., and J. THORNER, 2008a Septin stability and recycling during dynamic structural transitions in cell division and development. Current Biology **18:** 1203-1208.

MCMURRAY, M., THORNER, J., 2008 Biochemical properties and supramolecular architecture of septin hetero-oligomers and septin filaments, pp. 49-100 in *The Septins*, edited by P. HALL, RUSSELL, H. S.E. AND PRINGLE, J.R. John Wiley & Sons, Ltd., UK.

MCMURRAY, M. A., A. BERTIN, G. GARCIA, 3RD, L. LAM, E. NOGALES *et al.*, 2011 Septin filament formation is essential in budding yeast. Dev Cell **20:** 540-549.

MIMS, C., E. RICHARDSON and W. TIMBERLAKE, 1988 Ultrastructural analysis of conidiophore development in the fungusAspergillus nidulans using freeze-substitution. Protoplasma **144:** 132-141.

MINO, A., K. TANAKA, T. KAMEI, M. UMIKAWA, T. FUJIWARA *et al.*, 1998 Shs1p: A Novel Member of Septin That Interacts with Spa2p, Involved in Polarized Growth inSaccharomyces cerevisiae. Biochemical and Biophysical Research Communications **251:** 732-736.

MOMANY, M., 2001 Cell biology of the duplication cycle in fungi, pp. 120-125 in *Molecular and Cellular Biology of Filamentous Fungi*, edited by N. TALBOT. Oxford University Press, New York.

MOMANY, M., and J. HAMER, 1997a Septation in Aspergillus nidulans. Cell motility and the cytoskeleton **38:** 373-384.

MOMANY, M., and J. E. HAMER, 1996 The Aspergillus nidulans septin encoding gene, aspB, is essential for growth. Fungal Genet Biol **21:** 92-100.

OH, Y., and E. BI, 2011 Septin structure and function in yeast and beyond. Trends Cell Biol **21:** 141-148.

ORLANDO, K., X. SUN, J. ZHANG, T. LU, L. YOKOMIZO *et al.*, 2011 Exo-endocytic trafficking and the septin-based diffusion barrier are required for the maintenance of Cdc42p polarization during budding yeast asymmetric growth. Mol Biol Cell **22:** 624-633.

PABLO-HERNANDO, M. E., Y. ARNAIZ-PITA, H. TACHIKAWA, F. DEL REY, A. M. NEIMAN *et al.*, 2008 Septins localize to microtubules during nutritional limitation in Saccharomyces cerevisiae. BMC Cell Biol **9:** 55.

PAN, F., R. MALMBERG and M. MOMANY, 2007 Analysis of septins across kingdoms reveals orthology and new motifs. BMC Evolutionary Biology **7:** 103.

ROSENBERGER, R., and M. KESSEL, 1967 Synchrony of Nuclear Replication in Individual Hyphae of Aspergillus nidulans. J Bacteriol **94:** 1464-1469.

RUSSELL, S. E. H., and P. A. HALL, 2005 Do septins have a role in cancer?, pp. 499-503.

SCHMIDT, K., and B. J. NICHOLS, 2004 A barrier to lateral diffusion in the cleavage furrow of dividing mammalian cells. Curr Biol **14:** 1002-1006.

SPILIOTIS, E., M. KINOSHITA and W. NELSON, 2005 A mitotic septin scaffold required for Mammalian chromosome congression and segregation, pp. 1781-1785. American Association for the Advancement of Science.

SPILIOTIS, E., and W. NELSON, 2006 Here come the septins: novel polymers that coordinate intracellular functions and organization. Journal of Cell Science **119:** 4.

SUDBERY, P., 2001 The germ tubes of Candida albicans hyphae and pseudohyphae show different patterns of septin ring localization. Molecular Microbiology **41:** 19-31.

SURKA, M., C. TSANG and W. TRIMBLE, 2002 The mammalian septin MSF localizes with microtubules and is required for completion of cytokinesis. Molecular Biology of the Cell **13:** 3532.

SZEWCZYK, E., T. NAYAK, C. OAKLEY, H. EDGERTON, Y. XIONG *et al.*, 2007 Fusion PCR and gene targeting in Aspergillus nidulans.

TADA, T., A. SIMONETTA, M. BATTERTON, M. KINOSHITA, D. EDBAUER *et al.*, 2007 Role of Septin cytoskeleton in spine morphogenesis and dendrite development in neurons. Current Biology **17:** 1752-1758.

TAKIZAWA, P. A., J. L. DERISI, J. E. WILHELM and R. D. VALE, 2000 Plasma membrane compartmentalization in yeast by messenger RNA transport and a septin diffusion barrier. Science **290:** 341-344.

TIMBERLAKE, W., 1990 Molecular Genetics of Aspergillus Development. Annual Reviews in Genetics **24:** 5-36.

TRINCI, A., 1969 A kinetic study of the growth of Aspergillus nidulans and other fungi. J Gen Microbiol **57:** 11-24.

VERSELE, M., and J. THORNER, 2005 Some assembly required: yeast septins provide the instruction manual. Trends Cell Biol **15:** 414-424.

WARENDA, A., and J. KONOPKA, 2002 Septin function in Candida albicans morphogenesis. Molecular biology of the cell **13:** 2732.

WESTFALL, P. J., and M. MOMANY, 2002 Aspergillus nidulans septin AspB plays pre- and postmitotic roles in septum, branch, and conidiophore development. Mol Biol Cell **13:** 110-118.

WOLKOW, T., S. HARRIS and J. HAMER, 1996 Cytokinesis in Aspergillus nidulans is controlled by cell size, nuclear positioning and mitosis. Journal of Cell Science **109:** 2179.

XIANG, X., S. BECKWITH and N. MORRIS, 1994 Cytoplasmic dynein is involved in nuclear migration in Aspergillus nidulans. Proceedings of the National Academy of Sciences **91:** 2100-2104.

XIANG, X., and R. FISCHER, 2004 Nuclear migration and positioning in filamentous fungi. Fungal Genet Biol **41:** 411-419.

YANG, L., L. UKIL, A. OSMANI, F. NAHM, J. DAVIES *et al.*, 2004 Rapid Production of Gene Replacement Constructs and Generation of a Green Fluorescent Protein-Tagged Centromeric Marker in Aspergillus nidulans, pp. Am Soc Microbiol.

YELTON, M., J. HAMER and W. TIMBERLAKE, 1984 Transformation of Aspergillus nidulans by Using a trpC Plasmid. Proceedings of the National Academy of Sciences **81:** 1470-1474.

CHAPTER 3

INTERACTIONS OF THE *ASPERGILLUS NIDULANS* SEPTIN ASPB WITH OTHER CYTOSKELETAL ELEMENTS[1]

[1]Hernández-Rodríguez, Y., Cowden, S., and Momany, M. 2011. To be submitted to Eukaryotic Cell.

Abstract

The cell cytoskeleton plays key roles in vesicle, protein and organelle trafficking as well as cell growth and morphology. The coordination of these roles and modifications to the cell cortex ensure normal growth emergence. Therefore, different cytoskeletons interact to regulate these processes. The polarity machinery travels along the actin and microtubule cytoskeletons by association with motor proteins to reach future growth addition sites. Nevertheless, how these cytoskeletal elements interact and relay proteins, vesicles, and organelles is not clearly understood. Septins have been shown to interact and organize both cytoskeletons and to play roles in cell morphogenesis, division, vesicle trafficking, and form diffusion barriers for growth. It has been suggested that septins might bridge interactions between the actin and the microtubule cytoskeleton. Still, septin interactions with actin and microtubules are not completely understood. Here we explored these connections by studying the septin AspB and its interaction with actin and microtubules in the filamentous fungus *Aspergillus nidulans*. We show that AspB partially colocalizes with microtubules and actin and that these cytoskeletal elements are necessary for normal AspB localization. To further assess interactions of actin and microtubules with AspB, we followed hyperemergence of growth phenotypes in *ΔaspB* in the absence of actin and microtubule filaments. We found that microtubules, but not actin, facilitate hypergrowth emergence in *aspB* deletion mutants. In addition we showed that the tropomyosin TpmA (which blocks access of myosin to actin filaments) is not localized to actin filaments in Δ*aspB* and this mutant displays polarity defects during branch emergence in the absence of actin. Finally we showed that AspB colocalizes with endocytic vesicles (AbpA) and that the endocytic zone is of abnormal size and abnormally positioned in Δ*aspB*. Therefore our studies in *Aspergillus nidulans* suggest that the AspB septin might help stabilize polarity axes by

interacting and/or organizing actin, microtubules and endocytosis, and for that reason actin, microtubules and septins might interact to ensure normal polar growth.

Introduction

Septin heteropolymers form scaffolds that recruit proteins involved in many cellular processes and form diffusion barriers that compartmentalize cells to ensure proper cell division and growth. Septin studies have focused for many years on its role in cytokinesis, however more evidence accumulates that the different septin morphologies, and their interactions within a cell, dictate their vast variety of roles. As cytoskeletal elements, they are involved in cell morphology in fungal and animal cells. Studies in yeast have shown that septin defects arrest growth, can cause mislocalization of cortical markers, affect morphology, cytokinesis and can result in chains of cells (GLADFELTER 2010; GLADFELTER *et al.* 2001; GLADFELTER 2006; GLADFELTER *et al.* 2005; OH and BI 2011). More recently, filamentous fungi lacking individual septins have been shown to display abnormal morphology and growth emergence (ALVAREZ-TABARES and PEREZ-MARTIN 2010; LINDSEY *et al.* 2010a; OH and BI 2011). In animal cells, septins have been shown to also affect growth and morphology as defective expression of septins affected dendrite morphology and promoted actin-containing protrusions (OH and BI 2011; TADA *et al.* 2007; XIE *et al.* 2007).

In mammalian cells, septin filaments localize to membranes and to actin and microtubules in the cytoplasm (KINOSHITA 2006; SPILIOTIS and NELSON 2006; VERSELE and THORNER 2005). Septins can form scaffolds and diffusion barriers, and organize the cytoskeleton to allow morphogenesis and cell division (Oh and Bi 2011). Studies of septin associations and interactions with other cell cytoskeletons are still ongoing. Actin, and some actin binding proteins, interact with septins and show codependence *in vivo* and *in vitro*, still their exact

interaction is not completely clear (KINOSHITA 2003; KINOSHITA 2006; KINOSHITA *et al.* 2002; KINOSHITA *et al.* 1997). Microtubule interactions with septins are less understood, but recent studies point to septins organizing microtubules and controlling associations with modifying enzymes, microtubule binding proteins and motors (SPILIOTIS *et al.* 2008; SPILIOTIS and NELSON 2006; SPILIOTIS 2010). Therefore, septins might regulate microtubule dependent trafficking and growth.

For growth emergence, cells need to find mechanisms to overcome the stability of the cell cortex. Modifications of cortex rigidity can be accomplished by rearranging lipids within the membrane and binding actin, as well as lipid and actin associated proteins. Septins have been implicated in affecting the stability of the cortex, and consequently control growth emergence (Gilden and Krummel 2010). For these roles, septins have been shown to associate to membranes through lipids or associated proteins (BERTIN *et al.* 2008; BERTIN *et al.* 2010; MCMURRAY *et al.* 2011; TANAKA-TAKIGUCHI *et al.* 2009). For instance, SEPT5 in mammals localizes to membranes and negatively regulates vesicle docking which blocks growth emergence (AMIN *et al.* 2008; BEITES *et al.* 2005). Also, septin contacts with lipids can provide a network for actin-cortex interactions (GILDEN and KRUMMEL 2010; TANAKA-TAKIGUCHI *et al.* 2009). In mammals, septin interaction with myosin II has been suggested to also negatively regulate growth emergence (JOO *et al.* 2007). On the other hand, septin interactions with microtubules seem to allow growth emergence as SEPT2 in mammals promotes transport along microtubules and therefore polar growth (SPILIOTIS *et al.* 2008a; SPILIOTIS 2010b).

The actin and microtubule cytoskeletons have been extensively studied for their roles as tracks for vesicle trafficking, which is key for hyphal growth. Still, polar growth requires many machineries to work in unison to achieve this goal (LICHIUS *et al.* 2011). Rapid hyphal growth

requires microtubules and actin patches concentrating at the tip apex and endocytosis, as endocytic mutants can be lethal. In *A. nidulans* microtubules are necessary for rapid hyphal extension, endocytosis is coupled with actin patches at tips and the endocytic protein SlaB is essential (ARAUJO-BAZAN *et al.* 2008; HERVAS-AGUILAR and PENALVA 2010; HORIO and OAKLEY 2005; PENALVA 2010).

The septins, as a more recently discovered cytoskeletal element, have been shown to be important for many cellular roles and it is becoming evident that their interactions with actin and microtubules somehow dictate growth and morphology (LICHIUS *et al.* 2011). It seems that actin, microtubules and septin polymers roles integrate to allow for targeted secretion and trafficking for hyphal growth and morphogenesis (LICHIUS *et al.* 2011). The next step is to understand how all these cytoskeletons communicate. It has been suggested that septins might bridge interactions between actin and microtubules and work as diffusion barriers to ensure that polarity markers, as well as processes that ensure growth, such as endocytosis, remain polarized and localized to areas of new growth (GILDEN and KRUMMEL 2010; LICHIUS *et al.* 2011; SPILIOTIS 2010a). Here we explored this possibility by studying the septin AspB and its interaction with actin, microtubules and endocytic markers in the filamentous fungus *Aspergillus nidulans*. We show that AspB partially colocalizes with microtubules and actin, and that microtubules, but not actin, facilitate hypergrowth emergence in *aspB* deletion mutants. In addition we show that the tropomyosin TpmA (which blocks access of myosin to actin filaments) is not localized to actin filaments in Δ*aspB*. Interestingly, polarity defects are observed in *aspB* deletion mutants in the absence of actin during branch emergence. We also show that AspB localization is abnormal in the absence of actin or microtubule polymers. Finally we show that AspB colocalizes with actin decorated endocytic vesicles (AbpA) and that the endocytic zone is of abnormal size and

abnormally positioned in Δ*aspB*. Therefore our studies suggest that the septin AspB might help organize and/or stabilize actin and microtubules and endocytosis to ensure normal polar growth.

Materials and Methods

Strains and growth conditions

Experiments were carried out using *A. nidulans* strains presented in Table 3.1. Some of these strains have been previously used for other studies, donated by other labs or obtained by genetic crosses. Progeny from crosses were selected by auxotrophic markers of preference (considering future analysis and crosses) and verified by PCR as described in Yang et al. (YANG *et al.* 2004).

Fungal cultures for microscopy, crosses, DNA isolation and strain purification studies were grown in minimal medium (MM) (1 % glucose, nitrate salts, biotin, trace elements and 1% thiamine, pH 6.5) or in complete medium (CM) (1% glucose, 2% peptone, 1% yeast extract, 1% casamino acids, 0.01% vitamins and supplements, nitrate salts solution and trace elements, pH 6.5, 1.8% agar was added for solid medium.) (Kafer 1977). Additional supplements were added depending on strains' auxotrophic markers (i.e. pyridoxine HCl, p-aminobenzoate, riboflavin HCl, arginine and uridine and uracyl (Kaminskyj 2001). Strains were cultured at 30°C.

Microscopy

Culture preparation: Conidia were harvested from agar plates with sterile water. For fungal observation and characterization, 1 x 10^4 or 1 x 10^8 spores were grown in 5 or 10mls of MM or CM liquid in a petri dish containing a glass cover slip, and incubated at 30°C. To stain cell wall and septa, we followed previously published protocols (Momany 2001). Calcofluor Blankophour BDH was used to stain septa and Hoechst 33342 (for dormant conidia) and Hoechst 33258 bis-benzimide were used to stain nuclei. Samples were viewed using a Zeiss Axioplan

microscope with a Plan –NEOFLUAR 100X/1.30 NA oil immersion objective lens, X-cite Fluorescence Illumination System (EXFO), and were digitally photographed using a Zeiss Axiocam MRc CCD (charge-coupled device) camera and software. Photoshop CS3 was used to combine DIC or light images with fluorescence images and for micrograph organization, improve contrast and brightness and/or Hue saturation coloration. Microsoft Excel was used to make graphs and calculate statistics from biological replicates.

Fluorescence microscopy: For *in vivo* fluorescence observations, strains were incubated as described above until the appropriate time point at 30°C, and coverslips with attached fungus were not fixed, but mounted in 8-10µls of liquid medium onto slides. Incubation time points for examining fungal development at 30°C were as follow: isotropic growth (4-5 hrs), germ tube emergence (6-7 hrs), hyphal elongation and septation (9-11hrs), branching (12-16hrs).

Immunofluorescence microscopy: Strains were grown as described above. Coverslips with attached fungus were fixed for 30 minutes in 200mM PIPES, 500mM EGTA, 1M MgSO4, DMSO and 37% Formaldehyde (50ml 200mM PIPES pH 6.7, 10ml 500mM EGTA pH 8.5, 1ml 1M MgSO4, 10 ml DMSO, 20ml 37% Formaldehyde and 9ml ddH_2O), followed by three 10 minute washes with PBS. Coverslips were then transferred to 100µl of the digestive solution on parafilm in a humid chamber for 1hr at room temperature (1.5ml = 0.013g Drisilase, 0.096g Gluconex, 1.5µl Zymolase, 750µl Egg White, 50mM Sodium Citrate until 1.5ml); followed by three 10 minute washes with PBS. Coverslips were then incubated with pre-chilled methanol for 10 minutes at -20°C; followed by two 10 minute washes with PBS. Coverslips were transferred to a blocking solution for 15 minutes (TBST + 5% skim milk), and then washed twice with TBST for 5 minutes. Coverslips were incubated on 100µl of the primary antibody (1:500 TBST) on parafilm in a humid chamber for 1 hour at room temperature (or at 4°C overnight); followed

by four 10 minute washes with TBST. Primary antibodies used: monoclonal mouse anti α-Tubulin clone DM1A (Sigma T-9026), monoclonal mouse anti α-Tubulin Tyrosine (TuB-1A2) (Sigma T9028), monoclonal mouse anti α-actin N350 (Amershan). Coverslips were then incubated on 100µl of the secondary antibody (1:100 TBST) on parafilm in a covered (dark) humid chamber for 1 hour at room temperature, followed by four 10 minute covered (dark) washes with TBST. Secondary antibodies used: Goat α-mouse Dylight 488 and Goat α-mouse Dylight 549 (Jackson ImmunoResearch Inc). Coverslips were then stained for chitin and nuclei and mounted onto slide as previously described (Momany 2001); and stored at 4°C in the dark until viewing.

Depolymerization of actin and microtubules

Strains were grown until the suitable time point in 5mls of medium as described above. Spores were incubated at 30°C for 4hrs for germtube emergence and 8-10hr for branch emergence and cytoskeleton dependence analyses. To determine the concentration of Benomyl to use, depolymerization of microtubules was assessed at different concentrations by following the disappearance of microtubule filaments under Benomyl treatment in the *tubA-gfp* strain (6µg Benomyl/ml of DMSO; 1-1.5hrs). To determine the concentration of Cytochalasin A to use, depolymerization of actin was assessed at different concentrations by following the disappearance of actin filaments under Cytochalasin A treatment (1µg Cytochalasin A/ml of DMSO; 1-1.5hrs) in the TpmA-GFP labeled strain. For cytoskeleton dependence analysis, strains were viewed live (no fixing). For growth emergence phenotype analysis, cells were fixed and stained for chitin and nuclei as previously described (Momany 2001). Calcofluor Blankophour BDH was used to stain septa and Hoechst 33258 bis-benzimide was used to stain nuclei.

Results

AspB-GFP partially colocalizes with microtubules and the UncA kinesin, and depolymerization of microtubules results in abnormal AspB-GFP filaments

In our previous studies we showed that AspB forms filaments and bars reminiscent of mammalian septins and cytoskeletal elements, and *ΔaspB* strains showed clumped nuclei (Hernandez-Rodriguez *et al*. unpublished, (KINOSHITA 2003; KINOSHITA 2006; LINDSEY and MOMANY 2006; SURKA *et al.* 2002). In *Aspergillus nidulans*, nuclear migration and positioning is a coordinated process achieved by microtubules and other protein partners (HELMSTAEDT *et al.* 2008; SUELMANN and FISCHER 2000; VEITH *et al.* 2005; XIANG *et al.* 1994; XIANG and FISCHER 2004; YAMAMOTO and HIRAOKA 2003). To assess if AspB interacts with microtubules, we examined colocalization of AspB-GFP with microtubules. In the absence of alternative functional protein fluorescent tags, we did colocalization studies by using a combination of Immunofluorescence and GFP-based Fluorescence microscopy. Spores were incubated for 12-14hrs at 30°C. To label AspB, we used an *aspB-gfp* tagged strain (AYR35, Table 3.1) and to label microtubules we used mouse α-TubA antibodies and the goat α-mouse Dylight588 on the *aspB-gfp* tagged strain. We found that AspB-GFP partially colocalized with α-TubA labeled microtubules (Figure 3.1). We also observed AspB-GFP localization near Hoechst and H1-mRFP labeled nuclei (Figure 3.1, Figure 3.3 and Supplemental Figure 3.1).

To assess if AspB-GFP structures interact and depend on microtubules, we depolymerized microtubules with Benomyl and examined the effects on AspB-GFP structures. Spores were incubated for 8-10hrs at 30°C followed by Benomyl treatment (6μg Benomyl/ml of DMSO; 1-1.5hrs) and samples were imaged without fixing by Fluorescent microscopy. Depolymerization of microtubules was assessed by following the disappearance of microtubule filaments under

Benomyl treatment in the *tubA-gfp* strain. In the absence of microtubule filaments, AspB-GFP formed crossed or star filaments that seemed to be held by a ring (Figure 3.2). These crossed and star filaments typically had an AspB-GFP ring-like structure near the point where filaments crossed. More than 50% of the population showed AspB-GFP star filaments and more than 30% showed only cytoplasmic AspB-GFP localization (Supplemental Figure 3.2). These data indicates that AspB and microtubules partially colocalize and that microtubules are, for the most part, needed for normal AspB-GFP localization.

Septins in mammalian systems have been shown to partially colocalize with microtubules and some septins preferentially bind a specific population of microtubules for vesicle trafficking (GILDEN and KRUMMEL 2010; KINOSHITA *et al.* 2002; KREMER *et al.* 2005; LINDSEY and MOMANY 2006; SILVERMAN-GAVRILA and SILVERMAN-GAVRILA 2008; SPILIOTIS *et al.* 2008; SPILIOTIS 2010; SURKA *et al.* 2002). Recently it was shown that *A. nidulans* has a special population of tyrosinolated modified microtubules (Tyro-microtubules) (ZEKERT and FISCHER 2009). Because AspB-GFP only partially colocalized with α-TubA, we examined whether AspB has preferential binding to a subset of microtubules. We used a combination of Immunofluorescence and GFP-based Fluorescence microscopy. To label AspB we used the *aspB-gfp* tagged strain and to label Tyro-microtubules we used mouse α-Tyro-TubA antibodies and goat α-mouse Dylight588 on the *aspB-gfp* tagged strain. AspB-GFP partially colocalized with α-Tyro-TubA labeled microtubules (Figure 3.3). Zekert *et al.*, had also shown that the Kinesin motor UncA preferentially bound detyrosinolated microtubules (ZEKERT and FISCHER 2009). Since we only observed partial colocalizaiton of AspB with microtubules and tyrosinolated microtubules, we wondered if AspB could colocalize with UncA and detyrosinolated microtubules. In addition the *ΔuncA* strain showed more branching which was

also seen in *ΔaspB* (Hernandez-Rodriguez *et al.*, unpublished data (ZEKERT and FISCHER 2009)). We constructed doubled label strains carrying *aspB-gfp* and *mrfp-uncA*^{rigor}. Spores were incubated for 6-14hrs at 30°C and live Fluorescence microscopy was used. We found AspB-GFP also partially colocalized with mRFP-UncA^{rigor} (Figure 3.4). To this point we have only been able to observe partial colocalization with microtubules, tyrosinolated microtubules and UncA bound microtubules. Therefore, the AspB-microtubule interaction is still unclear.

In mammals, microtubules seem to somehow organize septins, still their codependence is unclear (SPILIOTIS 2010). To further assess whether AspB interacts with microtubules, we examined TubA-GFP labeled microtubules in the *ΔaspB* background. Spores were incubated for 6-12hrs at 30°C and live Fluorescence microscopy was used. In early germination we didn't find a clear pattern or phenotype of microtubules in *ΔaspB* (data not shown). However, we did observe phenotypes during branch emergence. To quantify the phenotype, we examined newly formed branches (≤5µm) closest to the conidial compartment for presence or absence of microtubule filaments. In wild type, microtubules form bundles that run along the hypha and branches. In newly formed branches, less than 5% of the population in wild type showed no microtubule filaments compared to more than 60% in *ΔaspB* (Figure 3.5). We also observed fewer microtubule bundles along *ΔaspB* hyphae than in wild type (data not shown). These data suggests that AspB might help organize/stabilize microtubules in emerging axes and might explain the abortive branching phenotype observed in *ΔaspB* (Hernandez-Rodriguez *et al.*, unpublished data).

TpmA-GFP is lost from actin filaments in *ΔaspB*

Septins and actin in mammals have been shown to be interdependent and septins use F-actin cables as templates for filament formation (KINOSHITA *et al.* 2002; SCHMIDT and NICHOLS

2004b). To further explore AspB interactions with the cytoskeleton, we examined AspB interactions with actin. To assess this interaction, we first attempted colocalization studies. In the absence of alternative functional protein fluorescent tags we attempted colocalization by using a combination of Immunofluorescence and GFP-based Fluorescence microscopy. Unfortunately partial cell wall digestion, to ensure that AspB-GFP filaments were present, hindered antibody labeling of actin filaments. Therefore, to evaluate AspB interactions with actin, we depolymerized actin with Cytochalasin A and examined the effects on the AspB-GFP structures. Spores were incubated for 8-10hrs at 30°C followed by Cytochalasin A treatment (1µg Cytochalasin A/ml of DMSO; 1-1.5hrs) and samples were imaged without fixing by Fluorescent microscopy. Depolymerization of actin was assessed by following the disappearance of actin filaments under Cytochalasin A treatment in the *tpmA-gfp* strain. Depolymerization of actin resulted in many small AspB-GFP free-floating cytoplasmic rings (Figure 3.6). To further assess if AspB interacts with actin, we used tropomyosin TpmA-GFP to label actin filaments in the *ΔaspB* background. Tropomyosin is an actin filament-stabilizing protein and TpmA-GFP has been shown to localize to septa, tips and actin filaments (PEARSON *et al.* 2004). Spores were incubated for 8-10hrs at 30°C and live Fluorescence microscopy was used. TpmA-GFP localizations to actin filaments and tips are lost in *ΔaspB* and localization to septa is very faint (Figure 3.7). To assess whether actin filaments are present in *ΔaspB*, we crossed a strain carrying *alcA(p)-lifeact-egfp* with *ΔaspB*. Actin filaments were visible in *ΔaspB* (Supplemental Figure 3.3). These data suggests that AspB helps maintain and/or stabilize TpmA localization to actin filaments and that actin filaments help maintain and/or stabilize AspB localization to its structures.

Depolymerization of actin affects AspB-GFP localization and results in polarity defects during branch emergence in *ΔaspB*, and hypergrowth emergence in *ΔaspB* is partially dependent on microtubules but not actin.

Together, colocalization studies, AspB-GFP structures under depolymerization of actin and microtubules, and actin and microtubule phenotypes in *ΔaspB* hint at some kind of interaction between these cytoskeletons and AspB. One of the prominent phenotypes observed in *ΔaspB* is the hyperemergence of germtubes and branches. To further assess interactions of actin and microtubules with AspB, we followed hyperemergence of growth phenotypes in *ΔaspB* in the absence of actin and microtubule filaments. We hypothesize that septins, actin and microtubules work together for normal polar growth and that perhaps septins organize both cytoskeletons. If this is true, then both cytoskeletons are disorganized promoting hyperemergence of growth in *ΔaspB*. Therefore, if the cytoskeletons are depolymerized, then hyperemergence of growth would reduce and growth occur wherever the polarity machinery could access without the aid of mediated-trafficking. To assess these hypotheses, spores were incubated for 4hrs (germtube emergence) and 10hr (branch emergence) at 30°C followed by depolymerization of microtubules or actin. Depolymerization of microtubules was assessed by following the disappearance of microtubule filaments under Benomyl treatment (6µg Benomyl/ml of DMSO; 1-1.5hrs) in the TubA-GFP labeled strain. Depolymerization of actin was assessed by following the disappearance of actin filaments under Cytochalasin A treatment (1µg Cytochalasin A/ml of DMSO; 1-1.5hrs) in the TpmA-GFP labeled strain. Samples were then transferred to fresh pre-warmed medium for recovery. TubA-GFP and TpmA-GFP localizations were recovered after switching to fresh medium (Supplemental Figure 3.4). Recovery lasted until wild type initiated germtube or branch emergence. Then samples were

fixed and stained with Calcofluor for septa and Hoechst for nuclei. We found that depolymerization of microtubules, but not actin, reduced hypergermtube and hyperbranch emergence in *ΔaspB* (Figure 3.8). In the microtubule depolymerization experiments, during germtube emergence, after recovery from the DMSO solvent control, only 2% of wild type showed hypergermtube emergence compared to almost 30% of *ΔaspB*. However, after recovery from microtubule depolymerization with Benomyl, 2% of wild type and *ΔaspB* showed 3 or more germtubes per conidium (hypergermtube emergence). During branch emergence, after recovery from the DMSO solvent control, only 2% of wild type showed hyperbranch emergence compared 51% of *ΔaspB*. However, after recovery from microtubule depolymerization with Benomyl, 4% of wild type and 11% of *ΔaspB* showed 3 or more branches per compartment (hyperbranch emergence) (Figure 3.8). These data suggests that hypergrowth emergence in *ΔaspB* is partially dependent on microtubules and that perhaps septins help organize and/or stabilize microtubules during growth emergence.

The effects of Cytochalasin A treatment during hyperemergence of growth phenotypes in *ΔaspB* were different (Figure 3.8). During germtube emergence, after recovery from the DMSO solvent control, 0% of wild type showed hypergermtube emergence compared to 4% of *ΔaspB*. After recovery from actin depolymerization with Cytochalasin A, 0% of wild type and 2% of *ΔaspB* showed 3 or more germtubes per conidium. During branch emergence, After recovery from the DMSO solvent control, only 1% of wild type showed hyperbranch emergence compared 11% in *ΔaspB*. After recovery from actin depolymerization with Cytochalasin A, 3% of wild type and 12% of *ΔaspB* showed 3 or more branches per compartment (hyperbranch emergence) (Figure 3.8). Because the comparison of growth emergence with and without depolymerization of actin did not result in large reductions of growth emergence as microtubule

depolymerization did, we suggest that depolymerization of F-actin does not reduce hypergrowth emergence in *ΔaspB*. However we did find some abnormalities during branch emergence after recovery from actin depolymerization with Cytochalasin A. For the data presented in Figure 3.8, assessment of hyperbranch emergence was done by counting the number of branches in the branching compartment closest to the conidial compartment after recovery from Cytochalasin A. In wild type identifying the conidial compartment was straightforward as hardly any swelling to the size of a conidial compartment (~5μm) was observed after Cytochalasin A treatment (Figure 3.9 and Supplemental Figure 3.5). We noticed that this assessment was difficult in *ΔaspB*. Interestingly, recovering hypha of *ΔaspB*, after depolymerization of actin during branch emergence, resulted in extreme swelling and compartment lysis which made determining the conidial compartment difficult (Figure 3.9). The emergence of 2-3 hyphal tubes was commonly observed from swelling compartments. This phenotype suggests problems in polarity and/or cell wall stability in *ΔaspB* during branch emergence in the absence of actin.

AspB colocalizes with an endocytic internalization marker and the endocytic zone is of abnormal size and abnormally positioned in *ΔaspB*

Actin and microtubules are necessary for holding the tip growth apparatus in position and together respectively, and play roles in exocytosis, which is key for polar growth (FISCHER-PARTON *et al.* 2000; PENALVA 2010). To further explore AspB roles with both cytoskeletons and polar growth, we colocalized an endocytic marker with AspB-GFP and examined endocytic zones in *ΔaspB*. For colocalization studies, we used the actin binding protein AbpA which has been shown to be an endocytic marker and to localize to cortical actin patches (not actin filaments) (ARAUJO-BAZAN *et al.* 2008). We constructed double labeled strains carrying *aspB-gfp* and *abpA-mrfp*. Spores were incubated for 12-14hrs at 30°C and live Fluorescence

microscopy was used. AspB-GFP partially colocalized with AbpA-mRFP at tips (Figure 3.10). This indicates that AspB partially localizes with actin patches and endocytic sites.

To further explore AspB roles in endocytosis, we examined SlaB-GFP localization in *ΔaspB*. We used SlaB because it also localizes to endocytic sites and it is more abundant and cortical than AbpA, making it easier to characterize endocytic sites in *ΔaspB* (ARAUJO-BAZAN *et al.* 2008). In addition SlaB has been shown to be essential and necessary for polarity maintenance in hyphal tips (HERVAS-AGUILAR and PENALVA 2010). Spores were incubated for 12-14hrs at 30°C and live Fluorescence microscopy was used. Hyphal tips were imaged by sequentially selecting areas where all tips were easily distinguished and not overlapping with other tips. To avoid bias, the selection of tips was done using DIC microscopy. Once the tip was positioned, the fluorescent SlaB-GFP image was taken. This avoided knowing the SlaB-GFP localization before collecting the data. Twenty five tips (~50 micrographs) were collected for each strain per time point. Biological replicates were done and the trend was the same. The data presented is a combination of time points which had similar statistics. In wild type, SlaB-GFP formed rings that are clearly excluded from the tip apex (~4.6µm exclusion in average) (Figure 3.11-12). In *ΔaspB*, SlaB-GFP zone showed none or half of the exclusion distance from the tip apex (~2.3µm exclusion in average). In wild type, the SlaB-GFP zone length was ~5.9µm in average. However in *ΔaspB*, the SlaB-GFP zone length was ~3.7µm in average. Therefore, SlaB-GFP showed less exclusion distance from tips and narrower endocytic zone lengths in *ΔaspB* suggesting that AspB might help maintain and/or organize endocytic sites.

Discussion

AspB interacts with microtubules and actin

Septins are cytoskeletal elements that are found in fungi and other eukaryotes but not in plants. Septin heteroligomeric filaments form diffusion barriers, organize the cytoskeleton and are involved in nuclear division, cytokinesis and vesicle trafficking (CAO *et al.* 2009; GILDEN and KRUMMEL 2010; SPILIOTIS and NELSON 2006). In fungi, the cell cytoskeleton is composed of actin, microtubules and septins, and their unified roles control organelle and protein transport, endocytosis, septation, and cell polarity (LICHIUS *et al.* 2011). Therefore, these cytoskeletal elements are key for determining the morphology and growth of fungal cells, but their individual roles depend on the extent to which polar growth is exhibited. For instance in budding yeast, microtubules do not appear to play as crucial roles as actin does for growth, but microtubules are key for nuclear division. Here, some septins are essential, play roles in cytokinesis, coordination of nuclear division and polar growth (DOUGLAS *et al.* 2005; GLADFELTER *et al.* 2005; OH and BI 2011). In filamentous fungi, microtubules are important for rapid polar growth, nuclear distribution, hyphal morphology and holding the tip growth apparatus in position, while actin is required for normal apical growth, hyphal tip shape and holding the tip growth apparatus together (GILDEN and KRUMMEL 2010; GLADFELTER 2010; LICHIUS *et al.* 2011). Here, septins have been shown to be important for controlling growth emergence (ALVAREZ-TABARES and PEREZ-MARTIN 2010; LINDSEY *et al.* 2010). Though many model systems have been used to understand septin-actin-microtubule interactions, there are still many unanswered questions. Here we show that in *Aspergillus nidulans* actin, microtubules and septins might interact to ensure normal polar growth.

In general, protein colocalization can serve as the intial step for providing useful clues to protein-protein interaction. Septins have been shown to colocalize with both actin and microtubules (HANAI *et al.* 2004; JUVVADI *et al.* 2011; KINOSHITA *et al.* 1997; NAGATA *et al.* 2003; PABLO-HERNANDO *et al.* 2008; SILVERMAN-GAVRILA and SILVERMAN-GAVRILA 2008; SPILIOTIS *et al.* 2008a; SPILIOTIS 2010a; SURKA *et al.* 2002; WU *et al.* 2003). Here we show that in *Aspergillus nidulans* the septin AspB partially colocalizes with actin and microtubules. We previously showed AspB-actin colocalization during septum formation, and here we show that AspB colocalizes with actin patches at the tips (HARRIS 2001; WESTFALL and MOMANY 2002). To better understand their interactions, we will examine AspB-actin colocalizations throughout fungal growth when actin fluorescent tags for *A. nidulans* become available. Here we also show that AspB partially colocalizes with microtubules, tyrosinolated microtubules and UncA bound microtubules, and occasionally localized near or in between nuclei. We were unable to assess whether these colocalizations are cell cycle dependant as chemical synchronization for nuclear division resulted in abnormal septins (data not shown). In the future, we are interested in synchronizing populations using cell cycle mutants and following AspB localization with microtubules and the UncA motor. This will help better understand septin-microtubule interactions and nuclear phenotypes observed in Δ*aspB*.

Septins display, to an extent, codependence with both actin and microtubules (BÖHMER *et al.* 2009; KINOSHITA *et al.* 2002; KINOSHITA *et al.* 1997; KREMER *et al.* 2005; NAGATA *et al.* 2003; SCHMIDT and NICHOLS 2004b; SILVERMAN-GAVRILA and SILVERMAN-GAVRILA 2008; SPILIOTIS *et al.* 2008a; SPILIOTIS 2010a). To further understand septin-actin and septin-microtubule interactions, we assessed codependency by following AspB arrangements in the absence of actin and microtubule polymers and vice versa. Depolymerization of actin resulted in many small

AspB-GFP free-floating cytoplasmic rings similar to phenotypes observed in mammals (KINOSHITA *et al.* 2002). Also, in the absence of AspB, tropomyosin (TpmA) did not localize to actin filaments and septa labeling was very faint. Still, actin filaments were present in the absence of AspB. Therefore, AspB and actin interactions might be somehow codependent as actin filaments might help maintain and/or stabilize AspB localization to its structures and AspB might help maintain and/or stabilize TpmA localization to actin filaments. This might in turn control growth emergence by controlling the tropomyosin block of motors to actin filaments. Likewise, depolymerization of microtubules mostly resulted in cytoplasmic or abnormal AspB-GFP filaments; and in the absence of AspB, microtubule bundles were less frequent in newly formed branches. This phenotype could explain the abortive branching observed in Δ*aspB* (Hernandez-Rodriguez *et al.*, unpublished data). These data suggests that AspB and microtubule interactions might be somehow codependent and AspB might help organize and/or stabilize microtubules in additional growing axes.

AspB might help stabilize and/or organize polar sites.

It has been suggested that septins might control growth addition to the cortex by its interaction with the cytoskeleton (GILDEN and KRUMMEL 2010). Our data also points in that direction. One of the striking phenotypes in Δ*aspB* is its hyperemergence of growth. This phenotype has also been reported for Δ*aspA* and Δ*aspC* (LINDSEY *et al.* 2010a). This suggests that septins are somehow involved in controlling polar growth. To investigate this role, we assessed growth emergence in Δ*aspB* after recovery from actin or microtubule depolymerization. Depolymerization of actin did not reduce hyperemergence of growth but resulted in swelling and lysis of hyphae during branch emergence in Δ*aspB*. In the absence of actin, during branch emergence, Δ*aspB* displayed polarity and/or cell wall defects. Therefore, actin might be

important for cell wall stability and maintaining polar growth during branch emergence in Δ*aspB*. On the contrary, depolymerization of microtubules reduced hypergermtube and hyperbranch emergence in Δ*aspB*. These data suggests that hypergrowth emergence in Δ*aspB* is partially dependent on microtubules, but not actin, and that perhaps septins help organize and/or stabilize microtubules during growth emergence.

Trafficking of vesicles by motors to growth emergence sites is key for polar growth. Septins have been shown to control the access of myosin motors to actin filaments (GILDEN and KRUMMEL 2010; JOO *et al.* 2007). Here we show that tropomyosin (TpmA), which blocks access of motors to actin, is lost from actin filaments. We propose that Δ*aspB* hypergrowth emergence might be, in part, a result of hyperaccess of motors to actin filaments which could result in more trafficking of the polar growth machinery. We are interested in following actin motor dynamics in Δ*aspB* to explore this possibility. Though hypergrowth emergence was not reduced in the absence of actin filaments, we did find polarity defects during branch emergence. Conversely, septin-microtubule interactions have been shown to have different roles in growth emergence (GILDEN and KRUMMEL 2010; KREMER *et al.* 2005; SPILIOTIS *et al.* 2008a). Septins can interact with microtubules and motors for trafficking of vesicles to promote growth emergence, but some septins can block access of vesicles to membranes so that growth is not added (AMIN *et al.* 2008; BEITES *et al.* 2005; BEITES *et al.* 1999; GILDEN and KRUMMEL 2010). Therefore, AspB might be acting as a negative regulator of growth, so that in its absence microtubule cargos have more access to the cortex and promote hyperemergence of growth; and/or AspB helps organize and/or stabilize microtubules to ensure trafficking and growth emergence to a specific area.

During polar growth, actin and microtubules serve as tracks for vesicle trafficking towards and away from the growing axes (GILDEN and KRUMMEL 2010; LICHIUS *et al.* 2011). Bridging

between these cytoskeletons is necessary to target protein vesicles to their final destinations. Though the cell cytoskeleton is very important for polar growth, endocytosis is also necessary for maintaining growth extension (ARAUJO-BAZAN *et al.* 2008; HERVAS-AGUILAR and PENALVA 2010; ORLANDO *et al.* 2011; PENALVA 2010). In addition, diffusion barriers are necessary to maintain endocytic areas. Septin form barriers that maintain asymmetric localization of the polarity machinery (ORLANDO *et al.* 2011; SCHMIDT and NICHOLS 2004a). Septin localization and interactions with the cytoskeleton, along with their roles as diffusion barriers, suggest that septins might help bridge interactions between actin and microtubules, and might form diffusion barriers to ensure normal endocytosis during polar growth. We have shown several lines of evidence that suggest AspB-actin interactions: 1) actin binding protein (ApbA) colocalizes with AspB, 2) actin filaments are necessary for normal AspB localization, 3) tropomyosin (TpmA) localization to actin filaments is lost in the absence of AspB, and 4) actin is important for polar growth during branch emergence in Δ*aspB*. In addition we have shown several lines of evidence that suggest AspB-microtubule interactions: 1) microtubules partially colocalize with AspB, 2) microtubules are necessary for normal AspB filaments, 3) microtubules are unable to populate all polarity axes in the absence of AspB, and 4) microtubules facilitate hypergrowth emergence in Δ*aspB*. Other lines of evidence from our previous studies also suggest AspB-microtubule interactions as microtubules are necessary for nuclear migration and Δ*aspB* results in clumped nuclei. Here we show that AspB-GFP can localize near nuclei. Even with all these lines of evidence, as in mammalian systems, AspB-microtubule interactions are still unclear (SPILIOTIS 2010a). In terms of septins roles related to endocytosis, we have shown that AspB colocalizes with an endocytic internalization marker and the endocytic zone is of abnormal size and abnormally positioned in Δ*aspB*. AspB partially colocalizes with AbpA and therefore with actin

patches and endocytic sites. SlaB, a more cortical endocytic site marker, is less or not excluded from tips and the smaller zone lengths in Δ*aspB* show that endocytic sites are abnormal. This suggests that AspB might help maintain and/or organize endocytic sites. All together we have shown that AspB might help stabilize polarity axes by possibly interacting and/or organizing actin, microtubules and endocytosis.

Acknowledgments

This work was supported by the Dissertation Completion Grant from the University of Georgia to Yainitza Rodriguez; and by the NSF grant MCB 0211787 and NSF grant DevMech 1051730 to Dr. Michelle Momany. We want to thank Stephen Osmani, Steve Harris, Miguel Peñalva, Reinhard Fisher and Hiroyuki Horiuchi for sharing strains.

Tables and Figures

Table 3.1: Strains used

Strain	Genotype	Reference
A850	*biA1;_argB::trpC_B;methG1; veA1; trpC801*	FGSC
A773	*pyrG89;wA3;pyroA4*	FGSC
HA344	*An-H1-chRFP::pyroAAf;(pyroA4;argB2);pyrG89;nkuA::argB*	Stephen Osmani
AAV122.1	*pyrG89;argB2;pyroA4Δnku::argB;tpm::gfp::pyr-4*	Steve Harris
AAV124.1	*pyrG89;argB2;pyroA4ΔnkuA::argB; tubA::gfp::pyr-4*	Steve Harris
SNZ54	*TNO2A3 transformed with pNZ520, pyroA4 (mRFP-UncA rigor)*	Reinhard Fisher
1794	*pyroA4 argB, nKuA::argB,argB2, slaB-GFP::pyrGAfpyrG89*	Miguel Peñalva
1417	*biA1 pantoB100 abpA::mRFP pyrG89*	Miguel Peñalva
A1149LA-1	*pyrG89::alcA(p)-lifeact-egfp-pyrG,pyroA4 nkuA::argB*	Hiroyuki Horiuchi
ASH59	*AYR32 X 1794*	This study
AYR1	*pyrG89*, aspB:: AfpyrG; pyroA4; riboB2*	Previous study
AYR6	*pyrG89, aspB::aspB-gfp- AfpyrG; argB2*	Previous study
AYR32	*AYR1 X A850*	Previous study
AYR33	*AYR6 X AAV124.1*	This study
AYR35	*AYR6 X A773*	Previous study
AYR40	*AYR6 X SNZ54*	This study
AYR50	*AYR35 X HA344*	This study
AYR63	*AYR35 X1417*	This study
AYR68	*AYR32 X AAV122.1*	This study
AYR70	*AYR32 X* A1149LA-1	This study

FGSC, Fungal Genetics Stock Center, Department of Microbiology, University of Kansas Medical Center (Kansas City, KS).

Figure 3.1. AspB-GFP partially colocalizes with α-TubA labeled microtubules. AspB-GFP can partially colocalize with microtubules. Arrows denote areas of colocalization of AspB-GFP and α-TubA. AspB-GFP was also found near or in between some nuclei. Nuclei are in blue, AspB in green and TubA in red. Spores were incubated for 12-14hrs at 30°C. Immunofluorescence microscopy was used. Nuclei were labeled with Hoechst 33258 bis-benzimide, AspB was labeled using the AspB-GFP strain and TubA was labled with α-TubA mouse antibodies (Sigma) and α-mouse Dylight 588 antibodies (Jackson ImmunoResearch). Micrographs were collected in black and white and Photoshop CS3 was used to combine, overlay, organize, improve contrast and brightness and/or colorize (Hue saturation) micrographs. Scale bar is 5μm.

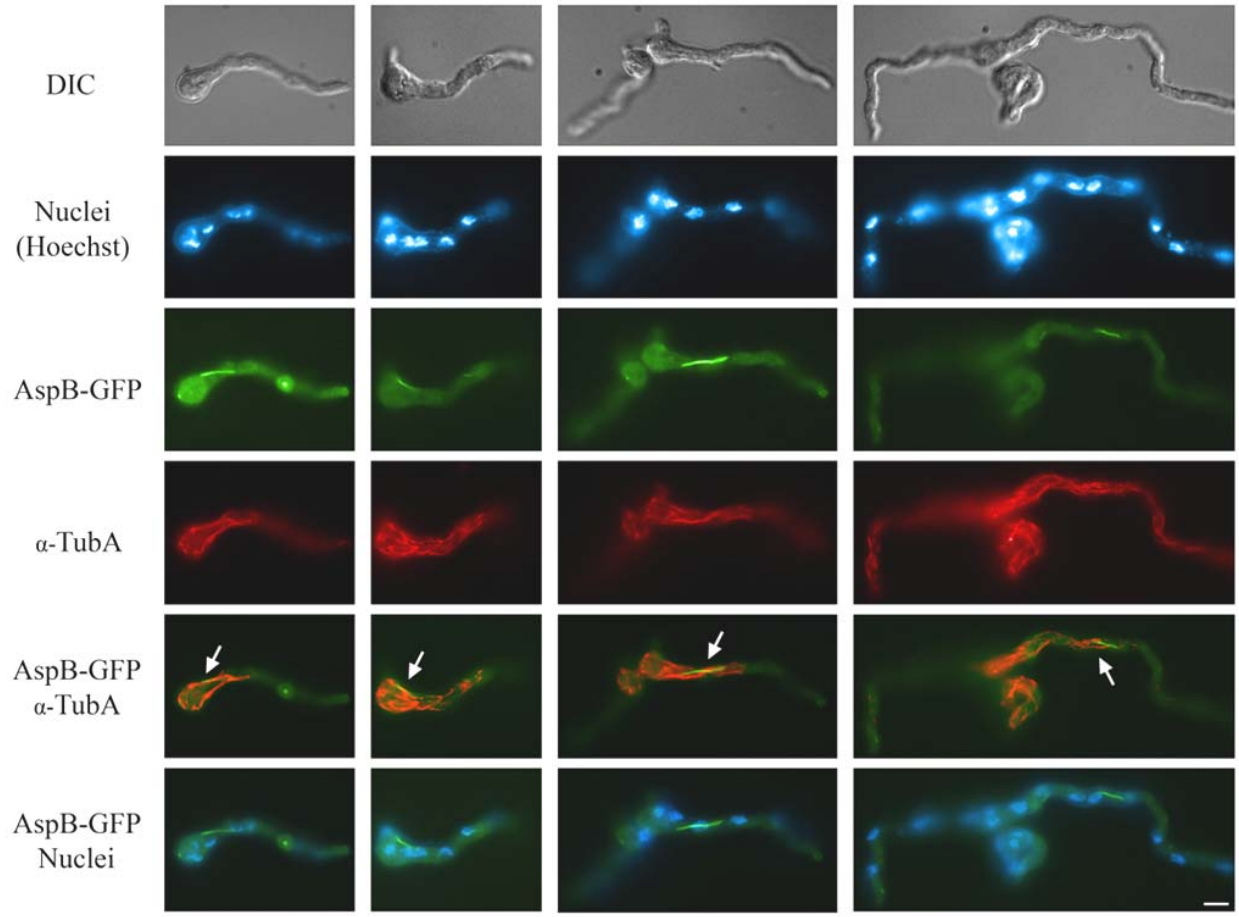
DIC
Nuclei
(Hoechst)
AspB-GFP
α-TubA
AspB-GFP
α-TubA
AspB-GFP
Nuclei

Figure 3.2. Depolymerization of microtubules results in AspB-GFP star filaments. (A) TubA-GFP filaments are not affected by DMSO. (B) TubA-GFP filaments are not observed under Benomyl treatment. (C) AspB-GFP filaments are not affected by DMSO. (D) AspB-GFP forms abnormal filament clusters and star filaments (*) under Benomyl treatment. (E) Enlarged star filaments from matched micrographs denoted by black lines. Star filaments showed a ring (^) that seemed to hold them together. Refer to Supplemental. Figure 3.2 for phenotypic counts. Spores were incubated for 8-10hrs at 30°C. Depolymerization of microtubules was assessed by following disappearance of microtubule filaments under Benomyl treatment (6µg Benomyl/ml of DMSO; 1-1.5hrs) in the TubA-GFP labeled strain. Live microscopy was used. Photoshop CS3 was used to combine, overlay, organize and improve contrast and brightness of DIC and fluorescent micrographs. Scale bar is 5µm.

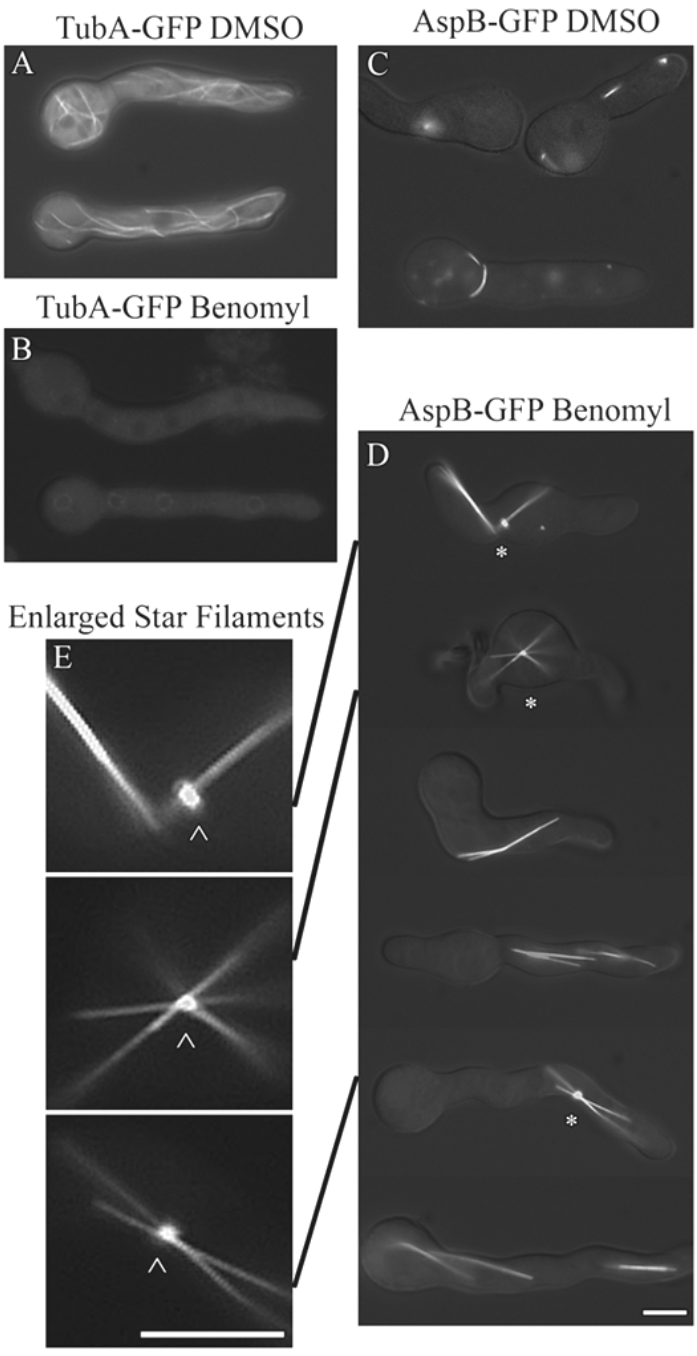
TubA-GFP DMSO
A
AspB-GFP DMSO
C
TubA-GFP Benomyl
B
AspB-GFP Benomyl
D
Enlarged Star Filaments
E

Figure 3.3. AspB-GFP partially colocalizes with α-Tyrosinolated TubA labeled microtubules. AspB-GFP can partially colocalize with Tyrosinolated microtubules. Arrows denote areas of colocalization of AspB-GFP and α-Tyrosinolated TubA. AspB-GFP was also found near or in between some nuclei. Nuclei are in blue, AspB in green and TubA in red. Spores were incubated for 6-14hrs at 30°C. Immunofluorescence microscopy was used. Nuclei were labeled with Hoechst 33258 bis-benzimide, AspB was labeled using the AspB-GFP strain and TubA was labled with α-Tyrosinolated TubA mouse antibodies (Sigma) and α-mouse Dylight 588 antibodies (Jackson ImmunoResearch). Micrographs were collected in black and white and Photoshop CS3 was used to combine, overlay, organize, improve contrast and brightness and/or colorize (Hue saturation) micrographs. Scale bar is 5μm.

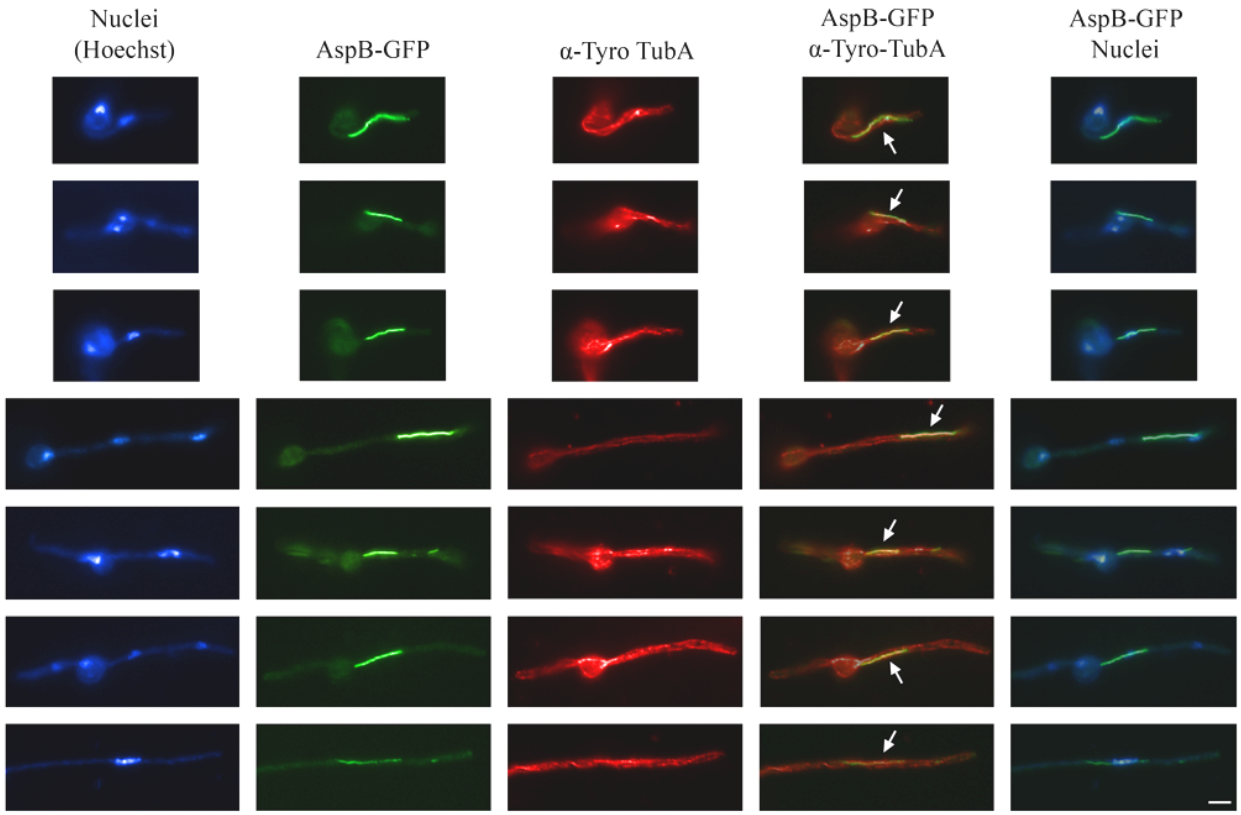
Nuclei
(Hoechst)
AspB-GFP
α-Tyro TubA
AspB-GFP
α-Tyro-TubA
AspB-GFP
Nuclei

Figure 3.4. AspB-GFP partially colocalizes with mRFP-UncA^{rigor}. AspB-GFP can partially colocalize with mRFP-UncA^{rigor}. Arrows denote areas of colocalization of AspB-GFP and mRFP-UncA^{rigor}. In early germination AspB-GFP seem to connect (^) or cross (*) mRFP-UncA^{rigor}. AspB-GFP is in green and mRFP-UncA^{rigor} in red. Spores were incubated for 6-12hrs at 30°C. Live microscopy was used. Micrographs were collected in black and white and Photoshop CS3 was used to combine, overlay, organize, improve contrast and brightness and/or colorize (Hue saturation) micrographs. Scale bar is 5μm.

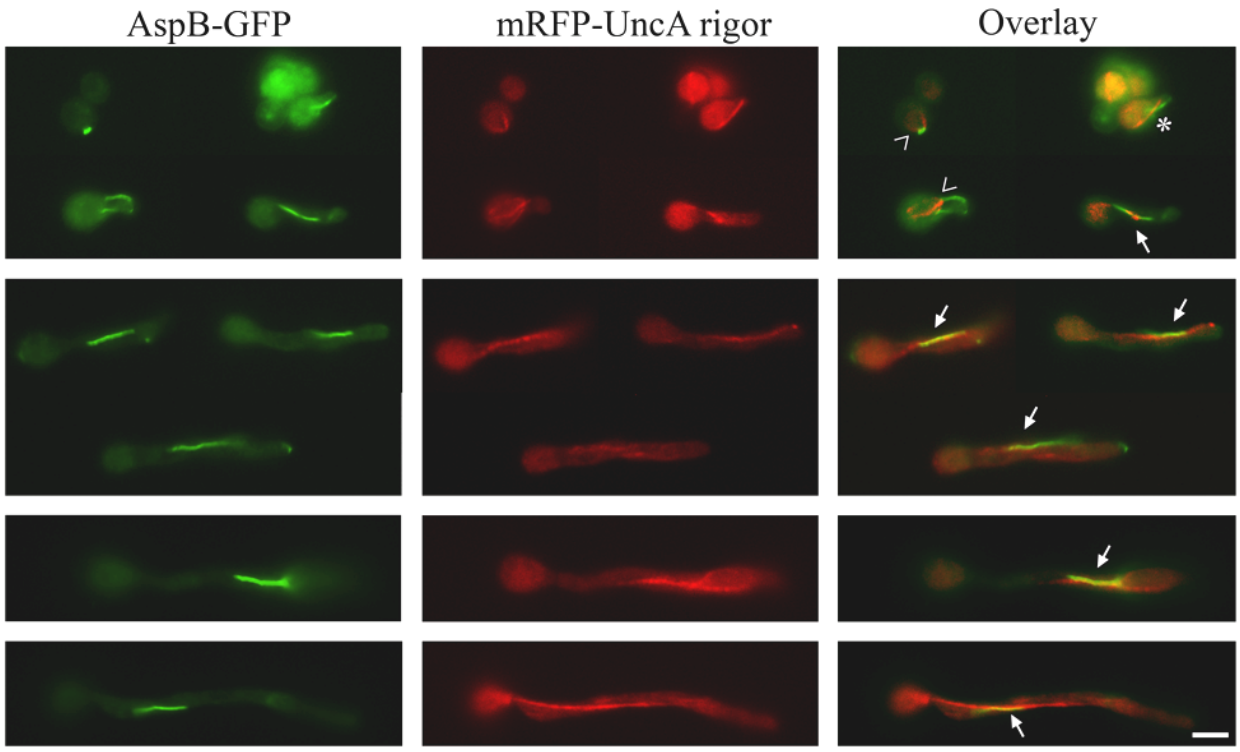
AspB-GFP
mRFP-UncA rigor
Overlay

Figure 3.5. *ΔaspB* showed less microtubule filaments in branches. (I.) *tubA-gfp* and *ΔaspB tubA-gfp strains*. *ΔaspB* showed more branches without microtubule filaments. Live microscopy was used. Photoshop CS3 was used to combine, overlay, organize and improve contrast and brightness of DIC and fluorescent micrographs. Scale bar is 5µm. (II.) *ΔaspB* has more newly formed branches without microtubule filaments compared to wild type. Spores were incubated for 12hrs at 30°C. Newly formed branches (≤5µm) were assessed for presence or absence of microtubule filaments (n=200). Live microscopy was used.

I.

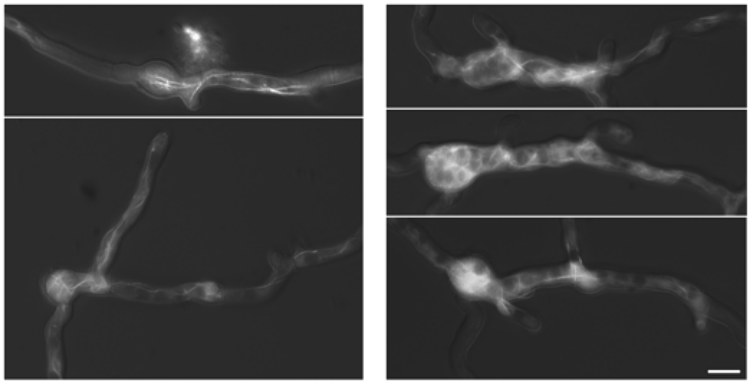

tubA-gfp *ΔaspB tubA-gfp*

II.

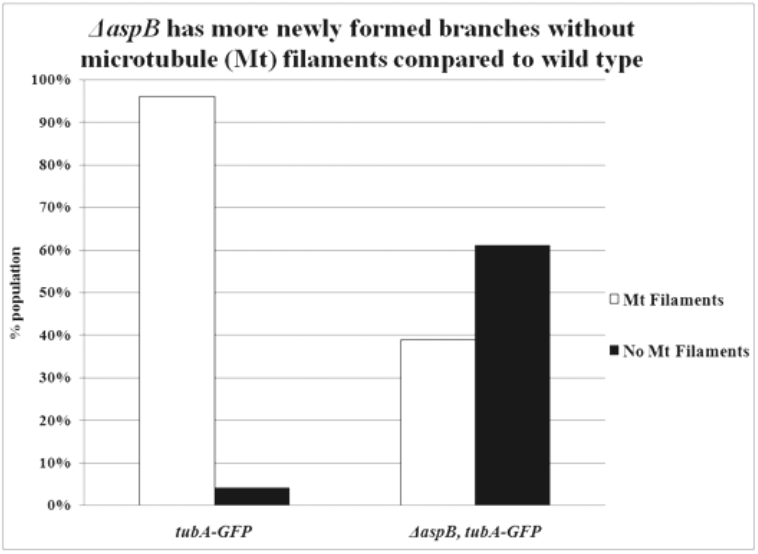

Figure 3.6. Depolymerization of actin results in many AspB-GFP free-floating cytoplasmic rings. AspB-GFP filaments are not affected by DMSO. AspB-GFP forms many free-floating cytoplasmic rings under Cytochalasin A treatment. Inset from zoomed in area (^) shows a closer view of the small cytoplasmic rings. Spores were incubated for 8-10hrs at 30°C. Depolymerization of actin was assessed by following the disappearance of actin filaments under Cytochalasin A treatment (1µg Cytochalasin A/ml of DMSO; 1-1.5hrs) in the TpmA-GFP labeled strain; see materials and methods for details. Live microscopy was used. Photoshop CS3 was used to combine, overlay, organize and improve contrast and brightness of DIC and fluorescent micrographs. Scale bar is 5µm.

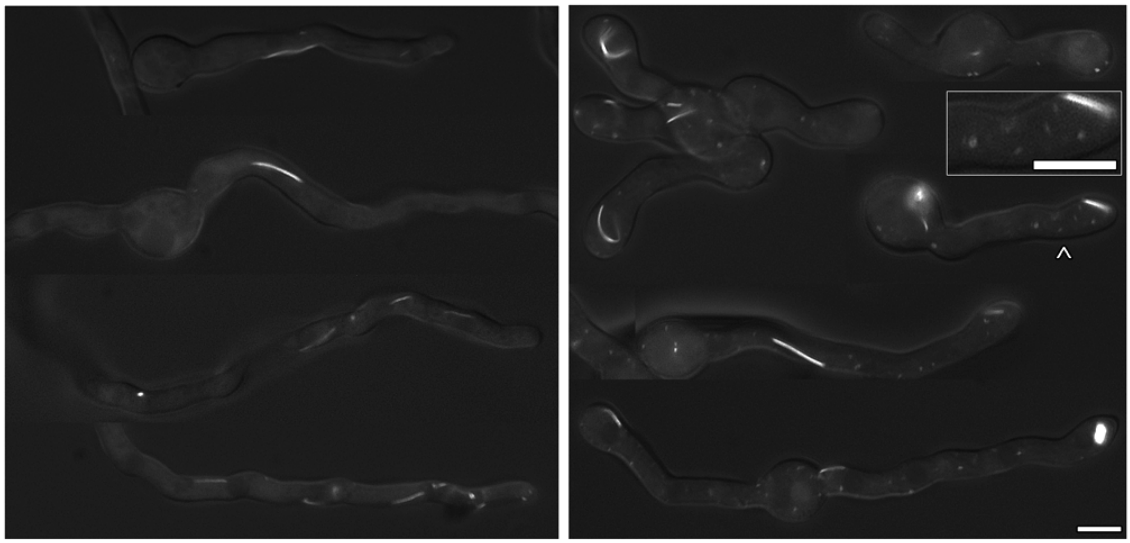

AspB-GFP DMSO

AspB-GFP Cytochalasin

Figure 3.7. TpmA-GFP localization to actin filaments and tips are lost in *ΔaspB*. (A) TpmA-GFP localizes to septa (S). (B-C) TpmA-GFP localizes to actin filaments (arrow head) and tips (*). (D) TpmA-GFP localizes faintly to septa in *ΔaspB*. (E-F) TpmA-GFP localization to actin filaments and tips are lost in *ΔaspB*. Spores were incubated for 12-14hrs at 30°C. Live microscopy was used. Photoshop CS3 was used to combine, overlay, organize and improve contrast and brightness of DIC and fluorescent micrographs. Scale bar is 5μm.

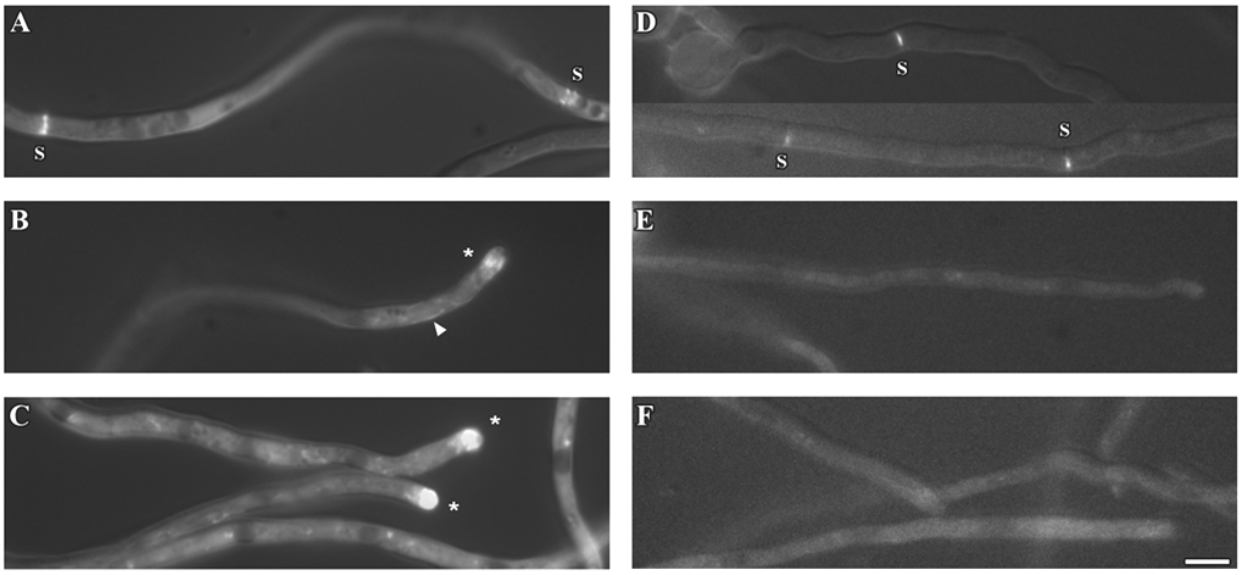

tpmA-gfp *ΔaspB tpmA-gfp*

Figure 3.8. Depolymerization of microtubules, but not actin, reduced hypergermtube and hyperbranch emergence in *ΔaspB*. The first part of the graphs compares germtube or branch emergence before treatment of wild type and *ΔaspB*. Then graphs compare germtube or branch emergence after treatment and recovery from Benomyl, Cytochalasin A or DMSO (solvent control) of wild type and *ΔaspB*. (A) Depolymerization of microtubules reduces hypergermtube emergence in Δ*aspB*. (B) Depolymerization of microtubules reduces hyperbranch emergence in Δ*aspB*. (C) Depolymerization of actin does not reduce hypergermtube emergence in Δ*aspB*. (D) Depolymerization of actin does not reduce hyperbranch emergence in Δ*aspB*. For hypergermtube emergence analyses the number of germtubes (gt) were counted and grouped as 0gt, 1gt, 2gt or 3 or more gt (≥3br); n=300. For hyperbranch emergence analyses, Calcofluor staining was used to delineate compartments and the number of branches (br) in the most basal compartment (closest to the conidal compartment) were counted and group as 0br, 1br, 2br or 3 or more br (≥3br); n=300. Spores were incubated for 4hrs (germtube emergence) and 10hr (branch emergence) at 30°C. Depolymerization of microtubules was assessed by following the disappearance of microtubule filaments under Benomyl treatment (6µg Benomyl/ml of DMSO; 1hr) in the TubA-GFP labeled strain. Depolymerization of actin was assessed by following the disappearance of actin filaments under Cytochalasin A treatment (1µg Cytochalasin A/ml of DMSO; 1hr) in the TpmA-GFP labeled strain. Recovery lasted until wild type initiated germtube or branch emergence. Coverslips were fixed and stained with Calcofluor Blankophour BDH for septa and Hoechst 33258 bis-benzimide for nuclei.

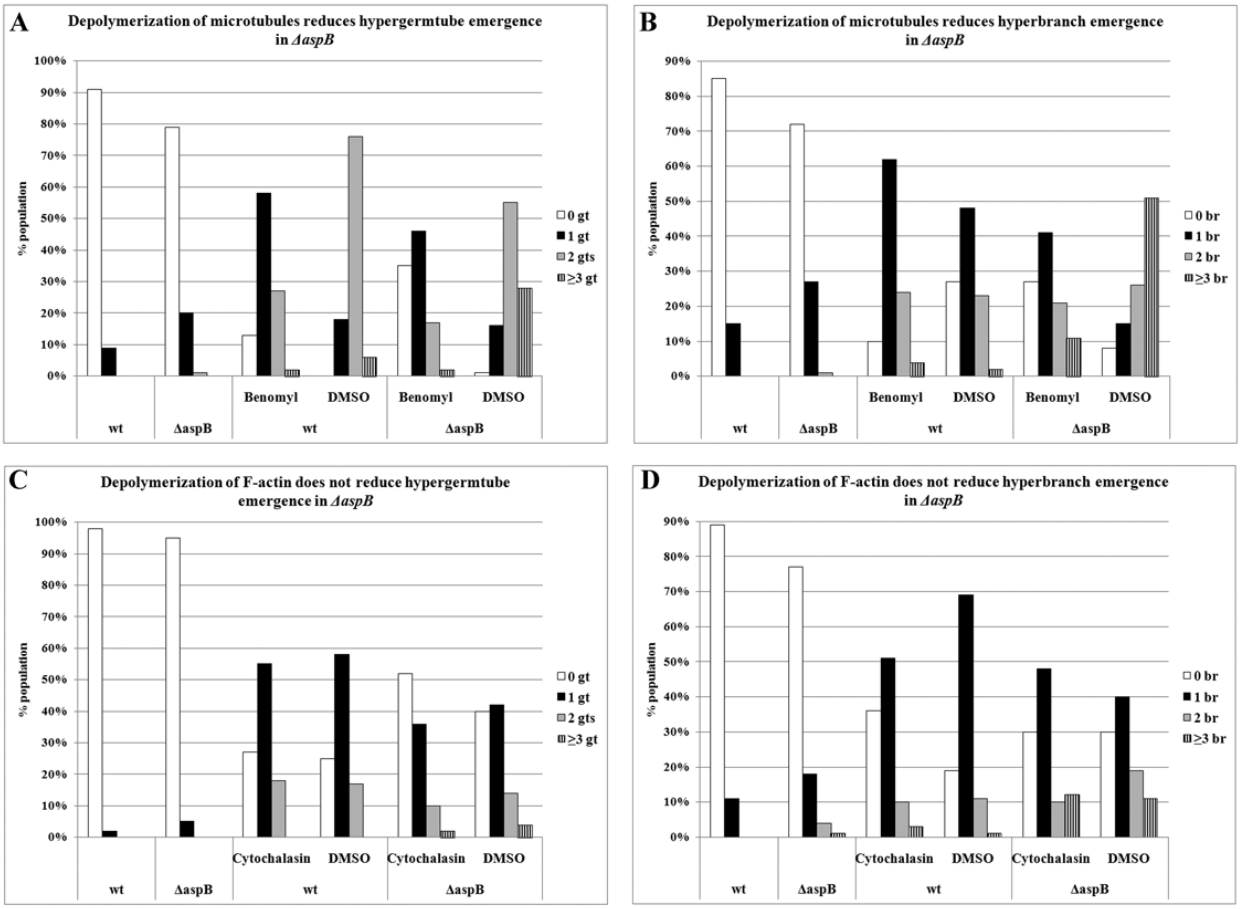
A
Depolymerization of microtubules reduces hypergermtube emergence in ΔaspB
% population
100%
90%
80%
70%
60%
50%
40%
30%
20%
10%
0%
0 gt
1 gt
2 gts
≥3 gt
Benomyl
DMSO
Benomyl
DMSO
wt
ΔaspB
wt
ΔaspB
B
Depolymerization of microtubules reduces hyperbranch emergence in ΔaspB
% population
0 br
1 br
2 br
≥3 br
Benomyl
DMSO
Benomyl
DMSO
wt
ΔaspB
wt
ΔaspB
C
Depolymerization of F-actin does not reduce hypergermtube emergence in ΔaspB
% population
0 gt
1 gt
2 gts
≥3 gt
Cytochalasin
DMSO
Cytochalasin
DMSO
wt
ΔaspB
wt
ΔaspB
D
Depolymerization of F-actin does not reduce hyperbranch emergence in ΔaspB
% population
0 br
1 br
2 br
≥3 br
Cytochalasin
DMSO
Cytochalasin
DMSO
wt
ΔaspB
wt
ΔaspB

Figure 3.9. Depolymerization of actin results in polarity defects during hyperbranch emergence in *ΔaspB*. (I.) *ΔaspB* showed extreme swelling and lysis (arrow) after treatment and recovery from Cytochalasin A and not DMSO as described in Figure 3.7 during hyperbranch emergence. Nuclear staining showed nuclei and cytoplasm leaking from lysed compartments. Lysis was not observed in wild type. See Supplemental Figure 3.4 for comparisons to wild type. Photoshop CS3 was used to combine, overlay, organize and improve contrast and brightness of DIC and fluorescent micrographs. Scale bar is 5μm. (II.) *ΔaspB* showed extreme swelling after actin depolymerization. Samples treated and recovered from Cytochalasin A as described in Figure 3.7 were assessed. Each individual was categorized as swelling if an area of equal or larger size than the conidial compartment or a swollen lysed area was observed; and non swelling if the conidial compartment was easily identified and no other swollen area was found (n= 200). Swollen areas in *ΔaspB* were larger than in wild type.

I.

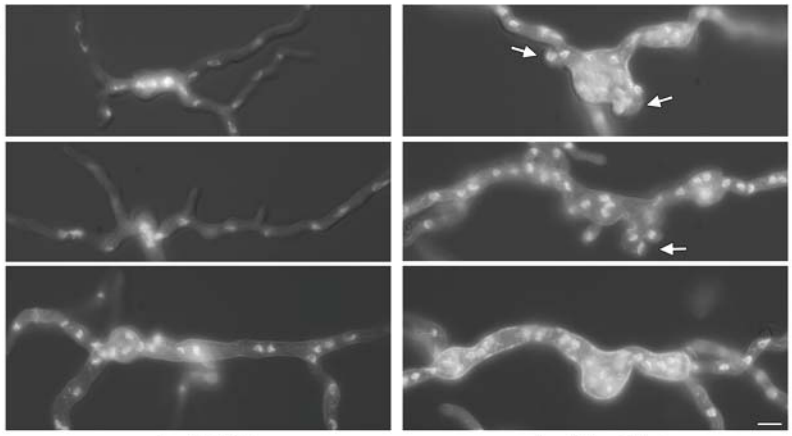

ΔaspB DMSO *ΔaspB* Cytochalasin

II.

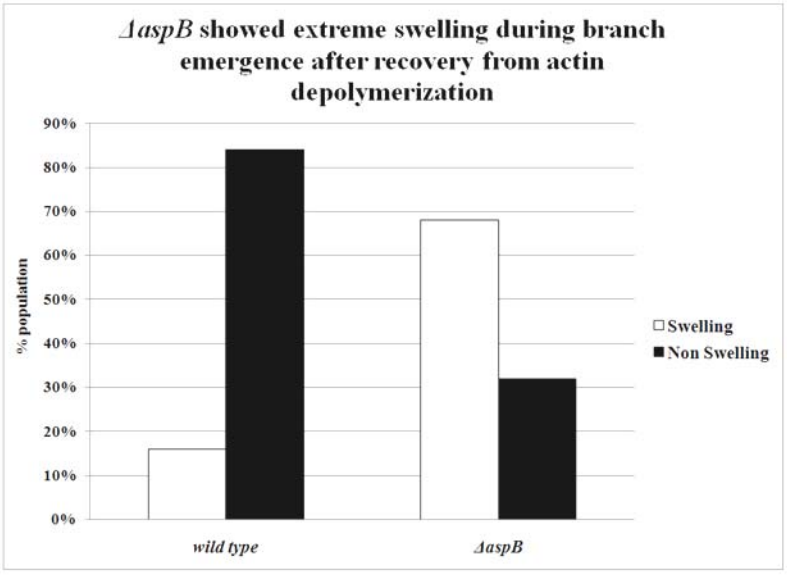

Figure 3.10. AspB-GFP partially colocalizes with AbpA. AspB-GFP can partially colocalize with AbpA-mRFP at tips. AspB-GFP is in green and AbpA-mRFP in red. Spores were incubated for 12-14hrs at 30°C. Live microscopy was used. Micrographs were collected in black and white and Photoshop CS3 was used to combine, overlay, organize, improve contrast and brightness and/or colorize (Hue saturation) micrographs. Scale bar is 5μm.

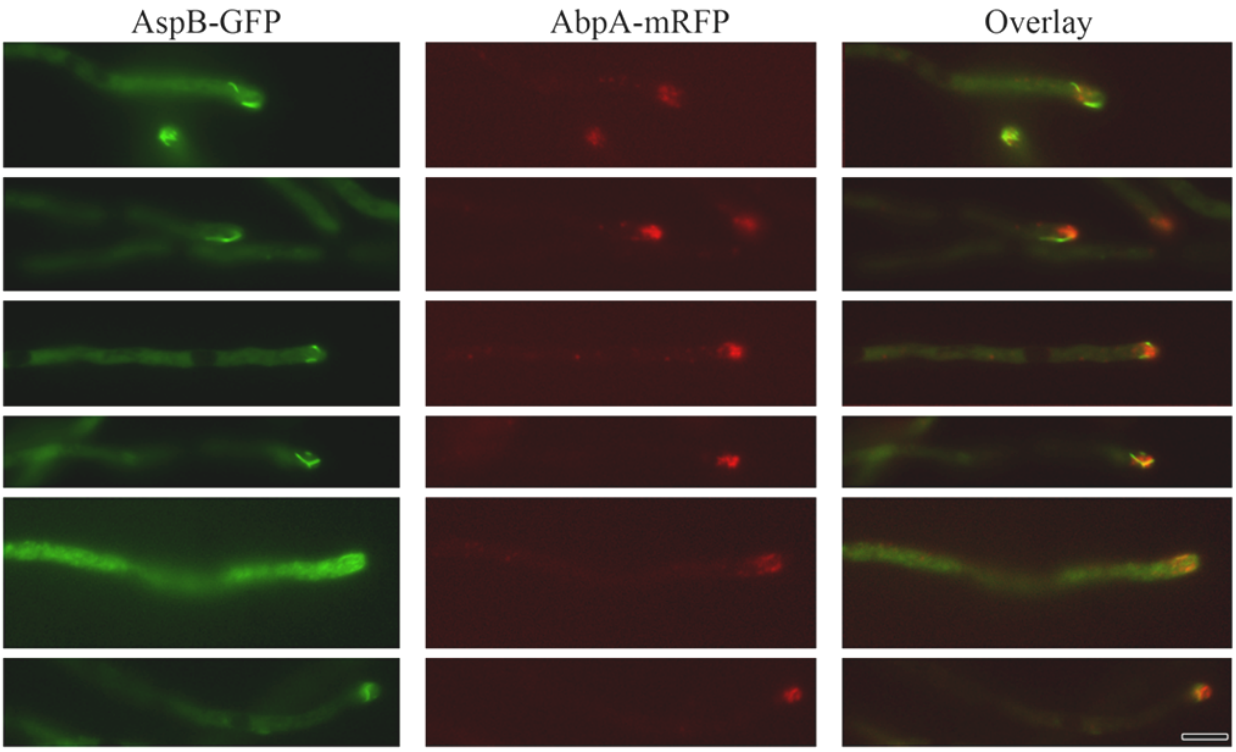
AspB-GFP
AbpA-mRFP
Overlay

Figure 3.11. SlaB-GFP showed less exclusion distance from tips and smaller zone lengths in *ΔaspB*. Spores were incubated for 12-14hrs at 30°C. Live microscopy was used. For measurements, micrographs of each individual were taken and analyzed using Photoshop CS3 to combine, overlay, organize, improve contrast and brightness and measure DIC and fluorescent micrographs. (A) *ΔaspB* showed less SlaB-GFP exclusion distance from the tip apex compared to wild type. Wild type: Mean 4.71µm and Median 4.4µm. *ΔaspB*: Mean 2.17µm and Median 2.5µm. n=50. (B) *ΔaspB* showed smaller SlaB-GFP zone lengths compared to wild type. Wild type: Mean 5.95µm and Median 5.85µm. *ΔaspB*: Mean 3.73µm and Median 3.75µm. n=50.

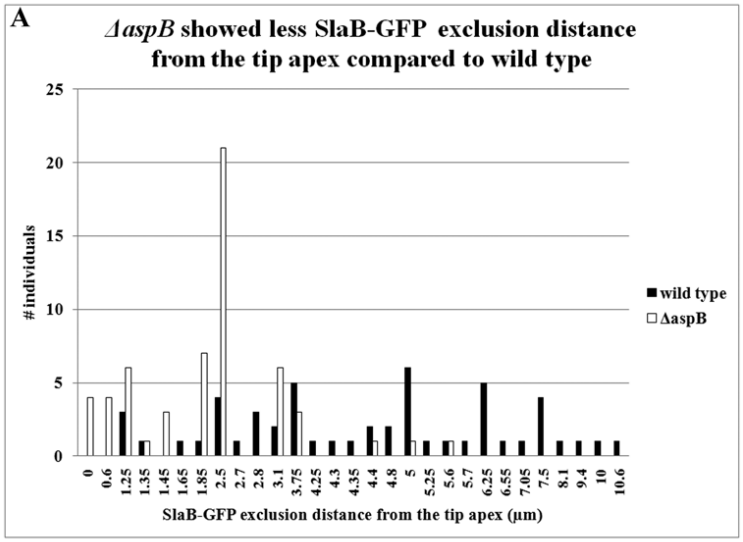
A
ΔaspB showed less SlaB-GFP exclusion distance from the tip apex compared to wild type
individuals
SlaB-GFP exclusion distance from the tip apex (µm)
wild type
ΔaspB

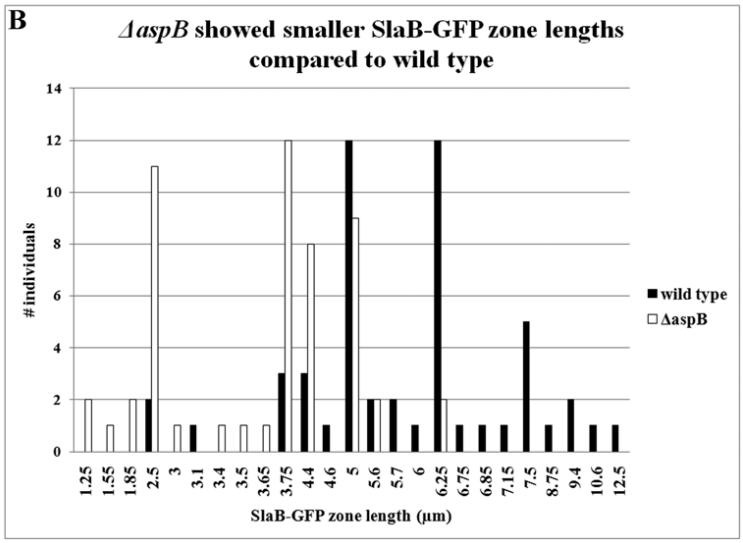
B
ΔaspB showed smaller SlaB-GFP zone lengths compared to wild type
individuals
SlaB-GFP zone length (µm)
wild type
ΔaspB

Figure 3.12. SlaB-GFP showed smaller zone lengths and localized at or very close to the tip apex in *ΔaspB*. Some micrographs used for Figure 3.11 analysis are shown to exemplify results. SlaB-GFP in the wild type background showed wide zones that are excluded from the tip. SlaB-GFP in the *ΔaspB* background showed narrower or no zone and localization was closer or not excluded from the tip. Photoshop CS3 was used to combine, overlay, organize and improve contrast and brightness of DIC and fluorescent micrographs. Scale bar is 5μm.

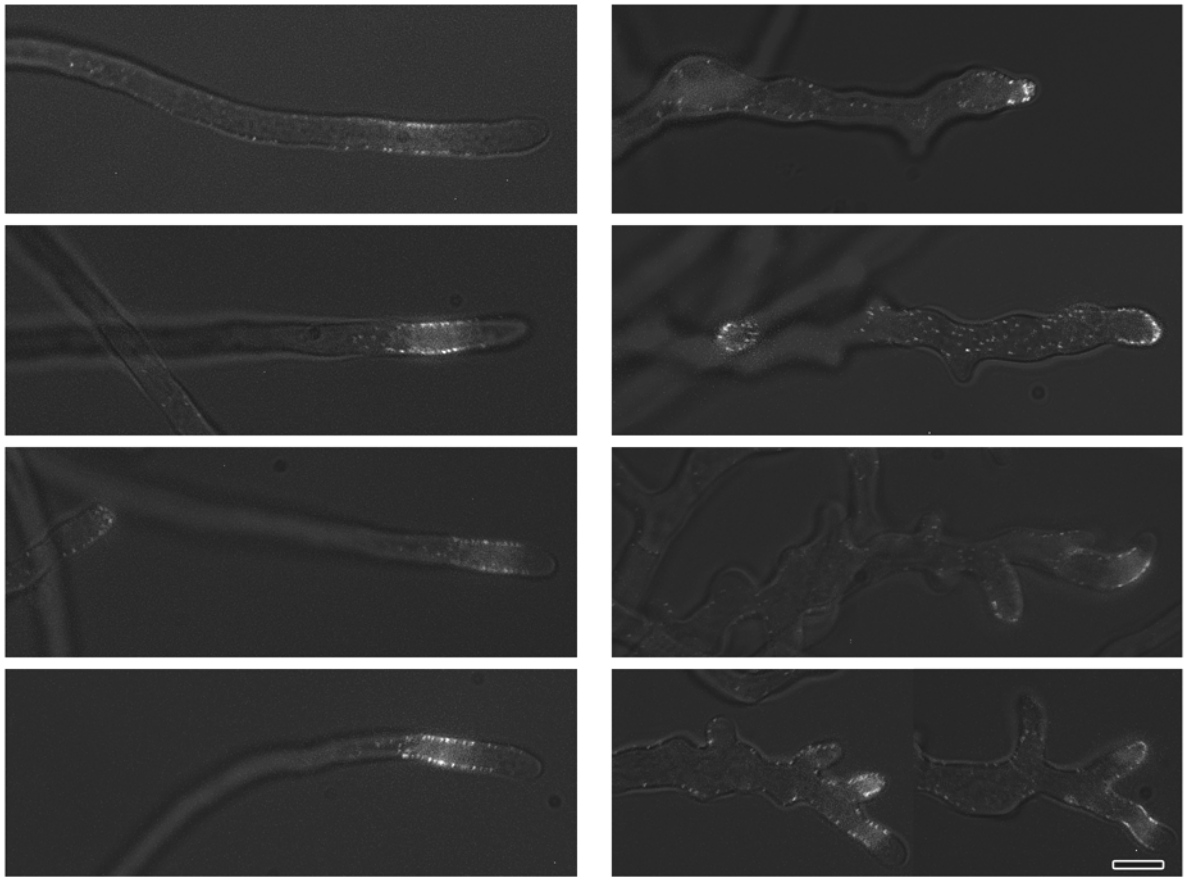

slaB-gfp *ΔaspB slaB-gfp*

Supplemental Figures

Supplemental Figure 3.1. AspB-GFP filaments and bars localize near nuclei. AspB-GFP filaments and bars can be found near nuclei from dormant conidia to mature hypha. H1mRFP was used to label nuclei. Live microscopy was used. Micrographs were collected in black and white and Photoshop CS3 was used to combine, overlay, organize, improve contrast and brightness and/or colorize (Hue saturation) micrographs. AspB-GFP in green and H1 labeled nuclei in blue. Scale bar is 5μm.

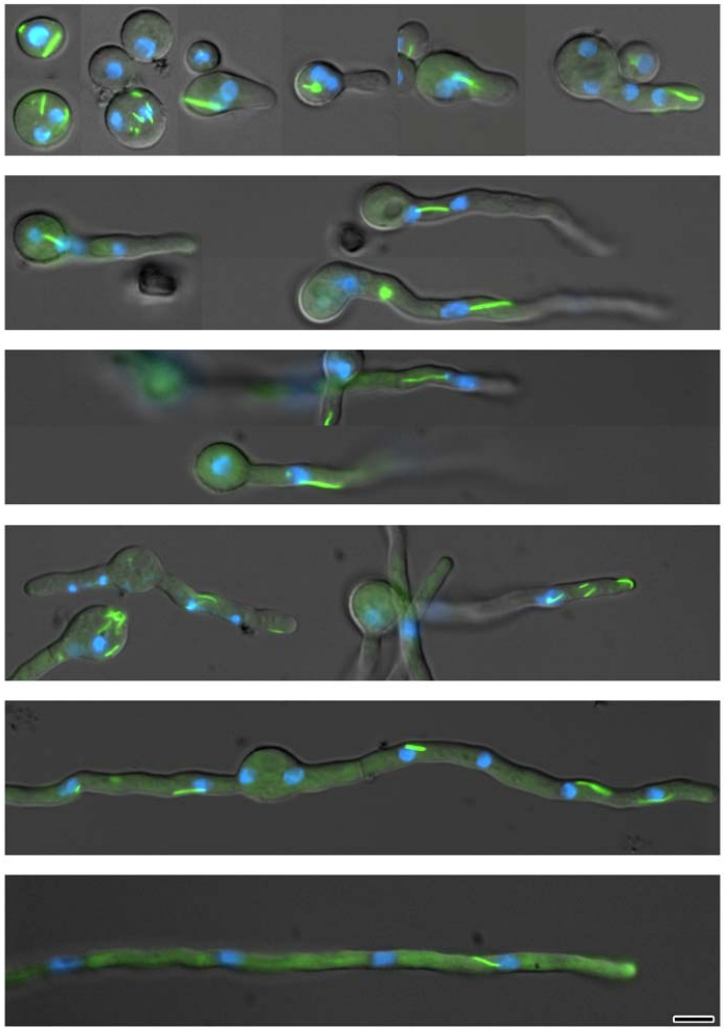

Supplemental Figure 3.2. Microtubule depolymerization results in AspB-GFP star filament formation. AspB-GFP localizations were assessed in Benomyl and DMSO treatments as described in Figure 3.2 and classified as: normal filaments, spots (rings, dots, bowties), cytoplasmic and star filaments. Under Benomyl treatment AspB-GFP localization was mostly cytoplasmic or as star filaments. Refer to Figure 3.2 for phenotypic micrographs. Conditions as described in Figure 3.2. n=300.

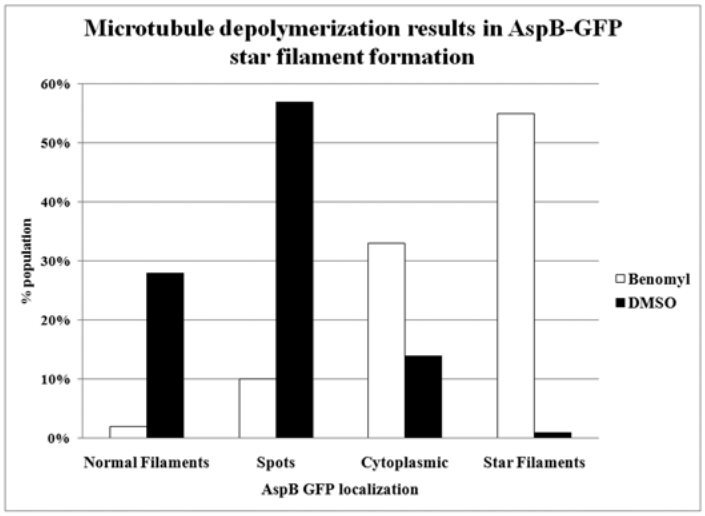
Microtubule depolymerization results in AspB-GFP star filament formation
60%
50%
40%
30%
20%
10%
0%
% population
Normal Filaments
Spots
Cytoplasmic
Star Filaments
AspB GFP localization
Benomyl
DMSO

Supplemental Figure 3.3. Actin filaments are present in *ΔaspB*. *alcA(p)-lifeact-egfp* was used to label actin and this construct was crossed into *ΔaspB*. Actin filaments (arrow head), localization to tips (*) and septa (s) are present in *ΔaspB*. Live microscopy was used. Photoshop CS3 was used to combine, overlay, organize and improve contrast and brightness of DIC and fluorescent micrographs. Scale bar is 5μm.

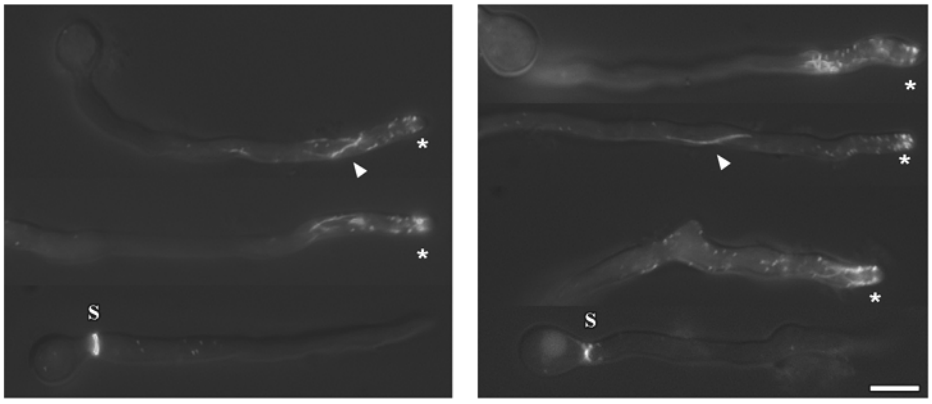

alcA(p)-lifeact-egfp *ΔaspB alcA(p)-lifeact-egfp*

Supplemental Figure 3.4. TubA-GFP and TpmA-GFP localizations under Benomyl and Cytochalasin A treatments respectively are reversible and not affected by DMSO. (A) TubA-GFP filaments (arrow) are not affected by DMSO. (B) TubA-GFP filaments are not observed under Benomyl treatment. (C) TubA-GFP filaments are recovered after switching coverslips to fresh pre-warmed medium; see materials and methods for details. (D) TpmA-GFP filaments (arrow head), localization to tips (*) and septa (S) are not affected by DMSO. (E) TubA-GFP localizations are not observed under Cytochalasin A treatment. (F) TpmA-GFP filaments are recovered after switching coverslips to fresh pre-warmed medium; see materials and methods for details. Conditions as described in Figure 3.7. Live microscopy was used. Photoshop CS3 was used to combine, overlay, organize and improve contrast and brightness of DIC and fluorescent micrographs. Scale bar is 5μm.

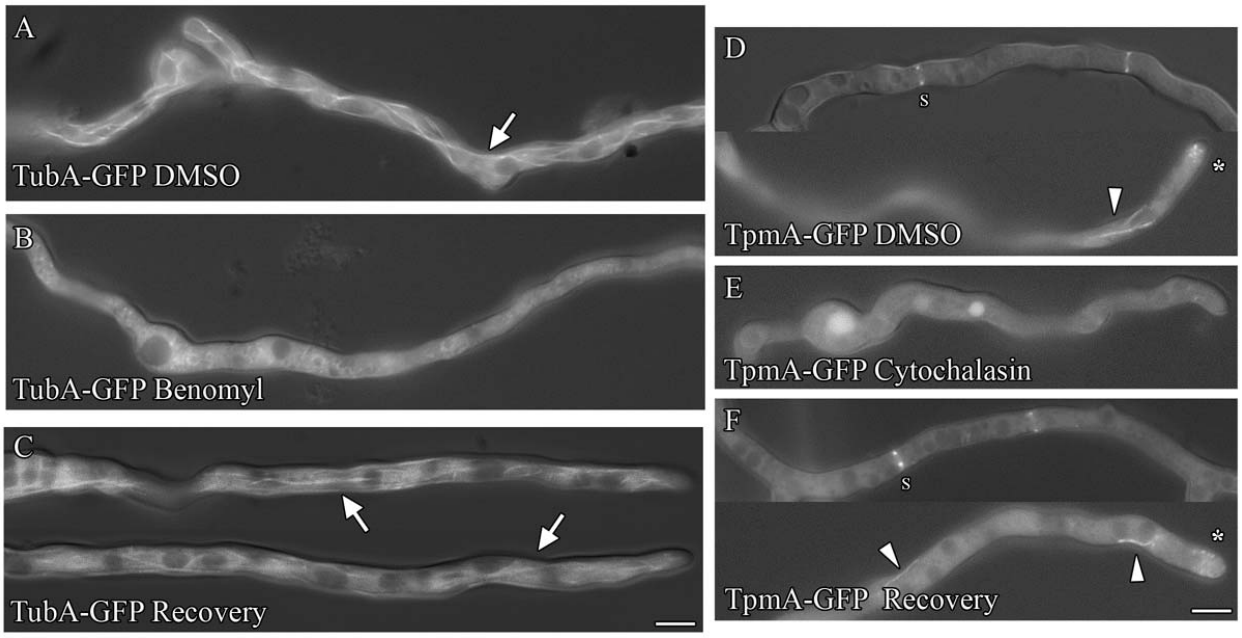
A
TubA-GFP DMSO
B
TubA-GFP Benomyl
C
TubA-GFP Recovery
D
s
*
TpmA-GFP DMSO
E
TpmA-GFP Cytochalasin
F
s
*
TpmA-GFP Recovery

Supplemental Figure 3.5. Wild type hardly shows swelling during branch emergence after recovery from Cytochalsin A treatment. Conditions as described in Figure 3.7 and 3.8 DIC image of wild type during branch emergence after recovery from Cytochalsin A treatment shows normal not swollen hypha. Refer to Figure 3.8 for phenotypic counts. Scale bar is 5µm.

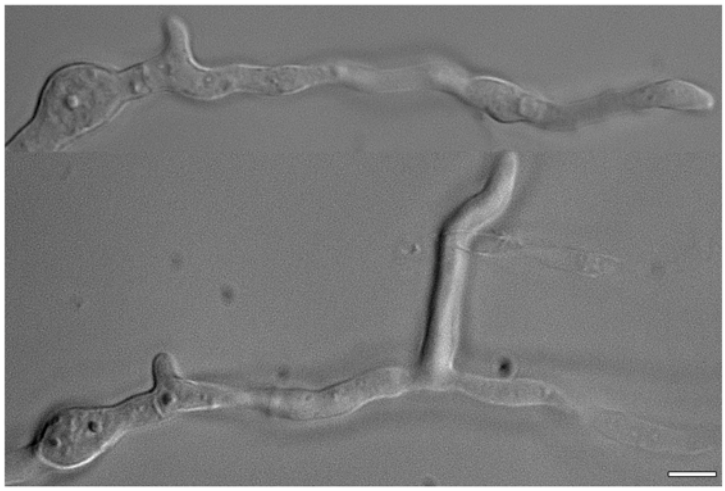

Wild type under Cytochalasin A treatment

References

ALVAREZ-TABARES, I., and J. PEREZ-MARTIN, 2010 Septins from the phytopathogenic fungus Ustilago maydis are required for proper morphogenesis but dispensable for virulence. PLoS ONE **5:** e12933.

AMIN, N. D., Y. L. ZHENG, S. KESAVAPANY, J. KANUNGO, T. GUSZCZYNSKI *et al.*, 2008 Cyclin-dependent kinase 5 phosphorylation of human septin SEPT5 (hCDCrel-1) modulates exocytosis. J Neurosci **28:** 3631-3643.

ARAUJO-BAZAN, L., M. A. PENALVA and E. A. ESPESO, 2008 Preferential localization of the endocytic internalization machinery to hyphal tips underlies polarization of the actin cytoskeleton in Aspergillus nidulans. Mol Microbiol **67:** 891-905.

BEITES, C. L., K. A. CAMPBELL and W. S. TRIMBLE, 2005 The septin Sept5/CDCrel-1 competes with alpha-SNAP for binding to the SNARE complex. Biochem J **385:** 347-353.

BEITES, C. L., H. XIE, R. BOWSER and W. S. TRIMBLE, 1999 The septin CDCrel-1 binds syntaxin and inhibits exocytosis. Nat Neurosci **2:** 434-439.

BERTIN, A., M. A. MCMURRAY, P. GROB, S. S. PARK, G. GARCIA, 3RD *et al.*, 2008 Saccharomyces cerevisiae septins: supramolecular organization of heterooligomers and the mechanism of filament assembly. Proc Natl Acad Sci U S A **105:** 8274-8279.

BERTIN, A., M. A. MCMURRAY, L. THAI, G. GARCIA, 3RD, V. VOTIN *et al.*, 2010 Phosphatidylinositol-4,5-bisphosphate promotes budding yeast septin filament assembly and organization. J Mol Biol **404:** 711-731.

BÖHMER, C., C. RIPP and M. BÖLKER, 2009 The germinal centre kinase Don3 triggers the dynamic rearrangement of higher-order septin structures during cytokinesis in Ustilago maydis. Molecular microbiology **74:** 1484-1496.

CAO, L., W. YU, Y. WU and L. YU, 2009 The evolution, complex structures and function of septin proteins. Cell Mol Life Sci **66:** 3309-3323.

DOUGLAS, L. M., F. J. ALVAREZ, C. MCCREARY and J. B. KONOPKA, 2005 Septin function in yeast model systems and pathogenic fungi. Eukaryot Cell **4:** 1503-1512.

FISCHER-PARTON, S., R. M. PARTON, P. C. HICKEY, J. DIJKSTERHUIS, H. A. ATKINSON *et al.*, 2000 Confocal microscopy of FM4-64 as a tool for analysing endocytosis and vesicle trafficking in living fungal hyphae. J Microsc **198:** 246-259.

GILDEN, J., and M. F. KRUMMEL, 2010 Control of cortical rigidity by the cytoskeleton: emerging roles for septins. Cytoskeleton (Hoboken) **67:** 477-486.

GLADFELTER, A., 2010 Guides to the final frontier of the cytoskeleton: septins in filamentous fungi. Current Opinion in Microbiology.

GLADFELTER, A., J. PRINGLE and D. LEW, 2001 The septin cortex at the yeast mother–bud neck. Curr Opin Microbiol **4:** 681-689.

GLADFELTER, A. S., 2006 Control of filamentous fungal cell shape by septins and formins, pp.

GLADFELTER, A. S., L. KOZUBOWSKI, T. R. ZYLA and D. J. LEW, 2005 Interplay between septin organization, cell cycle and cell shape in yeast. J Cell Sci **118:** 1617-1628.

HANAI, N., K. NAGATA, A. KAWAJIRI, T. SHIROMIZU, N. SAITOH *et al.*, 2004 Biochemical and cell biological characterization of a mammalian septin, Sept11. FEBS Lett **568:** 83-88.

HARRIS, S. D., 2001 Septum formation in Aspergillus nidulans. Curr Opin Microbiol **4:** 736-739.

HELMSTAEDT, K., K. LAUBINGER, K. VOSSKUHL, O. BAYRAM, S. BUSCH *et al.*, 2008 The nuclear migration protein NUDF/LIS1 forms a complex with NUDC and BNFA at spindle pole bodies. Eukaryot Cell **7:** 1041-1052.

HERVAS-AGUILAR, A., and M. A. PENALVA, 2010 Endocytic machinery protein SlaB is dispensable for polarity establishment but necessary for polarity maintenance in hyphal tip cells of Aspergillus nidulans. Eukaryot Cell **9:** 1504-1518.

HORIO, T., and B. R. OAKLEY, 2005 The role of microtubules in rapid hyphal tip growth of Aspergillus nidulans. Mol Biol Cell **16:** 918-926.

JOO, E., M. C. SURKA and W. S. TRIMBLE, 2007 Mammalian SEPT2 is required for scaffolding nonmuscle myosin II and its kinases. Dev Cell **13:** 677-690.

JUVVADI, P. R., J. R. FORTWENDEL, L. E. ROGG and W. J. STEINBACH, 2011 Differential localization patterns of septins during growth of the human fungal pathogen Aspergillus fumigatus reveal novel functions. Biochem Biophys Res Commun **405:** 238-243.

KAFER, E., 1977 Meiotic and mitotic recombination in Aspergillus and its chromosomal aberrations. Adv Genet **19:** 33-131.

KAMINSKYJ, S. G. W., 2001 Fundamentals of growth, storage, genetics and microscopy of Aspergillus nidulans, pp. in *FUNGAL GENETICS NEWSLETTER #48*. Fungal Genetic Stock Center.

KINOSHITA, M., 2003 Assembly of Mammalian Septins, pp. 491-496.

KINOSHITA, M., 2006 Diversity of septin scaffolds. Curr Opin Cell Biol **18:** 54-60.

KINOSHITA, M., C. M. FIELD, M. L. COUGHLIN, A. F. STRAIGHT and T. J. MITCHISON, 2002 Self- and actin-templated assembly of mammalian septins, pp. 791-802.

KINOSHITA, M., S. KUMAR, A. MIZOGUCHI, C. IDE, A. KINOSHITA *et al.*, 1997 Nedd5, a mammalian septin, is a novel cytoskeletal component interacting with actin-based structures. Genes Dev **11:** 1535-1547.

KREMER, B. E., T. HAYSTEAD and I. G. MACARA, 2005 Mammalian septins regulate microtubule stability through interaction with the microtubule-binding protein MAP4. Mol Biol Cell **16:** 4648-4659.

LICHIUS, A., A. BEREPIKI and N. D. READ, 2011 Form follows function-The versatile fungal cytoskeleton. Fungal Biology.

LINDSEY, R., S. COWDEN, Y. HERNANDEZ-RODRIGUEZ and M. MOMANY, 2010a Septins AspA and AspC are important for normal development and limit the emergence of new growth foci in the multicellular fungus Aspergillus nidulans. Eukaryot Cell **9:** 155-163.

LINDSEY, R., Y. HA and M. MOMANY, 2010b A septin from the filamentous fungus A. nidulans induces atypical pseudohyphae in the budding yeast S. cerevisiae. PLoS ONE **5:** e9858.

LINDSEY, R., and M. MOMANY, 2006 Septin localization across kingdoms: three themes with variations. Curr Opin Microbiol **9:** 559-565.

MCMURRAY, M. A., A. BERTIN, G. GARCIA, 3RD, L. LAM, E. NOGALES *et al.*, 2011 Septin filament formation is essential in budding yeast. Dev Cell **20:** 540-549.

MOMANY, M., 2001 Cell biology of the duplication cycle in fungi, pp. 120-125 in *Molecular and Cellular Biology of Filamentous Fungi*, edited by N. TALBOT. Oxford University Press, New York.

NAGATA, K., A. KAWAJIRI, S. MATSUI, M. TAKAGISHI, T. SHIROMIZU *et al.*, 2003 Filament formation of MSF-A, a mammalian septin, in human mammary epithelial cells depends on interactions with microtubules. Journal of Biological Chemistry **278:** 18538-18543.

OH, Y., and E. BI, 2011 Septin structure and function in yeast and beyond. Trends Cell Biol **21:** 141-148.

ORLANDO, K., X. SUN, J. ZHANG, T. LU, L. YOKOMIZO *et al.*, 2011 Exo-endocytic trafficking and the septin-based diffusion barrier are required for the maintenance of Cdc42p polarization during budding yeast asymmetric growth. Mol Biol Cell **22:** 624-633.

PABLO-HERNANDO, M. E., Y. ARNAIZ-PITA, H. TACHIKAWA, F. DEL REY, A. M. NEIMAN *et al.*, 2008 Septins localize to microtubules during nutritional limitation in Saccharomyces cerevisiae. BMC Cell Biol **9:** 55.

PEARSON, C., K. XU, K. SHARPLESS and S. HARRIS, 2004 MesA, a novel fungal protein required for the stabilization of polarity axes in Aspergillus nidulans. Molecular Biology of the Cell **15:** 3658.

PENALVA, M. A., 2010 Endocytosis in filamentous fungi: Cinderella gets her reward. Curr Opin Microbiol **13:** 684-692.

SCHMIDT, K., and B. J. NICHOLS, 2004a A barrier to lateral diffusion in the cleavage furrow of dividing mammalian cells. Curr Biol **14:** 1002-1006.

SCHMIDT, K., and B. J. NICHOLS, 2004b Functional interdependence between septin and actin cytoskeleton. BMC Cell Biol **5:** 43.

SILVERMAN-GAVRILA, R., and L. SILVERMAN-GAVRILA, 2008 Septins: new microtubule interacting partners. ScientificWorldJournal **8:** 611-620.

SPILIOTIS, E., S. HUNT, Q. HU, M. KINOSHITA and W. NELSON, 2008 Epithelial polarity requires septin coupling of vesicle transport to polyglutamylated microtubules. Journal of Cell Biology **180:** 295.

SPILIOTIS, E., and W. NELSON, 2006 Here come the septins: novel polymers that coordinate intracellular functions and organization. Journal of Cell Science **119:** 4.

SPILIOTIS, E. T., 2010 Regulation of microtubule organization and functions by septin GTPases. Cytoskeleton **67:** 339-345.

SUELMANN, R., and R. FISCHER, 2000 Nuclear migration in fungi--different motors at work. Res Microbiol **151:** 247-254.

SURKA, M. C., C. W. TSANG and W. S. TRIMBLE, 2002 The mammalian septin MSF localizes with microtubules and is required for completion of cytokinesis. Mol Biol Cell **13:** 3532-3545.

TADA, T., A. SIMONETTA, M. BATTERTON, M. KINOSHITA, D. EDBAUER *et al.*, 2007 Role of Septin cytoskeleton in spine morphogenesis and dendrite development in neurons. Current Biology **17:** 1752-1758.

TANAKA-TAKIGUCHI, Y., M. KINOSHITA and K. TAKIGUCHI, 2009 Septin-mediated uniform bracing of phospholipid membranes. Curr Biol **19:** 140-145.

VEITH, D., N. SCHERR, V. P. EFIMOV and R. FISCHER, 2005 Role of the spindle-pole-body protein ApsB and the cortex protein ApsA in microtubule organization and nuclear migration in Aspergillus nidulans. J Cell Sci **118:** 3705-3716.

VERSELE, M., and J. THORNER, 2005 Some assembly required: yeast septins provide the instruction manual. Trends Cell Biol **15:** 414-424.

WESTFALL, P. J., and M. MOMANY, 2002 Aspergillus nidulans septin AspB plays pre- and postmitotic roles in septum, branch, and conidiophore development. Mol Biol Cell **13:** 110-118.

WU, J. Q., J. R. KUHN, D. R. KOVAR and T. D. POLLARD, 2003 Spatial and temporal pathway for assembly and constriction of the contractile ring in fission yeast cytokinesis. Dev Cell **5:** 723-734.

XIANG, X., S. BECKWITH and N. MORRIS, 1994 Cytoplasmic dynein is involved in nuclear migration in Aspergillus nidulans. Proceedings of the National Academy of Sciences **91:** 2100-2104.

XIANG, X., and R. FISCHER, 2004 Nuclear migration and positioning in filamentous fungi. Fungal Genet Biol **41:** 411-419.

XIE, Y., J. P. VESSEY, A. KONECNA, R. DAHM, P. MACCHI *et al.*, 2007 The GTP-binding protein Septin 7 is critical for dendrite branching and dendritic-spine morphology. Curr Biol **17:** 1746-1751.

YAMAMOTO, A., and Y. HIRAOKA, 2003 Cytoplasmic dynein in fungi: insights from nuclear migration. J Cell Sci **116:** 4501-4512.

YANG, L., L. UKIL, A. OSMANI, F. NAHM, J. DAVIES *et al.*, 2004 Rapid Production of Gene Replacement Constructs and Generation of a Green Fluorescent Protein-Tagged Centromeric Marker in Aspergillus nidulans, pp. Am Soc Microbiol.

ZEKERT, N., and R. FISCHER, 2009 The Aspergillus nidulans kinesin-3 UncA motor moves vesicles along a subpopulation of microtubules. Molecular Biology of the Cell **20:** 673.

CHAPTER 4

CONCLUSIONS AND FUTURE EXPERIMENTS

Cells synchronize different processes through the interaction of organelles with a variety of machineries made of proteins, vesicles and/or enzymes to function and survive. Many of these interactions occur through the cell cytoskeleton, which is also key for providing cell structure and shape. Fungal cells have 3 cytoskeletons: actin, microtubules and septins. Actin and microtubules have been extensively studied for many years in a variety of model systems. Septins have been recently accepted as a cytoskeleton and its roles are less understood. Many questions remain in the field on how the cell cytoskeletons communicate. It has been suggested that septins might bridge these interactions (LICHIUS *et al.* 2011). Septins are an interesting group of proteins to study because of the diverse roles they play (BERTIN *et al.* 2008; CAO *et al.* 2009; DOUGLAS *et al.* 2005; GLADFELTER 2006; GLADFELTER *et al.* 2005; KINOSHITA 2006; KREMER *et al.* 2005; LICHIUS *et al.* 2011; LINDSEY and MOMANY 2006; MCMURRAY *et al.* 2011; OH and BI 2011; RODAL *et al.* 2005; SPILIOTIS and NELSON 2006a; SPILIOTIS and NELSON 2006b; VERSELE and THORNER 2005). Still, their roles seem to depend on the model system and/or the cell type being studied. Our work has focused on understanding septins roles in polar growth and their interaction with other cell cytoskeletons. Here we show that the septin AspB in *Aspergillus nidulans* plays roles in growth emergence. Our work also shows that AspB might interact with actin and microtubules. It is plausible to think that septins play roles in growth emergence by bridging interactions between the other cell cytoskeletons and their accessory proteins.

The first study on the septin AspB attempted to construct a knockout strain whose isolation depended on its ability to conidiate, and because a deletion mutant was never recovered it was identified as an essential gene (Momany and Hamer 1996). A second study identifying all septins in *Aspergillus nidulans* (AspA, AspB, AspC, AspD and AspE) showed that AspB is the mostly highly expressed septin during conidiation (MOMANY *et al.* 2001). In a third study, temperature sensitive mutants were used to characterize AspB, showing phenotypic abnormalities, irregular septa, high numbers of branches, and immature asexual reproductive structures (Westfall and Momany 2002). Polyclonal α-AspB antibodies showed that AspB localizes premitotically as a ring at sites of branching and secondary germ tube emergence and postmitotically to septation sites dependent on actin. Also, AspB antibodies labeled conidiophores transiently to the vesicle/metula and metula/phialide interfaces, and persistently to the phialide/conidiospore interface (Westfall and Momany 2002).

New gene targeting techniques for *Aspergillus nidulans* were described by Yang et al that provided a new era for studying, tagging and deleting genes (YANG *et al.* 2004). Using these techniques our lab decided to delete and construct protein tags for all septin genes. *aspB* was included in the study to ensure that it was essential. Surprisingly a deletion mutant for *aspB* was isolated and it showed very poor conidiation and abnormal colony coloration which explains why it was not isolated in the first study. None of the septins have been shown to be essential in *Aspergillus nidulans* and the characterization of AspA and AspC have been published, AspB is shown here and AspD and AspE are currently ongoing.

aspB-gfp and Δ*aspB* strains started the dissertation project presented here. The phenotypic characterization and localization studies provide powerful insights for understanding septin functions and allow us to hypothesize possible roles that will drive future research. In this

conclusion I will review all the phenotypes and localization studies presented in this dissertation and will use it as a base for hypothesizing and proposing possible roles and suggesting future experiments that could address these ideas.

AspB play roles in growth emergence and nuclear dynamics, and shows abnormal endocytic zones

Septins were first discovered in yeast for their roles in cell division and some septins were shown to be essential. Yeast show very limited polar growth during bud emergence which reverts back to isotropic growth, compared to filamentous fungi who exhibit a small window of isotropic growth, as they break dormancy, and committed nonreversible polar growth once the germ tube emerges. Septins have been extensively studied in yeast, and though studies are still ongoing, it serves as a basic model from which roles can be extrapolated to other systems. Studying septins in mammalian models brings further complications as humans have 14 septins with differential splicing that can add up to 30 different septin proteins. Still many studies in animal cells also allow us to extrapolate findings to simpler model systems. Studying septins in the filamentous fungus *Aspergillus nidulans* allows for a closer understanding of septin roles in multicellular organisms, as growth is divided by crosswalls creating different compartments that remain connected making it a multicellular organism, and roles in highly polar cells such as neurons.

When we recovered *aspB* deletion mutants we decided to characterize its phenotype throughout fungal growth and asexual reproduction and use nuclear and chitin staining to assess further roles. We assessed the number of nuclei in the freshly isolated conidia and noticed that a significant percentage of the population showed binucleated conidia when wild type shows uninucleated conidia. Because septins play roles in nuclear division in both yeast and animals,

this finding made us think of several possible scenarios taking place in the Δ*aspB* conidia: 1) conidia in Δ*aspB* germinate quicker and therefore display double the nuclear content compare to wild type, 2) conidia in Δ*aspB* do not arrest in interphase as wild type conidia do until the appropriate carbon source is sensed, 3) nuclear division in the phialide-conidia interface of the conidiophore is abnormal in Δ*aspB* and more nuclei are encapsulated in the conidia and/or 4) nuclear migration in the phialide-conidia interface of the conidiophore in Δ*aspB* is abnormal and more nuclei are encapsulated in the conidia. To distinguish from these scenarios several things could be done. For scenario #1, counts of wild type vs. Δ*aspB* at the same time point can be used to assess whether both strains are germinating at the same time. To quickly assess this phenotype, we did Hoechst staining of conidiophores and did counts of wild type vs. Δ*aspB* to assess whether they are germinating at the same time point. Staining of nuclei in conidiophores didn't provide much clues and it seemed that the number of nuclei in conidia was normal, but because these structures are thick with many conidia attached, focal resolution was not clear and perhaps Confocal microscopy could help clear these results. On the other hand, time point counts did reveal some clues. We found that Δ*aspB* strains germinated earlier than wild type as freshly harvested spores inoculated at the same time, concentration, media and temperature as wild type resulted in Δ*aspB* polarizing conidia while the majority of cells in wild type were still undergoing isotropic expansion. This hinted at the possibility that Δ*aspB* conidia are germinating earlier than wild type, though the exact reason is still not clear. For scenario #2, Flow cytometry could be used to compare the nuclear content of Hoechst stained nuclei of wild type vs. Δ*aspB*. For scenarios #3 and #4 nuclear staining and Confocal microscopy of conidiophores can provide clues. Time lapse and confocal microscopy of Δ*aspB* in combination with nuclear division mutants and/or markers, nuclear migration mutants and/or microtubule markers can be used to

see if nuclear division and/or migration is abnormal. We did attempt to look at microtubules in the Δ*aspB* strain to see if there were any abnormalities in conidiophores, but again the resolution at which we examined didn't provide clear results.

We also found that Δ*aspB* strains showed multiple germtubes. This phenotype was also reported for Δ*aspA* and Δ*aspC* but not to the extreme displayed by Δ*aspB*. During germtube emergence wild type forms 1 germtube per conidium which extends to form the hypha and later on produces a secondary germtube from the same conidium. In Δ*aspB*, 2-4 germtubes will emerge almost simultaneously from the same conidium. This hypergermtube emergence phenotype hints at two possible roles for AspB in growth emergence: 1) AspB acts as a negative regulator for growth, so that more sites are available for growth emergence in the absence of AspB, 2) AspB selects the area of growth by maintaining the growth machinery localized to one specific area, so that the polar machinery is diffused and growth emergences from several sites in the absence of AspB, 3) cytoskeletal elements involved in recruitment, maintenance and trafficking of the polarity machinery are disorganized in the absence of AspB and promote hyperemergence of growth. To assess scenario #1, overexpression mutants can be used, expecting that if AspB is a negative regulator of growth, then overexpression of AspB would reduce germtube emergence. We attempted to do so, but Real Time PCR showed that we fail to obtain overexpression of AspB and because of the puzzling results from the constructs we decided to explore overexpression phenotypes later on. For assessing scenario #2, polarity markers can be used, such as Cdc42 or the Tea proteins, and follow their localization in Δ*aspB*. Unfortunately there is no Spitzenkörper at this early stage to assess mislocalization or the presence of multiple Spitzenkörpers to evaluate if different polarity machinery centers are assembled at the same time, but the use of polarity markers should help answer this question. To

assess scenario #3, septin deletions phenotypes can be assessed in the absence of actin and microtubules. We studied this last scenario by depolymerizing both cytoskeletons in the absence of AspB. We found that depolymerization of microtubules, but not actin, in Δ*aspB* reduced hypergermtube emergence. This hints that septins organize/stabilize microtubules during germtube emergence.

Interestingly, though septins are key for cytokinesis in budding yeast and animal cells, we found that septation, which is *A. nidulans* equivalent to cytokinesis, is not disrupted but delayed. In *A. nidulans* the formation of cross walls called septa compartmentalize growth forming actively growing apical compartments and subapical compartments arrested in growth until the emergence of a branch (HARRIS 2001; HARRIS *et al.* 1994; MOMANY and HAMER 1997; MOMANY and TAYLOR 2000). Septation occurs concomitant with the third nuclear division and a hyphal size threshold (WOLKOW *et al.* 1996). We found that in Δ*aspB* septation was delayed as at a set time point Δ*aspB* hardly showed septated hyphae while the majority of hyphae in wild type were septated. Interestingly, branching in Δ*aspB* initiated before septation which was not seen in wild type. These phenotypes hint that perhaps AspB is not required for septation and in its absence recruitment, trafficking and/or maintenance of the septation related machinery is abnormal and/or delayed. To assess this scenario time lapse microcopy can be used to follow the localization of the septation related machinery during septum formation in wild type compared to Δ*aspB* and assess whether the recruitment and or maintenance of this machinery is abnormal in Δ*aspB.* We also noticed that Calcofluor staining of septa in Δ*aspB* bleached faster than in wild type, hinting that there are some abnormalities in the septum composition. To assess these abnormalities TEM analysis and chitin labeling could be done to compare wild type and Δ*aspB* septa morphology and composition.

We also found that Δ*aspB* strains showed hyperemergence of branches. This phenotype was also reported for Δ*aspA* and Δ*aspC*, but again not to the extreme displayed by Δ*aspB*. During branch emergence wild type forms 1-2 branches per compartment. In Δ*aspB*, we saw the emergence of numerous branches from the same compartment and some branches were abnormally thin and hooked. These branches seem abortive as they did not extend at later time points. These phenotypes hint at possible defects and roles: 1) As proposed for germtube emergence, AspB acts as a negative regulator for growth, so that in the absence of AspB, more sites are available for growth emergence, 2) As proposed for germtube emergence, AspB selects the area of growth by maintaining the growth machinery localize to one specific area, so that in the absence of AspB the polar machinery is diffused and growth emergences from several sites, 3) because Δ*aspB* showed branching before septation and multiple abnormal branches emergence, perhaps delayed septation impedes compartmentalization of the growth machinery that allows for the emergence of 1-2 branches per compartment and therefore a diffuse machinery initiates multiple branches simultaneously, but only the ones with the appropriate amount of polarity factors are able to maintain polarity and the remaining display abnormal morphologies and abort growth, and/or 4) perhaps cytoskeletal elements involved in requirement, maintenance and trafficking of the polarity machinery are disorganized in the absence of AspB promoting hyperemergence of growth and only the axes where the cytoskeletons continue to be present are able to maintain polar growth. To assess scenario #1 overexpression of the septins can be used to determine if they are negative regulators and if so we would expect a reduction in the emergence of growth upon overexpression. For scenarios #2 and #3 localization of polarity markers can be followed by time lapse microscopy to identify if the machinery is diffused and mislocalized at certain developmental stages in Δ*aspB*. For

scenario #4, septin deletion phenotypes can be assessed in the absence of actin and microtubules. We studied this last scenario by depolymerizing both cytoskeletons in the absence of AspB. We found that depolymerization of microtubules, but not actin, reduced hyperbranch emergence in Δ*aspB*. This hints that septins organize/stabilize microtubules during branch emergence. Interestingly, actin depolymerization during branch emergence in Δ*aspB* resulted in polarity defects (swelling and lysis) hinting that septins organize/stabilize actin for normal polar growth during branch emergence.

When isolating Δ*aspB* we noticed that colonies were brown-pink on plates, looked very sick and produced very little conidia. Higher resolution studies showed that conidiophores were abnormal in 100% of the population. These displayed merged layers and/or absence of layers, high deposition of chitin in the phialide-conidia interphase and poor production of conidia. These phenotypes show that AspB is key for asexual reproduction and conidiophore morphology, but how exactly it controls it is not understood. Perhaps construction of double mutants of *aspB* and genes already identified to play roles in conidiation can be assessed to find interactions and indentify pathways in which AspB might be working.

Nuclear related phenotypes were also observed in hyphae of Δ*aspB*. We observed clumping of nuclei particularly near branches and a high number of nuclei in conidial compartments of older hyphae. These phenotypes point to several possible roles: 1) AspB is part of the nuclear migration machinery in *A. nidulans*, and/or 2) nuclear division is continuous or abnormal in conidial compartments. To evaluate scenarios #1 and #2 time lapse microscopy using microtubule and nuclear labels in Δ*aspB* can be used to follow nuclear division and migration. We assessed microtubules in Δ*aspB* strains and observed less bundles in hyphae and

less bundles invading newly formed branches. These particular phenotypes also support that in the absence of AspB, reduced microtubule bundles could result in abortive branches in Δ*aspB*.

Endocytosis is important for polar growth (Penalva 2010). Because we observed hyperemergence of growth in Δ*aspB* we assessed endocytosis in this mutant. We found that endocytic zones are of abnormal size and abnormally positioned in Δ*aspB* as the SlaB endocytic marker showed smaller zones and none or less exclusion from hyphal tips compared to wild type. These phenotypes point that endocytosis is abnormal in Δ*aspB* and/or perhaps endocytic vesicles are targeted or moved to inappropriate zones leaving the machinery diffused or attached to abnormal areas and promoting hyperemergence of growth. These ideas could be assessed by time lapse microscopy and FRAP of endocytic markers and following their recycling and destinations. Actin and microtubule labels could be added to these experiments to complement the proposed ideas of cytoskeleton disorganization promoting hyperemergence of growth.

AspB forms bars and filaments, interacts with AspA, AspC and AspE, and colocalizes with nuclei, actin and microtubules

We found that AspB localizes throughout development and growth. In dormant conidia we observed the localization of AspB bars. The presence of bars in dormant spores shows that the AspB septin structure is assembled before isotropic and polar growth. From these observations we can propose that these bars might be storage areas of preassembled septins that are “ready to go” when the cell breaks dormancy and starts growth. Another possibility is that this bar serves as a diffusion barrier that allows for the emergence of growth in only one area of the conidium and maintains polarity related machinery localized and concentrated to the hemisphere of the conidium where growth will emerge. To assess these ideas, time lapse of Cdc42, other polarity establishment machinery, actin and microtubules could be followed and

colocalized as the cell breaks dormancy, grows isotropically and initiates polar growth. These experiments will provide great insights on why the septins bars are present in dormant cells and persist throughout germtube emergence. To assess if AspB bars are storage areas, FRAP can be used in conjunction to the above experiments and see how septin dynamics affect polarity establishment dynamics and germ tube emergence. Because septins have been shown to be recycled in *S. cerevisiae*, it would be interesting to follow the fate of "pre-assembled septins" compared to new septins similar to what was done by the Thorner lab in *S. cerevisiae* (McMurray and Thorner 2008). We also observed the formation of rings at the base of emerging growth (germtubes, branches and conidiophore layers) hinting that AspB shapes and/or controls the emergence of growth. In conjunction to the deletion phenotypes and experiments described above to understand septin roles in the control of growth emergence, FRAP experiments could also assess what would happen to the emergence of growth in relation to septin dynamics and how AspB ring dynamics compare to rings in *S. cerevisiae*.

In elongated hyphae we observed filaments that localized to areas of active growth and bars that remained localized to subapical areas with no growth emergence. These two structures could be displaying different roles. Bars could be: 1) negatively regulating the emergence of growth in those areas, 2) pre-assembled septins ready to go for when new growth is added and/or 3) could be forming diffusion barriers to ensure that the polarity machinery is recruited and or remains localized to areas for new growth. To assess these ideas, experiments proposed in the previous section looking at the machinery dynamics in the absence of septins, with FRAP of the septin bars and following the effects on localization of the growth machinery could help distinguish between these scenarios. We have seen that AspB can colocalize with microtubules, the UncA kinesin motor and actin endocytic vesicles and in Δ*aspB* growth emergence is

abnormal and endocytic zones are abnormally position and of abnormal length. Perhaps AspB filaments at tips help to bridge interactions of actin and microtubules and the polarity machinery to ensure normal polar growth. Time lapse microscopy and colocalization of septins, actin, microtubules, endocytic vesicles and associated proteins, will help assess these possible roles.

We also observed the localization of bars and filaments to conidiophores as well as rings at the base of emerging layers. AspB bars were only seen in regions where layers were not actively emerging. The presence of septin bars in dormant conidia and quiescent regions of hyphae and conidiophores is consistent with bars playing a role in suppressing emergence of new growth and experiments like the ones proposed above could also address this in conidiophores.

Septins form heteropolymers and the absence of certain septins can affect complex assembly and function (AN *et al.* 2004; BERTIN *et al.* 2008; BERTIN *et al.* 2010; CAO *et al.* 2009; MCMURRAY *et al.* 2011; OH and BI 2011; SPILIOTIS and NELSON 2006b; VERSELE *et al.* 2004; VERSELE and THORNER 2005). We observed that AspB structures could be affected in the absence of septin partners. In the absence of AspA, AspC and both, all AspB structures were lost and only cytoplasmic fluorescence was observed. In elongated hyphae of Δ*aspE*, AspB filaments and bars were extremely reduced. This shows that septin–septin interactions are needed for bars and filament structures of AspB, that AspA and AspC interact with AspB and that perhaps AspE, a septin only found in filamentous fungi, helps stabilize filaments in longer polar cells. To further assess these interactions our lab is working on following structures of all septins in different septin deletion backgrounds. Also, preliminary experiments, not shown in this dissertation, showed that in protein pull downs using AspB as bait, septins AspA, B, C and D were identified. Further protein immunoprecipitation and MS analyses as well as colocalization studies and protein crystallography will help understand septin-septin interactions.

We also found that AspB colocalized with microtubules, tyrosinolated microtubules and UncA bound microtubules. This data does not address direct interaction between septins and microtubules, but the AspB localization near and between nuclei, nuclei clumping in Δ*aspB*, AspB colocalization with microtubules, AspB abnormal filaments after depolymerization of microtubules, microtubule bundle defects in Δ*aspB*, and reduced hypergrowth emergence in Δ*aspB* after depolymerization of microtubules, hint at septin-microtubule interactions. Perhaps septins interact with microtubules for nuclear migration and the experiments described above can help address this. Perhaps septins interact with microtubules during growth emergence and the experiments described above can also address this as well as colocalization and time lapse studies of AspB with microtubule binding proteins and motors and time lapse microscopy of microtubule motors in Δ*aspB*. In addition septin protein pull downs may identify proteins that bind or interact with microtubules which will also help understand their interaction.

We found that AspB colocalized with AbpA labeled vesicles and therefore actin as AbpA is an actin binding protein. This data does not address direct interaction between septins and actin, but the AspB colocalization with AbpA, previously reported septin localization to septa being dependent on actin (Westfall and Momany 2002), AspB abnormal free-floating cytoplasmic rings after depolymerization of actin, loss of tropomyosin TpmA localization to actin filaments and faint localization to septa in Δ*aspB*, and polarity defects during branch emergence after actin depolymerization in Δ*aspB*, hint at septin-actin interaction. Perhaps septins interact with actin during growth emergence and the experiments described above can also address this. The fact that tropomyosin, which blocks myosin motors from actin filaments, is lost from actin filaments in Δ*aspB*, suggests that hypergrowth emergence could be caused by hyperaccess of myosin to actin filaments. Following myosin motors along actin filaments by

time lapse microscopy in Δ*aspB* could provide clues as well as colocalization and time lapse studies of AspB with myosin motors.

Concluding perspective

In general there are many tools in *Aspergillus nidulans* including a classical genetic system with many mutants and proteins tags available for assessing the proposed scenarios. Time lapse and Confocal microscopy are powerful tools for assessing many of these hypotheses in the septin deletion mutants and colocalization dynamics with fluorescent protein tags. Also, Electron microscopy could answer many questions related to cell wall and morphological abnormalities observed in Δ*aspB*. We are continuing studies with AspB and investigating its interactions with actin and microtubules and their associated proteins. In addition we will conduct septin-septin and septin-protein interaction studies looking at proteins that interact with AspB at certain developmental stages and monitor *aspB* expression patterns from germination to septation. All these studies will possibly show septins diverse roles in nuclear dynamics, morphology, growth and its interaction with other cytoskeletons. We expect that these studies will further support the idea that the key to septin function in any organism or in any moment in development is based on its structural arrangements and protein partners.

References

AN, H., J. L. MORRELL, J. L. JENNINGS, A. J. LINK and K. L. GOULD, 2004 Requirements of fission yeast septins for complex formation, localization, and function. Mol Biol Cell 15: 5551-5564.

BERTIN, A., M. A. MCMURRAY, P. GROB, S. S. PARK, G. GARCIA, 3RD *et al.*, 2008 Saccharomyces cerevisiae septins: supramolecular organization of heterooligomers and the mechanism of filament assembly. Proc Natl Acad Sci U S A 105: 8274-8279.

BERTIN, A., M. A. MCMURRAY, L. THAI, G. GARCIA, 3RD, V. VOTIN *et al.*, 2010 Phosphatidylinositol-4,5-bisphosphate promotes budding yeast septin filament assembly and organization. J Mol Biol 404: 711-731.

CAO, L., W. YU, Y. WU and L. YU, 2009 The evolution, complex structures and function of septin proteins. Cell Mol Life Sci 66: 3309-3323.

DOUGLAS, L. M., F. J. ALVAREZ, C. MCCREARY and J. B. KONOPKA, 2005 Septin Function in Yeast Model Systems and Pathogenic Fungi, pp. Am Soc Microbiol.

GLADFELTER, A. S., 2006 Control of filamentous fungal cell shape by septins and formins. Nat Rev Microbiol 4: 223-229.

GLADFELTER, A. S., L. KOZUBOWSKI, T. R. ZYLA and D. J. LEW, 2005 Interplay between septin organization, cell cycle and cell shape in yeast. J Cell Sci 118: 1617-1628.

HARRIS, S. D., 2001 Septum formation in Aspergillus nidulans. Curr Opin Microbiol 4: 736-739.

HARRIS, S. D., J. L. MORRELL and J. E. HAMER, 1994 Identification and characterization of Aspergillus nidulans mutants defective in cytokinesis. Genetics 136: 517-532.

KINOSHITA, M., 2006 Diversity of septin scaffolds. Curr Opin Cell Biol 18: 54-60.

KREMER, B. E., T. HAYSTEAD and I. G. MACARA, 2005 Mammalian septins regulate microtubule stability through interaction with the microtubule-binding protein MAP4. Mol Biol Cell 16: 4648-4659.

LICHIUS, A., A. BEREPIKI and N. D. READ, 2011 Form follows function-The versatile fungal cytoskeleton. Fungal Biology.

LINDSEY, R., and M. MOMANY, 2006 Septin localization across kingdoms: three themes with variations. Curr Opin Microbiol 9: 559-565.

MCMURRAY, M., and J. THORNER, 2008 Septin Stability and Recycling during Dynamic Structural Transitions in Cell Division and Development. Current Biology 18: 1203-1208.

MCMURRAY, M. A., A. BERTIN, G. GARCIA, 3RD, L. LAM, E. NOGALES *et al.*, 2011 Septin filament formation is essential in budding yeast. Dev Cell 20: 540-549.

MOMANY, M., and J. HAMER, 1997 Septation in Aspergillus nidulans. Cell motility and the cytoskeleton 38: 373-384.

MOMANY, M., and J. E. HAMER, 1996 The Aspergillus nidulans septin encoding gene, aspB, is essential for growth. Fungal Genet Biol 21: 92-100.

MOMANY, M., and I. TAYLOR, 2000 Landmarks in the early duplication cycles of Aspergillus fumigatus and Aspergillus nidulans: polarity, germ tube emergence and septation. Microbiology-Sgm 146: 3279-3284.

MOMANY, M., J. ZHAO, R. LINDSEY and P. J. WESTFALL, 2001 Characterization of the Aspergillus nidulans septin (asp) gene family. Genetics 157: 969-977.

OH, Y., and E. BI, 2011 Septin structure and function in yeast and beyond. Trends Cell Biol 21: 141-148.

PENALVA, M. A., 2010 Endocytosis in filamentous fungi: Cinderella gets her reward. Curr Opin Microbiol 13: 684-692.

RODAL, A. A., L. KOZUBOWSKI, B. L. GOODE, D. G. DRUBIN and J. H. HARTWIG, 2005 Actin and septin ultrastructures at the budding yeast cell cortex. Mol Biol Cell 16: 372-384.

SPILIOTIS, E., and W. NELSON, 2006a Here come the septins: novel polymers that coordinate intracellular functions and organization, pp. 4-10. © The Company of Biologists Limited 2006.

SPILIOTIS, E. T., and W. J. NELSON, 2006b Here come the septins: novel polymers that coordinate intracellular functions and organization. J Cell Sci 119: 4-10.

VERSELE, M., B. GULLBRAND, M. J. SHULEWITZ, V. J. CID, S. BAHMANYAR *et al.*, 2004 Protein-protein interactions governing septin heteropentamer assembly and septin filament organization in Saccharomyces cerevisiae. Mol Biol Cell 15: 4568-4583.

VERSELE, M., and J. THORNER, 2005 Some assembly required: yeast septins provide the instruction manual. Trends Cell Biol 15: 414-424.

WESTFALL, P. J., and M. MOMANY, 2002 Aspergillus nidulans septin AspB plays pre- and postmitotic roles in septum, branch, and conidiophore development. Mol Biol Cell 13: 110-118.

WOLKOW, T., S. HARRIS and J. HAMER, 1996 Cytokinesis in Aspergillus nidulans is controlled by cell size, nuclear positioning and mitosis. Journal of Cell Science 109: 2179.

YANG, L., L. UKIL, A. OSMANI, F. NAHM, J. DAVIES *et al.*, 2004 Rapid Production of Gene Replacement Constructs and Generation of a Green Fluorescent Protein-Tagged Centromeric Marker in Aspergillus nidulans, pp. Am Soc Microbiol.

CHAPTER 5

APPENDICES

GROWTH POLARITY[1]

SEPTINS ASPA AND ASPC ARE IMPORTANT FOR NORMAL DEVELOPMENT AND LIMIT THE EMERGENCE OF NEW GROWTH FOCI IN THE MULTICELLULAR FUNGUS *ASPERGILLUS NIDULANS*[1]

ASPERGILLUS TERREUS ACCESSORY CONIDIA ARE MULTINUCLEATED, HYPERPOLARIZING STRUCTURES THAT DISPLAY DIFFERENTIAL DECTIN STAINING AND CAN INDUCE HEIGHTENED INFLAMMATORY RESPONSES IN A PULMONARY MODEL OF ASPERGILLOSIS[1]

[1] Reprinted here with permission of publisher.

Aspergillus fumigatus and Aspergillosis
Edited by J.-P. Latgé and W. J. Steinbach

Chapter 11

Growth Polarity

MICHELLE MOMANY AND YAINITZA HERNÁNDEZ-RODRÍGUEZ

ASPERGILLOSIS AND POLAR GROWTH

All filamentous fungi use highly polar extension, adding new materials to the tips of hyphae and branches, to explore their environments in search of nutrients. Highly polar growth allows *Aspergillus fumigatus* to explore and invade blood vessels and tissues, resulting in the necrosis characteristic of invasive aspergillosis (Denning and Stevens, 1990; Latgé, 2001).

The small (3-μm) conidia of *A. fumigatus* are ubiquitous in the environment and are frequently inhaled (Beffa et al., 1998; Latgé, 2001; Pitt, 1994). In individuals with competent immune systems, alveolar macrophages and neutrophils internalize and destroy conidia before they cause disease. Conidia can also be internalized by cells which do not destroy them. Endothelial and epithelial cells have been shown to take up conidia (Lopes Bezerra and Filler, 2004; Paris et al., 1997; Wasylnka and Moore, 2002). Conidia within epithelial lung cells eventually germinate and grow. Their hyphae penetrate the cell from the inside and escape to the extracellular space (Wasylnka and Moore, 2002).

A. fumigatus conidia that survive to germinate eventually elaborate hyphae that invade blood vessels and from there disseminate to other sites in the host (Denning et al., 1992; Latgé, 1999) and continue to extend by polar growth, forming the filamentous, branching network common in histological sections from invasive aspergillosis patients.

A. FUMIGATUS POLAR GROWTH IN VITRO

Most of the more detailed knowledge we have of polar growth in *A. fumigatus* has come from in vitro characterization of early development in both *A. fumigatus* and *Aspergillus nidulans*. One thing that is clear from in vitro studies is that early development is characterized by predictable, synchronous switches between isotropic (round) and polar (tubular) morphologies. Dormant conidia are round with a uniform size and nuclei arrested in interphase (Bergen and Morris, 1983; Harris, 1997; Robinow and Canten, 1969). When *A. fumigatus* conidia are inoculated into medium containing a carbon source, they break dormancy and begin synchronous nuclear division and morphological development. Nuclear division and morphological development remain roughly synchronous for several nuclear divisions, at about 12 h in rich medium at 37°C (Fig. 1) (Momany and Taylor, 2000; A. Breakspear and M. Momany, unpublished data). After breaking dormancy conidia expand isotropically for approximately 4 h at 37°C. They polarize and send out the first germ tube by 6 h. Germ tubes continue polar growth to become hyphae, with the first septa forming near the bases of the hyphae by 10 h. At about the same time, the first branches emerge on the apical sides of septa. Hyphae continue polar growth, extending and branching to give rise to visible colonies by 24 h (Fig. 2). Within 36 h conidiophores develop. These asexual reproductive structures include several isotropic cell layers and produce isotropic dormant conidia, beginning the whole cycle again.

MECHANISMS OF FUNGAL POLARITY

Saccharomyces cerevisiae undergoes polar growth, although the growth is less dramatic than that seen in filamentous fungi (Pruyne and Bretscher, 2000). Unbudded yeast cells expand isotropically, switching to polar growth with bud emergence. For bud expansion, growth is once more isotropic. In a broad overview, polar growth in *S. cerevisiae* can be thought of as having three steps: (i) cortical markers specify the position for polar growth; (ii) signaling proteins such as the Rho GTPase

Michelle Momany and Yainitza Hernández-Rodríguez • Dept. of Plant Biology, University of Georgia, Athens, GA 30602.

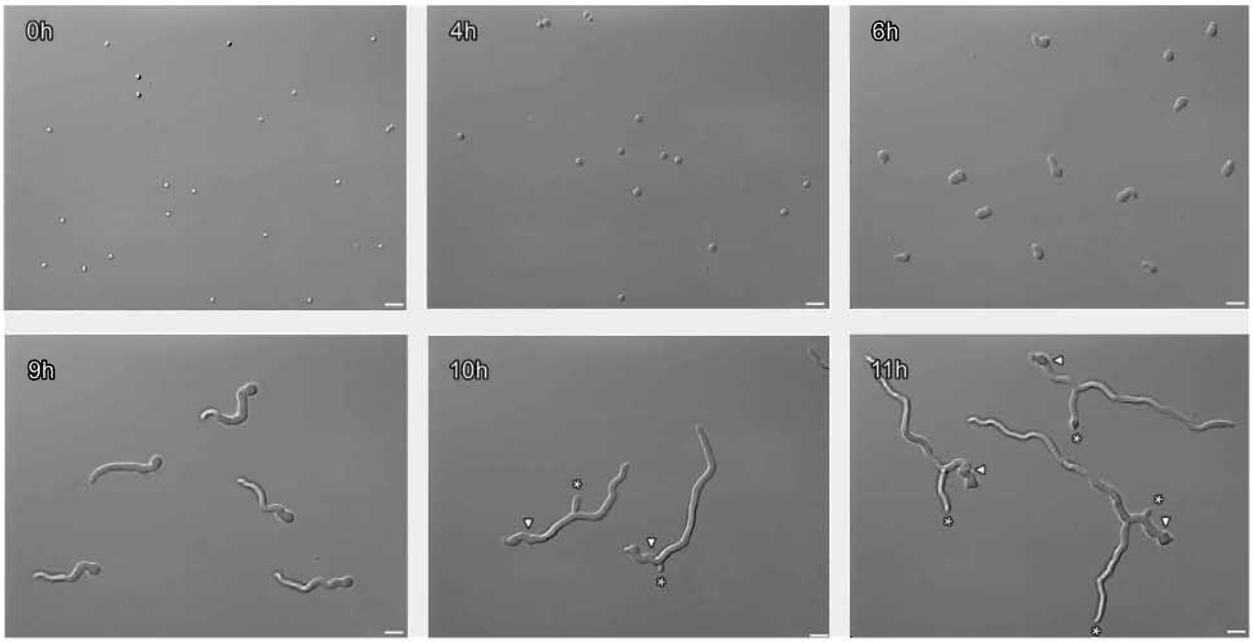

Figure 1. *A. fumigatus* conidia were inoculated into complete medium and incubated at 37°C. Samples were fixed at the time points indicated. Arrowheads indicate septa. Asterisks indicate branches. Bars, 10 μm. (Images courtesy of Andrew Breakspear.)

Cdc42 and its associated proteins relay this information to the morphogenetic machinery; (iii) the morphogenetic machinery deposits new cellular material in the appropriate area. The morphogenetic machinery includes everything needed to make and direct new cellular material: the cytoskeleton, secretory system, and cell wall biosynthetic machinery. Filamentous fungi generally lack homologs of the *S. cerevisiae* cortical markers, suggesting that cortical markers are very divergent in different fungi or that filamentous fungi use a different system for establishing positional information (Harris, 2006; Harris and Momany, 2004). One intriguing possibility is that the polarity axis in filamentous fungi is established in a stochastic manner and then becomes

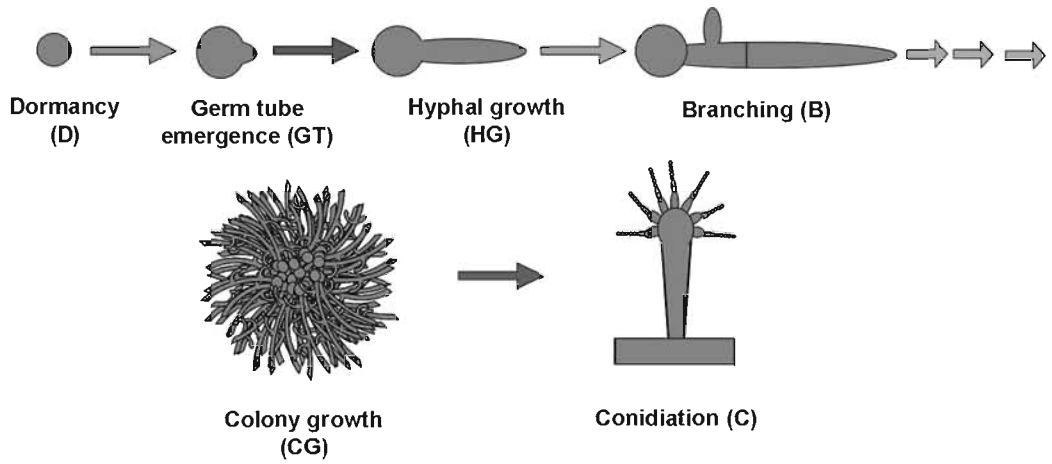

Figure 2. Diagrammatic representation of *A. fumigatus* growth stages. See text for details.

stabilized (Harris, 2006). In contrast to cortical markers, Rho GTPases and their associated proteins and the morphogenetic machinery proteins are highly conserved among fungi.

Despite sharing core machinery, important differences between polar growth in filamentous fungi and yeasts are beginning to emerge. A recent review of polar growth in filamentous fungi highlighted several of the unique features, most notably a role for microtubules in polar growth of filamentous fungi and the importance of the Spitzenkorpefer, a collection of vesicles at the tip that appears to be analogous to the polarisome (Harris, 2006). In the last few years, several *A. fumigatus* mutations have been described that affect the isotropic-to-polar switch at germ tube emergence or the ability to maintain polar growth once it is established in the hypha. These polarity-related mutations fall into one of two categories. They are either mutations in signaling genes or in cell wall genes. It should be noted that because filamentous fungi are characterized by polar extension, in many cases it is difficult to say whether the inability to properly polarize results from a polarity defect or is a consequence of a more general growth defect.

POLARITY-RELATED SIGNALING GENES

Calcineurin A is a serine/threonine-specific protein phosphatase involved in the antigenic response through calcium signaling. Deletion of the calcineurin A catalytic subunit, *cnaA*, or the Ca^{2+}-calmodulin binding subunit, *calA*, results in conidia with reduced surface rodlets and attenuated virulence. Deletion of *calA* also results in polarized conidia (a teardrop rather than round shape) that are unable to germinate (da Silva Ferreira et al., 2007; Steinbach et al., 2006).

rasA and *rasB* encode GTPases involved in morphogenesis and signaling. Mutation of *rasA* causes reduced polarization and other morphological abnormalities. Deletion of *rasB* results in delayed polarization and a failure to properly maintain polar growth seen as dichotomous branching. Deletion of *rasB* also results in a loss of virulence (Fortwendel et al., 2004, 2005).

mpkA encodes a mitogen-activated protein kinase involved in cell wall integrity and signaling (Du et al., 2006; Valiante et al., 2007). Deletion of *mpkA* results in broad, hyperpolar hyphae (hyperbranching) with no reduction in virulence.

Protein kinase A (PKA) is involved in cyclic AMP signaling, which is important for development and virulence. *pkaC1* encodes the catalytic subunit of PKA, and deletion of *pkaC1* results in a delay of polarization (Liebmann et al., 2004). Deletion of the regulatory subunit *pkaR* also results in delayed polarization along with broader germ tubes and hyphae (Zhao et al., 2006). Deletion of either PKA subunit also causes a loss of virulence.

POLARITY-RELATED CELL WALL GENES

The conidial cell wall is composed of chitin, galactomannan, α-1,3-glucan, and β-1,3-glucan (Latgé et al., 2005). *A. fumigatus* has seven different chitin synthase genes (Af*chsA*, Af*chsB*, Af*chsC*, Af*chsD*, Af*chsE*, Af*chsF*, and Af*chsG*). Strains with a deletion of any single chitin synthase gene do not show a phenotype. However, Δ*chsG* Δ*chsE* double deletion conidia show improper polarization, taking on a teardrop shape, and have less chitin and more α-1,3-glucans in their walls. Interestingly, the Δ*chsG* Δ*chsE* mutant germinates early but shows no reduction in virulence (Aufauvre-Brown et al., 1997; Mellado et al., 1996, 2003).

ags1, ags2, and *ags3* encode α-1,3-glucan synthases. Ags1 localizes to the cell wall periphery, while Ags2 localization is intracellular. Deletion of *ags1* results in reduced α-1,3-glucan in the cell wall. Deletion of *ags1* and *ags2* results in tip splitting, basically a failure to maintain polarity. Deletion of *ags1* and *ags2* does not affect virulence (Beauvais et al., 2005). Deletion of *ags3* results in early germination, an increase in melanin in the conidial cell wall, and increased virulence (Maubon et al., 2006).

gel1 and *gel2* encode glycosylphosphatidyinositol (GPI)-anchored β-1,3-glucanosyltranferases involved in cell wall biosynthesis. Though deletion of *gel1* shows no phenotype, deletion of *gel2* or both *gel1* and *gel2* results in hyperpolarized phialides on conidiophores which produce conidia without melanin. Virulence of these mutants is reduced (Mouyna et al., 2005).

ecm33 encodes a GPI-anchored protein involved in fungal morphology. Its deletion results in conidia with an increased diameter, defective separation, and increased chitin content (Chabane et al., 2006; Romano et al., 2006). Interestingly, Δ*ecm33* shows an early switch to polar growth (germination) and increased virulence.

Af*pig-a* encodes the catalytic subunit of the GPI–*N*-acetylglucosaminyl-transferase complex, which is involved in biosynthesis of GPI-anchored proteins. Deletion of Af*pig-a* results in swollen conidia, an early switch to polar growth (germination), cell lysis, and early conidiation. Interestingly, in this case early germination and conidiation don't result in increased virulence, but rather in decreased virulence (Li et al., 2007).

Af*pmt1* encodes a protein mannosyl transferase that adds mannose to serine or threonine residues of target proteins. In systems where targets have been identified, they are mostly cell wall or secreted proteins. De-

Table 1. Polarity-related genes in *A. fumigatus*[a]

Related function and gene(s)	Protein	Defects upon deletion	Deletion fully virulent?	Reference(s)
Signaling-related genes				
cnaA	Calcineurin A (Ser/Thr protein phosphatase) catalytic subunit	Conidia lack surface rodlets; abnormal hyphae; reduced colony growth and conidiation	No[b]	Steinbach et al., 2006
calA	Calcineurin A (Ser/Thr protein phosphatase) Ca^{2+}/calmodulin-binding unit	Conidia have reduced surface rodlets, some with abnormal polarized morphology (teardrop) and some unable to polarize; hyperpolarized hyphae (hyperbranching); reduced colony growth	No[b]	da Silva Ferreira et al., 2007
rasA	Ras GTPase	Dominant-negative mutants have reduced polarization; dominant-active mutants have reduced conidiation and abnormal conidiophores	NT	Fortwendel et al., 2004
rasB	Ras GTPase	Delayed polarization, failure to maintain polarized hyphae (dichotomous branching) and reduced colony growth	No[b]	Fortwendel et al., 2005
mpkA	MAP kinase	Thick hyperpolarized (hyperbranching) hyphae and reduced colony growth	Yes	Valiante et al., 2007
pkaC1	PKA catalytic subunit, cAMP signaling pathway	Delayed polarization and reduced colony growth and conidiation	No[b]	Liebmann et al., 2004
pkaR	PKA regulatory subunit	Reduced and delayed polarization, broader germ tubes and hyphae, reduced colony growth and conidiation, and abnormal conidiophores	No[b]	Zhao et al., 2006
Cell wall-related genes				
chsG and *chsE*	Chitin synthases	Double mutant has polarized conidia (teardrop); early switch to polar growth; reduced colony growth	Yes	Mellado et al., 2003
ags1 and *ags2*	α-1,3-Glucan synthase	Double deletion does not maintain polarized growth integrity (dichotomous branching); abnormal conidiophores and poor conidiation	Yes	Beauvais et al., 2005
ags3	α-1,3-Glucan synthase	Thicker conidial cell wall; increased melanin; early switch to polar growth	Yes, hypervirulent	Maubon et al., 2006
gel1 and *gel2*	GPI-anchored β-1,3-glucanosyl transferase	*gel2* or double deletion; no melanin in conidia; germination requires special medium; slow colony growth rate; some hyperpolarized phialides	No[b]	Mouyna et al., 2005
ecm33/*sps2*	GPI-anchored protein involved in fungal morphology	Increased conidial diameter; early switch to polar growth	Yes, hypervirulent	Chabane et al., 2006; Romano et al., 2006
Af*pig-a*	GPI-anchored protein; biosynthesis of GPI anchors	Swollen conidia; early switch to polar growth, cell lysis and early conidiation	No[b]	Li et al., 2007
Af*pmt1*	PMT O-mannosyl-transferases	Thin conidial cell wall; early switch to polar growth; reduced colony growth and poor conidiation ar 42°C	Yes	Zhou et al., 2007

[a]NT, not tested; MAP, mitogen-activated protein; cAMP, cyclic AMP.
[b]Attenuated or no virulence.

letion of Af*pmt1* results in conidia that switch early to polar growth (early germination) and have thin walls. Strains with *Afpmt1* deleted are fully virulent (Zhou et al., 2007).

CONCLUSIONS

Because polar extension is critical to robust growth of filamentous fungi, one could predict that it is critical for virulence in invasive aspergillosis. Bearing in mind the caveats that it is often difficult to distinguish polarity defects from general growth defects and that the number of polarity-related genes so far examined is small, the recent literature supports the idea that polarity is needed for virulence. In most cases the deletion of polarity-related signaling genes leads to reduced or late polarization as measured by germ tube emergence. Deletion or mutation of *calA, rasA, rasB, pkaC1*, and *pkaR* all resulted in delayed or reduced germination and reduced virulence (Table 1). The only polarity-related signaling gene whose mutation did not lead to reduced polar growth was *mpkA*, which showed hyperpolarization. Consistent with the idea that polar growth is critical for virulence, Δ*mpkA* showed no reduction in virulence.

In most cases the deletion of polarity-related cell wall genes leads to early polarization as measured by germ tube emergence. Deletion of *chsG* and *chsE* or of *ags3, ecm33*, Af*pig-a*, or Af*pmt1* lead to early germ tube emergence (Table 1). With the exception of ΔAf*pig-a*, these mutants were fully virulent. Indeed, two of the deletions with early germ tube emergence, Δ*ags3* and Δ*ecm33*, were more virulent than wild type. ΔAf*pig-a*, the deletion strain that showed early germ tube emergence along with a decrease in virulence, also showed cell lysis, perhaps offsetting the advantages of early polarization.

At this point it is still difficult to say how much of the correlation between polarity and virulence is simply a correlation between rapid, robust growth of the pathogen and increased virulence. A better understanding of the mechanisms underlying polar growth of *A. fumigatus* in vitro and in vivo might allow the contributions of polarity and of robust growth to the organism's pathogenesis to be separated.

REFERENCES

Aufauvre-Brown, A., E. Mellado, N. A. R. Gow, and D. W. Holden. 1997. *Aspergillus fumigatus chsE*: a gene related to *CHS3* of *Saccharomyces cerevisiae* and important for hyphal growth and conidiophore development but not pathogenicity. *Fungal Genet. Biol.* 21: 141–152.

Beauvais, A., D. Maubon, S. Park, W. Morelle, M. Tanguy, M. Huerre, D. S. Perlin, and J. P. Latgé. 2005. Two α(1-3) glucan synthases with different functions in *Aspergillus fumigatus*. *Appl. Environ. Microbiol.* 71:1531–1538.

Beffa, T., F. Staib, J. Lott Fischer, P. F. Lyon, P. Gumowski, O. E. Marfenina, S. Dunoyer-Geindre, F. Georgen, R. Roch-Susuki, L. Gallaz, et al. 1998. Mycological control and surveillance of biological waste and compost. *Med. Mycol.* 36(Suppl. 1):137–145.

Bergen, L. G., and N. R. Morris. 1983. Kinetics of the nuclear division cycle of *Aspergillus nidulans*. *J. Bacteriol.* 156:155–160.

Chabane, S., J. Sarfati, O. Ibrahim-Granet, C. Du, C. Schmidt, I. Mouyna, M. C. Prevost, R. Calderone, and J. P. Latgé. 2006. Glycosylphosphatidylinositol-anchored Ecm33p influences conidial cell wall biosynthesis in *Aspergillus fumigatus*. *Appl. Environ. Microbiol.* 72:3259–3267.

da Silva Ferreira, M. E., T. Heinekamp, A. Hartl, A. A. Brakhage, C. P. Semighini, S. D. Harris, M. Savoldi, P. F. de Gouvea, M. H. de Souza Goldman, and G. H. Goldman. 2007. Functional characterization of the *Aspergillus fumigatus* calcineurin. *Fungal Genet. Biol.* 44:219–230.

Denning, D. W., and D. A. Stevens. 1990. Antifungal and surgical treatment of invasive aspergillosis: review of 2,121 published cases. *Rev. Infect. Dis.* 12:1147–1200.

Denning, D. W., P. N. Ward, L. E. Fenelon, and E. W. Benbow. 1992. Lack of vessel wall elastolysis in human invasive pulmonary aspergillosis. *Infect. Immun.* 60:5153–5156.

Du, C., J. Sarfati, J. P. Latgé, and R. Calderone. 2006. The role of the sakA (Hog1) and tcsB (sln1) genes in the oxidant adaptation of *Aspergillus fumigatus*. *Med. Mycol.* 44:211–218.

Fortwendel, J. R., J. C. Panepinto, A. E. Seitz, D. S. Askew, and J. C. Rhodes. 2004. *Aspergillus fumigatus rasA* and *rasB* regulate the timing and morphology of asexual development. *Fungal Genet. Biol.* 41:129–139.

Fortwendel, J. R., W. Zhao, R. Bhabhra, S. Park, D. S. Perlin, D. S. Askew, and J. C. Rhodes. 2005. A fungus-specific Ras homolog contributes to the hyphal growth and virulence of *Aspergillus fumigatus*. *Eukaryot. Cell* 4:1982–1989.

Harris, S. D. 1997. The duplication cycle in *Aspergillus nidulans*. *Fungal Genet. Biol.* 22:1–12.

Harris, S. D. 2006. Cell polarity in filamentous fungi: shaping the mold. *Int. Rev. Cytol.* 251:41–77.

Harris, S. D., and M. Momany. 2004. Polarity in filamentous fungi: moving beyond the yeast paradigm. *Fungal Genet. Biol.* 41:391–400.

Latgé, J. P. 1999. *Aspergillus fumigatus* and aspergillosis. *Clin. Microbiol. Rev.* 12:310–350.

Latgé, J. P. 2001. The pathobiology of *Aspergillus fumigatus*. *Trends Microbiol.* 9:382–389.

Latgé, J. P., I. Mouyna, F. Tekaia, A. Beauvais, J. P. Debeaupuis, and W. Nierman. 2005. Specific molecular features in the organization and biosynthesis of the cell wall of *Aspergillus fumigatus*. *Med Mycol* 43(Suppl. 1):S15–S22.

Li, H., H. Zhou, Y. Luo, H. Ouyang, H. Hu, and C. Jin. 2007. Glycosylphosphatidylinositol (GPI) anchor is required in *Aspergillus fumigatus* for morphogenesis and virulence. *Mol. Microbiol.* 64:1014–1027.

Liebmann, B., M. Muller, A. Braun, and A. A. Brakhage. 2004. The cyclic AMP-dependent protein kinase a network regulates development and virulence in *Aspergillus fumigatus*. *Infect. Immun.* 72: 5193–5203.

Lopes Bezerra, L. M., and S. G. Filler. 2004. Interactions of *Aspergillus fumigatus* with endothelial cells: internalization, injury, and stimulation of tissue factor activity. *Blood* 103:2143–2149.

Maubon, D., S. Park, M. Tanguy, M. Huerre, C. Schmitt, M. C. Prevost, D. S. Perlin, J. P. Latgé, and A. Beauvais. 2006. AGS3, an α(1-3)glucan synthase gene family member of *Aspergillus fumigatus*, modulates mycelium growth in the lung of experimentally infected mice. *Fungal Genet. Biol.* 43:366–375.

Mellado, E., A. Aufauvre-Brown, N. A. R. Gow, and D. W. Holden. 1996. The *Aspergillus fumigatus chsC* and *chsG* genes encode class III chitin synthases with different functions. *Mol. Microbiol.* 20: 667–679.

Mellado, E., G. Dubreucq, P. Mol, J. Sarfati, S. Paris, M. Diaquin, D. W. Holden, J. L. Rodriguez-Tudela, and J. P. Latgé. 2003. Cell wall biogenesis in a double chitin synthase mutant ($chsG^-/chsE^-$) of *Aspergillus fumigatus*. *Fungal Genet. Biol.* 38:98–109.

Momany, M., and I. Taylor. 2000. Landmarks in the early duplication cycles of *Aspergillus fumigatus* and *Aspergillus nidulans*: polarity, germ tube emergence and septation. *Microbiology* 146:3279–3284.

Mouyna, I., W. Morelle, M. Vai, M. Monod, B. Lechenne, T. Fontaine, A. Beauvais, J. Sarfati, M. C. Prevost, C. Henry, et al. 2005. Deletion of GEL2 encoding for a β(1-3)glucanosyltransferase affects morphogenesis and virulence in *Aspergillus fumigatus*. *Mol. Microbiol.* 56:1675–1688.

Paris, S., E. Boisvieux-Ulrich, B. Crestani, O. Houcine, D. Taramelli, L. Lombardi, and J. P. Latgé. 1997. Internalization of *Aspergillus fumigatus* conidia by epithelial and endothelial cells. *Infect. Immun.* 65:1510–1514.

Pitt, J. I. 1994. The current role of *Aspergillus* and *Penicillium* in human and animal health. *J. Med. Vet. Mycol.* 32(Suppl. 1):17–32.

Pruyne, D., and A. Bretscher. 2000. Polarization of cell growth in yeast. I. Establishment and maintenance of polarity states. *J. Cell Sci.* 113:365–375.

Robinow, C. F., and C. E. Canten. 1969. Mitosis in *Aspergillus nidulans*. J. Cell Sci. 5:403–431.

Romano, J., G. Nimrod, N. Ben-Tal, Y. Shadkchan, K. Baruch, H. Sharon, and N. Osherov. 2006. Disruption of the *Aspergillus fumigatus* ECM33 homologue results in rapid conidial germination, antifungal resistance and hypervirulence. *Microbiology* 152:1919–1928.

Steinbach, W. J., R. A. Cramer, Jr., B. Z. Perfect, Y. G. Asfaw, T. C. Sauer, L. K. Najvar, W. R. Kirkpatrick, T. F. Patterson, D. K. Benjamin, Jr., J. Heitman, et al. 2006. Calcineurin controls growth, morphology, and pathogenicity in *Aspergillus fumigatus*. *Eukaryot. Cell* 5:1091–1103.

Valiante, V., T. Heinekamp, R. Jain, A. Hartl, and A. A. Brakhage. 2007. The mitogen-activated protein kinase MpkA of *Aspergillus fumigatus* regulates cell wall signaling and oxidative stress response. *Fungal Genet Biol.* 45:618–627.

Wasylnka, J. A., and M. M. Moore. 2002. Uptake of *Aspergillus fumigatus* conidia by phagocytic and nonphagocytic cells in vitro: quantitation using strains expressing green fluorescent protein. *Infect. Immun.* 70:3156–3163.

Zhao, W., J. C. Panepinto, J. R. Fortwendel, L. Fox, B. G. Oliver, D. S. Askew, and J. C. Rhodes. 2006. Deletion of the regulatory subunit of protein kinase A in *Aspergillus fumigatus* alters morphology, sensitivity to oxidative damage, and virulence. *Infect. Immun.* 74:4865–4874.

Zhou, H., H. Hu, L. Zhang, R. Li, H. Ouyang, J. Ming, and C. Jin. 2007. *O*-Mannosyltransferase 1 in *Aspergillus fumigatus* (AfPmt1p) is crucial for cell wall integrity and conidium morphology, especially at an elevated temperature. *Eukaryot. Cell* 6:2260–2268.

EUKARYOTIC CELL, Jan. 2010, p. 155–163 Vol. 9, No. 1
1535-9778/10/$12.00 doi:10.1128/EC.00269-09

Septins AspA and AspC Are Important for Normal Development and Limit the Emergence of New Growth Foci in the Multicellular Fungus *Aspergillus nidulans*[▽]

Rebecca Lindsey,† Susan Cowden, Yainitza Hernández-Rodríguez, and Michelle Momany*

Department of Plant Biology, University of Georgia, Athens, Georgia 30602

Received 14 September 2009/Accepted 23 November 2009

Septins are cytoskeletal proteins found in fungi, animals, and microsporidia, where they form multiseptin complexes that act as scaffolds recruiting and organizing other proteins to ensure normal cell division and development. Here we characterize the septins AspA and AspC in the multicellular, filamentous fungus *Aspergillus nidulans*. Mutants with deletions of *aspA*, *aspC*, or both *aspA* and *aspC* show early and increased germ tube and branch emergence, abnormal septation, and disorganized conidiophores. Strains in which the native *aspA* has been replaced with a single copy of *aspA-GFP* driven by the native septin promoter or in which *aspC* has been replaced with a single copy of *aspC-GFP* driven by the native promoter show wild-type phenotypes. AspA-GFP and AspC-GFP show identical localization patterns as discrete spots or bars in dormant and expanding conidia, as rings at forming septa and at the bases of emerging germ tubes and branches, and as punctate spots and filaments in the cytoplasm and at the cell cortex. In conidiophores, AspA-GFP and AspC-GFP localize as diffuse bands or rings at the bases of emerging layers and conidial chains and as discrete spots or bars in newly formed conidia. AspA-GFP forms abnormal structures in Δ*aspC* strains while AspC-GFP does not localize in Δ*aspA* strains. Our results suggest tbat AspA and AspC interact with each other and are important for normal development, especially for preventing the inappropriate emergence of germ tubes and branches. This is the first report of a septin limiting the emergence of new growth foci in any organism.

Septins are novel cytoskeletal proteins first discovered in a screen for *Saccharomyces cerevisiae* cell cycle mutants (14). The core septin proteins, Cdc3, Cdc10, Cdc11, and Cdc12, localize to the mother/bud neck, where they assemble into heteropolymers that organize proteins necessary to complete cytokinesis and ensure proper coordination between bud formation and nuclear division (4, 16, 37, 38).

S. cerevisiae septins first appear as a cortical patch at the future bud site. They later form a ring through which the bud emerges and then develop into an hourglass-shaped complex at the base of the bud that splits into two rings to complete cytokinesis (8, 10, 23). In the dimorphic fungus *Candida albicans*, septins assemble during the formation of buds and pseudohyphae, localize to prebud sites, and form rings at the mother/bud neck. During hyphal growth septins localize to hyphal tips and transiently as a basal band within germ tubes (33, 39). The genome of the filamentous fungus *Ashbya gossypii* is 90% homologous and syntenic with the genome of *S. cerevisiae*, though it grows in the filamentous morphology rather than the yeast morphology (6). In *A. gossypii* septins localize as discrete filamentous bars at septation sites, at tips of hyphae, and at the bases of emerging branches. *A. gossypii* septins are not essential, though they have been shown to be involved in mitosis, sporulation, hyphal morphogenesis, and septum formation (5, 9).

In mammals, septins ensure proper growth, cell migration, vesicle trafficking, and cell division (19, 32, 35, 42). Mammalian septins form distinct filaments that colocalize with and appear to organize the actin and microtubule cytoskeletons (19, 31, 35), punctate patterns at neuron terminals and vesicles, and rings in sperm cells (2, 15, 18, 43).

Aspergillus nidulans is a multicellular filamentous fungus which has five septins, AspA, AspB, AspC, AspD, and AspE (29). All five septins are expressed during vegetative and asexual growth, with AspB having the highest expression levels (29). Immunofluorescence studies showed that AspB localizes to septa and conidiophore layers and anticipates the sites of branch emergence (40). To better understand the roles of septins in shaping the growth of multicellular organisms, we characterized *A. nidulans* septins AspA and AspC, orthologs of *S. cerevisiae* Cdc11 and Cdc12, respectively (30). Septin deletion mutants were characterized throughout vegetative and asexual development. AspA and AspC are necessary for normal development and morphogenesis as well as sporulation. AspA and AspC were found to localize as rings, caps, puncta, or filaments throughout development. Localization of AspA and that of AspC appear to be mutually dependent, as AspC was unable to localize in the Δ*aspA* strain and AspA localization was abnormal in the Δ*aspC* strain.

MATERIALS AND METHODS

Strains and media. Strains used in this study are listed in Table 1. Media used were previously described (13). Strain construction and growth were done by standard *A. nidulans* techniques (13, 17). All incubations were at 30°C and in

* Corresponding author. Mailing address: Department of Plant Biology, University of Georgia, Athens, GA 30602. Phone: (706) 542-2014. Fax: (706) 542-1805. E-mail: momany@plantbio.uga.edu.

† Present address: U.S. Department of Agriculture, Agricultural Research Service, Bacterial Epidemiology and Antimicrobial Resistance Research Unit, Richard B. Russell Agricultural Research Center, 950 College Station Road, Athens, GA 30605-2720.

▽ Published ahead of print on 30 November 2009.

TABLE 1. *A. nidulans* strains used in this paper

Strain	Genotype[a]	Source or reference
A28	*pabaA6 biA1*	FGSC[b]
A773	*pyrG89 wA3 pyroA4*	FGSC
A850	*biA1 argB::trpC_B methG1 veA1 trpC801*	FGSC
A1147	*pyrG89 argB2 pabaB22 nkuA::argB riboB2*	FGSC
A1145	*pyrG89 pyroA4 nkuA::argB riboB2*	FGSC
ASH5	*aspA::argB2 biA1 argB::trpC_B methG1 veA1 trpC801*	This study
ASH26	*aspA::argB2 pyrG89 wa3* argB::*trpC_B methG1 pyroA4*	This study
ARL141	*aspA-GFP-AfpyrG pyrG89 biA1 argB::trpC_B methG1 veA1 trpC801*	This study
ARL157	*aspC::AfpyrG pyrG89 pyroA4*	This study
ARL159	*aspC-gfp-AfpyrG pabaA6 biA1*	This study
ARL161	*aspC::AfpyrG pyrG89 biA1 argB::trpC_B methG1 veA1 trpC801*	This study
ARL162	*aspA::argB2 aspC::AfpyrG pyrG89 pyroA4 biA1 ΔargB::trpC_B veA1 trpC801*	This study
ARL182	*aspC-GFP-AfpyrG aspA::argB2 argB::trpC_B methG1 pabaA6*	This study
ARL183	*aspC-gfp-AfpyrG aspA::argB2 argB::trpC_B pabaA6*	This study
ARL184	*aspC-gfp-AfpyrG aspA::argB2 argB::trpC_B pabaA6*	This study
ARL185	*aspC-gfp-AfpyrG ΔaspA::argB2 argB::trpC_B*	This study
ARL198	*aspC::AfpyrG aspA-gfp-AfpyrG pyrG89 pyroA4*	This study
ARL201	*aspC::AfpyrG aspA-gfp-AfpyrG pyrG89 pyroA4*	This study
ARL205	*aspA-gfp-AfpyrG**pyrG89 wA3 pyroA4*	This study
ARL206	*aspC-gfp-AfpyrG**biA1 argB::trpC_B methG1 veA1 trpC801*	This study

[a] The symbol \\ indicates haploids fused to make diploid strain.
[b] FGSC, Fungal Genetics Stock Center, Department of Microbiology, University of Kansas Medical Center (Kansas City, KS).

complete medium (1% glucose, 0.2% peptone, 0.1% Casamino Acids, 0.1% yeast extract, trace elements, nitrate salts, and 0.01% vitamins, pH 6.5) with amino acid supplements (17) except where noted. Green fluorescent protein (GFP) diploid strains were generated as previously reported (12) by mixing conidiospores from a wild-type strain (A773 or A850) with those from the AspA-GFP (ARL141) or AspC-GFP (ARL159) strain, respectively. Heterokaryotic germlings were plated into minimal agar from which only diploids could emerge. The resulting diploid conidia were streaked for isolation two times to yield strains ARL205 and ARL206, respectively. Localization was examined in four GFP bright strains for each diploid.

Growth conditions and microscopic observations. Preparation and growth of cells were as previously reported (28). Briefly, conidia were inoculated on sterile coverslips in liquid complete or minimal medium and incubated at 30°C in a petri dish. Cells were fixed, septa were stained with calcofluor (American Cyanamid, Wayne, NJ), and nuclei were stained with Hoechst 33258 (Sigma, St. Louis, MO). Microscopic observations were made using a Zeiss (Thornwood, NY) Axioplan microscope with appropriate filters, and digital images were acquired using an Axion (Axion Technologies) digital imaging system. For all GFP fusion observations, recipient strains that had not been transformed with GFP cassettes were viewed under identical settings to verify that there was no autofluorescence. Images were prepared using Photoshop cs version 8.0 (Adobe, Mountain View, CA). For quantitation of phenotypes, counts of 200 cells were done. All experiments were repeated at least three times with similar results. A representative data set is shown.

Asexual structures. Preparation of conidiophores was as previously reported (20). Briefly, conidia were inoculated on the edges of a square of complete agar medium which was sandwiched between two coverslips and placed on top of water agar to prevent the complete agar from drying out. Plates were incubated inverted at 30°C for 2 days. To observe conidiophore structures, coverslips with

TABLE 2. Primers

Construct and primer type or target	Sequence
aspA deletion	
Flank 1	Forward: GCTCTAGAGACCCGCAAGGGCCCACGAAAG
	Reverse: CGGGATCCGATGGACGATAGGGGGGGATGG
Flank 2	Forward: CCTAAGCTTCTTTGTTCGCGGGTAACGGCT
	Reverse: GGGGTACCGGAACAAACAGCCAGACCTGCT
Δ*aspA* check	Forward: TCCCTTCATCTTTCTCTTTCTCCATCCCCC
	Reverse: AATAAAAGCAGCCTAGTGTCTCCAATTATC
aspA-gfp	
Native *aspA*	Forward: ATGTCGTCCGCCTACAACCCG
	Reverse: CTGCTCGGCCTCGGCGGCTTC
Plasmid pFNO3 (GA5-*gfp-AfpyrG* amplification)	Forward: AGCCAGGGAGAAGCCGCCGAGGCCGAGCAGGGAGCTGGTGCAGGCGCT GGAGCCGGT
	Reverse: CTGTCTGAGAGGAGGCACTGATGCGTGATGGGCAAGCCGTTACCCGCGA ACAAAGATC
Downstream native *aspA*	Forward: GATCTTTGTTCGCGGGTAACGG
	Reverse: GCCAACACTCGCTGCAGTACTCAG
aspA-gfp check	Forward: CCTTACGATATCGAGGAAGACG
	Reverse: CGAGTAAGTCATGAGCGGTAATG
aspC deletion	
Upstream native *aspC*	Forward: GAGCAAAGTCGATCTCCCCGTCCC
	Reverse: GAGGACGGTACAACAACCAAAAGGCTTC
Plasmid pFNO3 (*AfpyrG* amplification)	Forward: GAAGCCTTTTGGTTGTTGTACCGTCCTCGCCTCAAACAATGCTTCACCCTC
	Reverse: GTGTCAAATGATGAACACTGATAGGAAGAACTGTCTGAGAGGAGGCACT GATGCG
Downstream native *aspC*	Forward: TTCTTCCTATCAGTGTTCATCATTTGACAC
	Reverse: GAATTTCGAATTATCCGCAGCAAC
Δ*aspC* check	Forward: GAGCAAAGTCGATCTCCCCGTCCC
	Reverse: CAGCGCTTGTGCCCCTCCATCTCC
aspC-gfp	
Native *aspC*	Forward: ATGGCCCCCGTCAACGAGACCGCTTC
	Reverse: GCGACGGCCGTGGCTACGAGTCGATG
Plasmid pFNO3 (*GA5-gfp-AfpyrG* amplification)	Forward: GCTCATCGACTCGTAGCCACGGCCGTCGCGGAGCTGGTGCAGGCGCTGG AGCCGGT
	Reverse: CTGTCTGAGAGGAGGCACTGATGCGTGATGCACCTGCTTTCAGTGGTATA GAATATTGT
Downstream native *aspC*	Forward: ACAATATTCTATACCACTGAAAGCAGGTG
	Reverse: GTAATGTCCCAGTTCGTAAGCCTAAG
aspC-gfp check	Forward: CAGATCAAAAAAAGTCGGCC
	Reverse: CAAGCAATGGTGAGAAAATTG

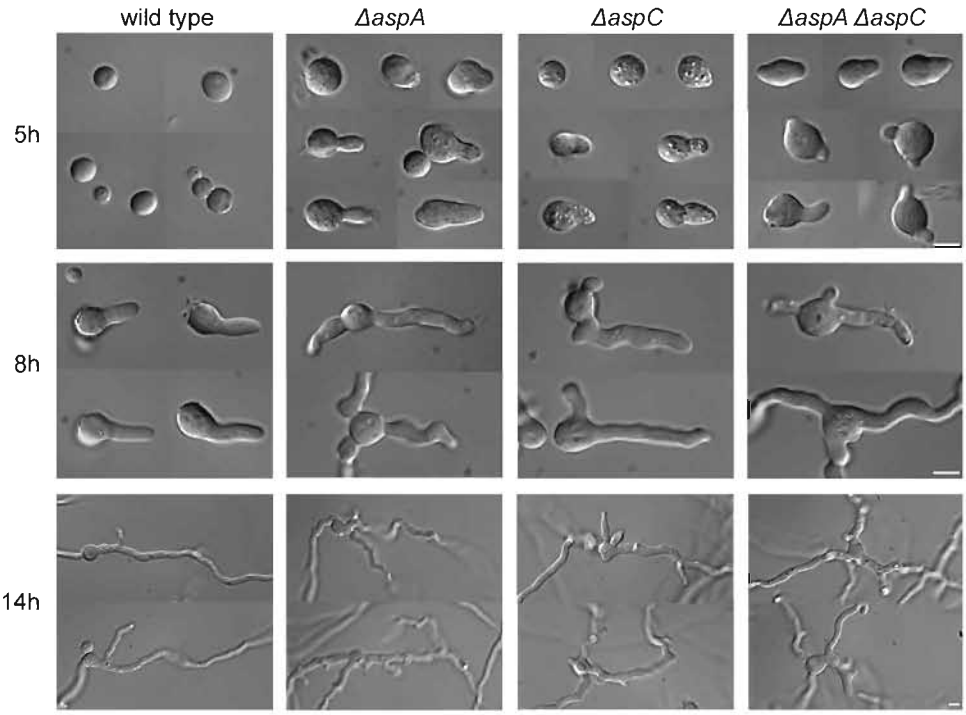

FIG. 1. Multiple germ tubes and branches emerge from Δ*aspA*, Δ*aspC*, and Δ*aspA* Δ*aspC* strains. Conidia of wild-type and mutant strains were inoculated into liquid medium and incubated for 5, 8, or 14 h; fixed; and photographed with differential interference contrast optics. Panels show composites of multiple cells from each time point. Scale bar, 5 μm.

aerial hyphae and conidiophores attached were fixed, mounted on slides, and observed microscopically.

Fluorescent tags and gene knockouts. The Δ*aspA* strain was generated by transforming *A. nidulans* A850 with plasmid pOAS15 using the protoplasting method. Approximately 800 bp upstream of the *aspA* gene (flank 1) was amplified using the Molecular Bio Products EasyStart Micro 20 kit (San Diego, CA) with primers AspAko_XbaI_1 and AspAko_BamHI_1 (Table 2), which introduced XbaI and BamHI sites, respectively. Approximately 1,000 bp downstream of the *aspA* gene (flank 2) were PCR amplified using the Molecular Bio Products EasyStart Micro 20 kit (San Diego, CA) with primers AspAko_HindIII_2 and AspAko_KpnI_2 (Table 2), which introduced HindIII and KpnI sites, respectively. The PCR products were cut with the appropriate restriction enzymes and then ligated on either side of the *argB* gene in the pArgB2 plasmid, resulting in plasmid pOAS15. Flank 1 is located at the 3′ end of the *argB* gene, and flank 2 is located at the 5′ end of the *argB* gene. After pOAS15 was confirmed by restriction digestion, it was used to transform *A. nidulans* A850 by the protoplasting method. The resulting transformants were checked by PCR (primers listed in Table 2) and confirmed by Southern blotting to ensure that a single homologous integration under the endogenous promoter was obtained.

All PCRs and fusion PCRs were conducted using Invitrogen AccuPrime *Pfx* DNA polymerase as previously described (44). The Δ*aspC* strain was generated by a complete replacement of the *aspC* gene with the *AfpyrG* gene. This was done by amplifying three separate fragments: the first fragment was 1 kb upstream of the *aspC* start codon (A850 template), the second fragment was 1 kb downstream of the *aspC* stop codon (A850 template), and the third fragment was the *AfpyrG* gene (pFNO3 plasmid template), which included 30 bp before the *aspC* start codon and 30 bp after the stop of the *aspC* stop codon added to facilitate fusion PCR (primers listed in Table 2). Each DNA fragment was run on an 0.8% agarose gel, and the bands were excised and cleaned with the Qiagen QIAquick gel extraction kit (Maryland). Equal amounts of each fragment were used in the fusion PCR. The fusion PCR product was then run on a gel to ensure that a single band was obtained, and the band was then excised and gel purified with the Qiagen QIAquick gel extraction kit (Maryland). The cleaned DNA was used to transform *A. nidulans* Δ*nkuA* strains by protoplasting. The resulting transformants were checked by PCR, which utilized primers in the 5′ region of the cassette and the *pyrG* region of the cassette (Table 2). The colonies that were positive for the fusion cassette were analyzed by Southern blotting to confirm that only a single copy of the cassette was incorporated by homologous recombination at the desired location.

Cassettes for GFP fusions were created in the S. Osinani lab and obtained through the Fungal Genetics Stock Center (http://www.fgsc.net/) (44). GFP strains were constructed by amplifying the target gene (*aspA* or *aspC*) excluding the stop codon (A850 template), 2 kb downstream of the target gene (A850 template), and the GFP *AfpyrG* cassette (pFNO3 template) with the addition of approximately 30 bp before and after the stop codon added to the 5′ and 3′ ends to facilitate the fusion PCR (primers listed in Table 2). Each PCR product was run on an 0.8% agarose gel, and the band was excised and cleaned with the Qiagen QIAquick gel extraction kit (Maryland). Equal amounts of each fragment were used for the fusion PCR. After fusion PCR the DNA was run on a gel, excised to ensure that a single band was obtained, and gel purified with the Qiagen QIAquick gel extraction kit (Maryland). *A. nidulans* Δ*nkuA* strains were then transformed with the cleaned DNA by the protoplasting method. The resulting transformants were checked by PCR, which utilized primers that flanked the entire fusion PCR product (Table 2). The colonies that were positive for the fusion cassette were analyzed by Southern blotting to confirm that only a single copy of the cassette was incorporated by homologous recombination at the desired location. At least four independent transformants were characterized.

RESULTS

In Δ*aspA*, Δ*aspC*, and Δ*aspA* Δ*aspC* strains, germ tubes emerge early, germ tube and branch emergence increases, and septation and conidiation are reduced. In the filamentous fungus *A. nidulans* development begins when uninucleate asexual

conidiospores break dormancy in the presence of a carbon source. Soon after conidia break dormancy, nuclear division begins and a single primary germ tube emerges and grows by tip extension (11, 13, 27). After germlings pass a critical size threshold, nuclear division triggers septum formation (41). This normally occurs when germlings contain 8 to 16 nuclei. At about the same time a secondary germ tube emerges from the conidium in a bipolar pattern, opposite from the site where the first germ tube emerged. After subapical and apical compartments are formed through septation, generally only one branch emerges per active subapical compartment of the hypha (21). To determine if the septins AspA and AspC play roles in *A. nidulans* development, we compared wild-type strains to strains in which individual septin genes were deleted (Δ*aspA*, ASH5, and Δ*aspC*, ARL161) or in which both septins were deleted (Δ*aspA* Δ*aspC*, ARL162). After 5 h at 30°C, no germ tubes were yet visible in the wild type, while 52 to 58% of deletion strain cells had germ tubes (n = 200; Fig. 1 and 2). When incubated for 8 h, 92% of wild-type cells had one germ tube, while 75 to 82% of single deletion mutants and 95% of double deletion mutants had two or more germ tubes (Fig. 1 and 2). If two germ tubes formed in the wild-type strain, they were usually separated by 180°. In the septin deletion mutants multiple germ tubes were adjacent to each other or separated by 45°, 90°, or 180° (data not shown). Branch emergence was assayed by counting the number of hyphae that had formed at least one branch. When cells were incubated for 14 h, branches emerged in 7% of wild-type cells, 58% of Δ*aspA* cells, 56% of Δ*aspC* cells, and 82% of the double deletion mutants (n = 200; Fig. 1 and 2). In addition to branching early, the mutants also showed more branches or branch initials relative to wild type.

Because septin deletion mutants appeared to develop more rapidly than wild type and because nuclear division is known to trigger septation (41), we scored septation based on nuclear number rather than time of incubation. After 11 h of incubation, nuclei and septa were labeled and only hyphae with 16 nuclei were scored. All wild-type cells, 12% of Δ*aspA* cells, and 3% of Δ*aspC* cells with 16 nuclei had septa (n = 200). No Δ*aspA* Δ*aspC* cells with 16 nuclei contained septa (data not shown). To determine whether septation in the septin deletion mutants was reduced or simply delayed, we examined cells after 15 h of incubation, a time when all hyphae had >32 nuclei. All wild-type cells and 95% of Δ*aspA* cells had at least one septum. In contrast, only 28% of Δ*aspC* and 38% of Δ*aspA* Δ*aspC* cells had at least one septum (n = 200; Fig. 2). The intensity of septum staining with calcofluor was reduced and difficult to see and photograph in Δ*aspC* and Δ*aspA* Δ*aspC* cells compared to wild-type and Δ*aspA* cells (data not shown). In plate assays of growth, we saw no obvious defect of septin deletion mutants with addition of the cell wall-perturbing agent calcofluor and no obvious difference in radial growth rate at restrictive temperature (data not shown).

During asexual reproduction (conidiation), an aerial hypha emerges from the main hypha and swells at its tip to form a vesicle. From the vesicle two ordered layers of cells emerge sequentially (metulae and phialides), ultimately giving rise to chains of conidiospores.

We compared conidiophores (asexual structures) of wild type to septin-deleted strains (Fig. 3). Wild type had regular layers and a chain of conidiospores (Fig. 3A). Δ*aspA*, Δ*aspC*, and Δ*aspA* Δ*aspC* mutants had irregular and fused layers in the conidiophore and produced fewer spores (Fig. 3B to H).

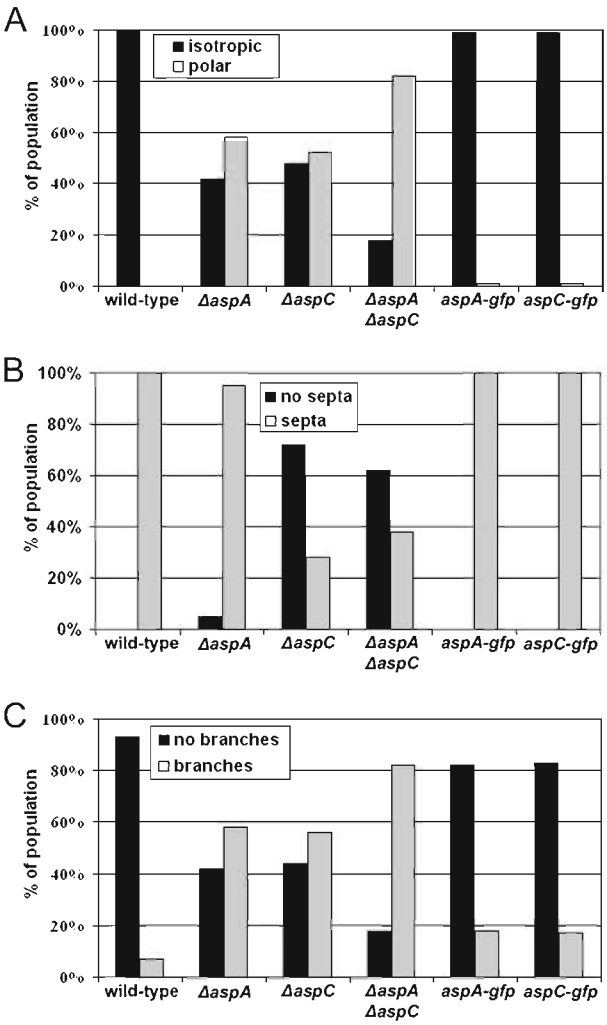

FIG. 2. Δ*aspA*, Δ*aspC*, and Δ*aspA* Δ*aspC* strains show early germ tube and branch emergence and delayed septation relative to wild-type and septin-GFP strains. Wild-type, deletion, and septin-GFP strains were incubated and fixed, and phenotypes were scored (n = 200). (A) Strains were incubated for 5 h at 30°C, and morphology was scored. Isotropic denotes round, swollen conidia. Polar denotes early germ tube emergence. (B) Strains were incubated for 15 h at 30°C, fixed, and stained with calcofluor and Hoechst 33258 to visualize septa and nuclei, respectively. The presence of septa was scored. (C) Strains were incubated for 14 h at 30°C, fixed, and labeled to visualize septa and nuclei. The presence of branches was scored.

AspA and AspC localize to dormant conidia, emerging germ tubes, emerging branches, septa, and emerging conidiophore layers. To localize the septins, we made in-frame fusions of GFP to the 3′ end of the open reading frames encoding AspA and AspC. To make expression as close to wild-type levels as

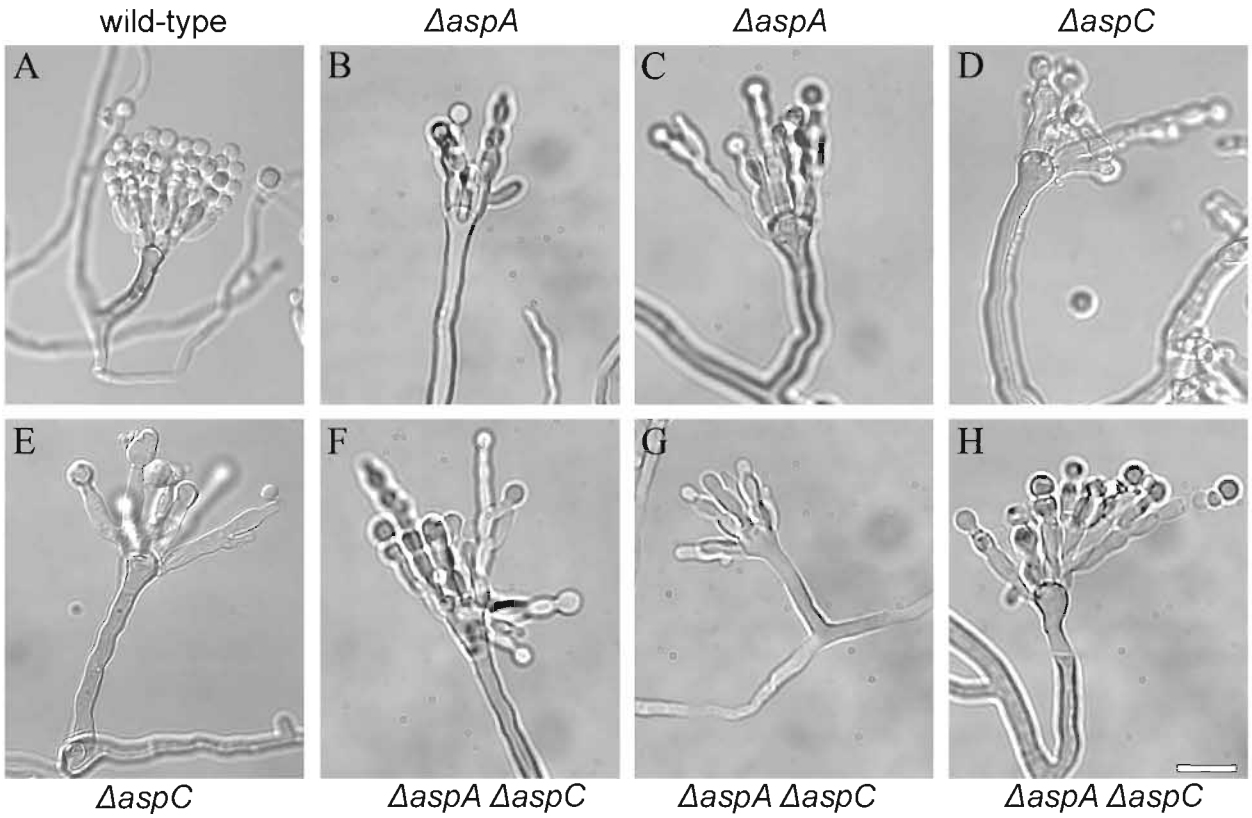

FIG. 3. Δ*aspA*, Δ*aspC*, and Δ*aspA* Δ*aspC* strains show abnormal conidiophores. (A) Wild-type conidiophores develop regular layers and conidiospore chains. (B to H) Δ*aspA*, Δ*aspC*, and Δ*aspA* Δ*aspC* mutants had irregular and fused conidiophore layers and produced fewer spores, with the double mutant phenotype being more severe than either single mutant. Scale bar, 5 μm.

possible, fusions were integrated at the *aspA* or *aspC* locus behind the native *asp* promoter, replacing the wild-type gene. To determine whether the GFP tag might interfere with septin function, we compared the phenotypes of Asp-GFP fusion strains (AspA-GFP, ARL141, and AspC-GFP, ARL161) with those of wild-type and septin-deleted strains. Germ tube and branch emergence, septation, and conidiation were all wild type in the septin-GFP strains, indicating that the GFP tag does not interfere with function (Fig. 2 and data not shown).

AspA-GFP was visible as spots or short rods in dormant conidia. There was generally a single very bright spot either alone or with dimmer spots (Fig. 4A). As the conidium expanded, AspA-GFP localization became more punctate and cortical (Fig. 4A and B), and as polarization occurred, AspA-GFP was found at the base and growing tip of the germ tube (Fig. 4B). In hyphae, AspA-GFP showed cytoplasmic localization that was often punctate at the cortex and brighter at hyphal tips and emerging branches (Fig. 4C, D, E, and G). AspA-GFP was also visible as a ring or cap at forming septa and emerging branches (Fig. 4E and F). In conidiophores, AspA-GFP localized transiently to each individual layer as it emerged, persistently to the phialide-conidiospore interface at the base of the forming chain of spores and generally as a single bright spot in each conidium, either alone or with dimmer spots (Fig. 5). Localization of AspA-GFP was also examined in a heterozygous diploid strain containing one copy of *aspA-GFP* and one of native *aspA* (ARL205). Localization of AspA-GFP in the heterozygous diploid strains was identical to localization in the haploid strain (data not shown). Localization of AspC-GFP was virtually indistinguishable from AspA-GFP at all stages examined in both haploid and heterozygous diploid strains (data not shown).

AspA localizes abnormally in Δ*aspC* cells, and AspC fails to localize in Δ*aspA* cells. In most cases where septins have been studied, different septins interact to form heteropolymers. To investigate whether AspA and AspC require each other for localization, we made strains in which one septin was fused to GFP and the other septin was deleted. From crosses of AspC-GFP and Δ*aspA* strains, we examined four progeny that contained both the deletion and the GFP fusion based on PCR analysis (ARL182 to ARL185). In all cases we no longer observed specific localization of AspC in the Δ*aspA* background in vegetative or asexual growth (Fig. 6A). From crosses of AspA-GFP and Δ*aspC* strains, we examined two progeny that contained both the deletion and the GFP fusion based on PCR analysis (ARL198 and ARL201). AspA-GFP in Δ*aspC* cells localized as a tiny bright dot in conidia (Fig. 6B). AspA-GFP

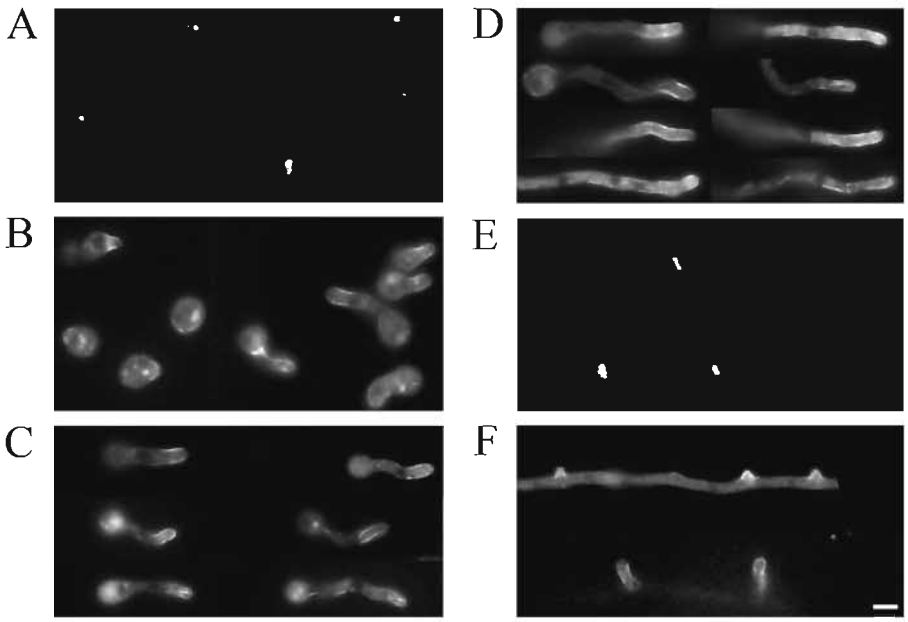

FIG. 4. AspA localizes to dormant conidia, emerging germ tubes, emerging branches, and septa. The AspA-GFP strain was incubated, and live cells were photographed using fluorescence microscopy. Panels show composites of multiple cells for each developmental stage. (A) Dormant conidia; (B) newly emerging germ tubes; (C) germlings; (D) hyphae; (E) septating hyphae; (F) branching hyphae. Scale bar, 5 μm.

continued to localize as a single very bright dot or a short bar at different locations during the remaining developmental stages (Fig. 6B), except in the conidiophore where multiple dots were seen (Fig. 6B).

DISCUSSION

AspA and AspC interact genetically and have similar functions in germ tube and branch emergence, septation, and conidiation. Our finding that Δ*aspA*, Δ*aspC*, and Δ*aspA* Δ*aspC* strains are viable is in sharp contrast to findings in *S. cerevisiae*, where the orthologous genes, *CDC11* (*aspA* ortholog) and *CDC12* (*aspC* ortholog), are essential (7). Phenotypes of Δ*aspA* and Δ*aspC* strains were almost identical in *A. nidulans*, with both strains showing early and increased germ tube emergence, increased branch emergence, delayed or reduced septation, and disorganized conidiophores. The only phenotype that differed between the deletion strains was seen after 15 h of incubation, at which time Δ*aspA* cells made normal levels of septa after an initial delay, while Δ*aspC* cells showed a reduction in the total number of septa.

The very similar phenotypes in Δ*aspA* and Δ*aspC* strains suggest that AspA and AspC play very similar roles in germ tube and branch emergence, septation, and conidiation. The identical localization patterns of AspA-GFP and AspC-GFP are consistent with the view that these septins have similar functions. However, the increased severity of all phenotypes in the Δ*aspA* Δ*aspC* double mutant suggests that there might be subtle differences between these septins. One possible difference would be the individual positions of AspA and AspC within multiseptin complexes. In *S. cerevisiae*, AspA ortholog Cdc11 and AspC ortholog Cdc12 associate directly with each other in the bud neck septin complex, where Cdc12 is thought to be the central septin associating with both Cdc11 and Cdc3 and linking them into the complex (3, 37). Our finding that AspA localizes to abnormal structures in strains lacking AspC and that AspC does not localize at all in strains lacking AspA suggests that the Cdc11 ortholog AspA might be the central septin in the *A. nidulans* septin complex and/or that AspA might be needed for the retention of AspC in complexes.

AspA and AspC localize as spots, rings, collars, and filaments. Consistent with the idea that AspA and AspC play similar roles, AspA and AspC show virtually identical localization patterns. Typically, fungal septins localize as rings or collars through which new growth emerges, cross walls delineating compartments, or caps at hyphal tips (22). AspA and AspC show these typical fungal localization patterns, forming rings or collars through which germ tubes, branches, and conidiophore layers emerge; septa delineating hyphal compartments; and diffuse caps at tips of actively growing hyphae (Fig. 4 and 5). In addition to these typical fungal localization patterns, AspA and AspC localize as dots or short bars, puncta, or elongated filaments, patterns previously described mainly for animal septins (Fig. 4) (22).

AspA and AspC are involved in, but not required for, septation. While *S. cerevisiae* strains with mutations in septin core complex members make no septa and cannot complete cytokinesis (16), *Schizosaccharomyces pombe* septin mutants form septa and divide, though the process is delayed in some mutants (24, 34). Thus, it was not too surprising that *A. nidulans* Δ*aspA*, Δ*aspC*, and Δ*aspA* Δ*aspC* strains made at least some septa. After an initial delay, Δ*aspA* strains made near-wild-type

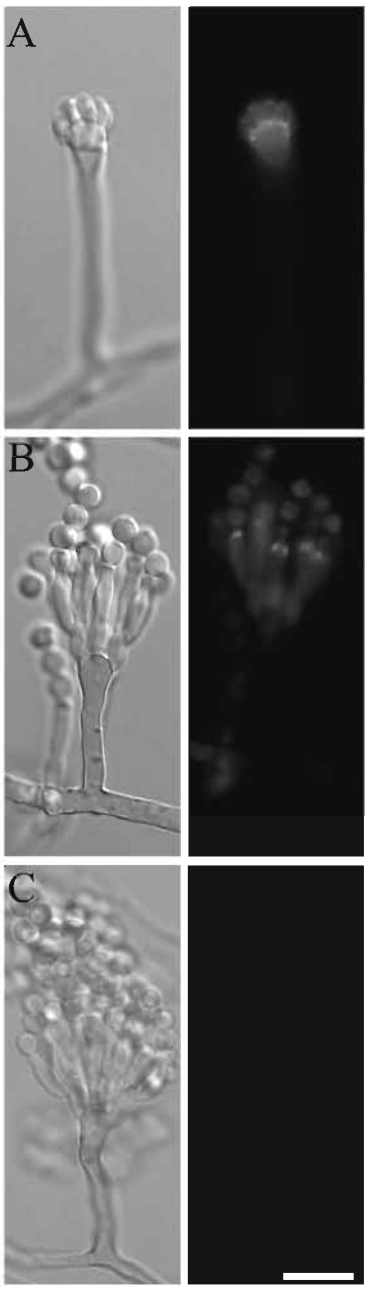

FIG. 5. AspA localizes to emerging conidiophore layers. The AspA-GFP strain was incubated on agar between glass coverslips, and live cells were photographed using fluorescence microscopy. AspA-GFP at vesicle-metula interface (A) and phialide-conidiospore interface (B and C). Scale bar, 5 μm.

levels of apparently normal septa. This is very close to the situation in *S. pombe*, where a mutant lacking Spn3, the AspA ortholog, shows normal cytokinesis (1). In contrast, Δ*aspC* strains made only one-third of the number of septa that the wild type did and these septa appeared to be abnormal based on staining with the chitin-binding dye calcofluor, suggesting that AspC has a unique role in septation and that this role cannot be filled by other septins. This is somewhat similar to the case in *S. pombe*, where a mutant in Spn4, the AspC ortholog, shows delayed cytokinesis, a more severe effect than loss of Spn3 (1). These differences in septin defects are consistent with recent literature showing that though different septins interact for proper function, septin dynamics within a complex can vary (5).

AspA and AspC influence the number of new growth foci and their patterns. During vegetative growth Δ*aspA*, Δ*aspC*, and Δ*aspA* Δ*aspC* mutants showed increased emergence of new growth foci, making extra germ tubes and branches (Fig. 1). In addition to having too many germ tubes, their spatial pattern is disrupted in Δ*aspA*, Δ*aspC*, and Δ*aspA* Δ*aspC* mutants. In wild-type *A. nidulans*, a single germ tube emerges from the conidium and is generally followed later by emergence of a second germ tube 180° relative to the first (27). In contrast, second germ tubes in the Δ*aspA*, Δ*aspC*, and Δ*aspA* Δ*aspC* mutants emerge axial or at 45°or 90° relative to the first germ tube, indicating a disruption of spatial pattern. In wild-type hyphae generally a single branch emerges from each compartment delineated by septa (21). Thus, we cannot predict the normal position for a second branch within a compartment and so cannot determine whether the multiple, closely spaced branches that emerge from compartments of Δ*aspA*, Δ*aspC*, and Δ*aspA* Δ*aspC* mutants indicate a disruption of spatial pattern or simply an increase in the number of new growth foci.

During asexual reproduction in *A. nidulans*, a regular, organized, multilayered conidiophore that bears chains of spores (conidia) is made by a process that closely resembles budding in yeast (36). During conidiation in Δ*aspA*, Δ*aspC*, and Δ*aspA* Δ*aspC* mutants, the multiple layers of the conidiophore are disorganized and the number of conidia is reduced (Fig. 3). This disorganization appears to affect different layers of the multilayered structure in individual conidiophores within a population. In some conidiophores the deletion phenotype appears to be a patterning defect, and in others it appears to be a cell division or separation defect.

In *S. cerevisiae*, septin mutants show disruption of normal axial and bipolar budding patterns (24, 26), and so the disruption of germ tube emergence patterns in Δ*aspA*, Δ*aspC*, and Δ*aspA* Δ*aspC* mutants was not too surprising. However, we were very surprised to see the increased germ tube and branch emergence in the *A. nidulans* septin mutants. Though *S. cerevisiae* septin mutants form cells with multiple buds, this multibud phenotype is thought to result from failure to complete cytokinesis, which normally separates buds from the mother cell, not from simultaneous emergence of new buds (25). During vegetative growth of filamentous fungi like *A. nidulans*, there is no separation of germ tubes and branches from the hypha comparable to the separation of buds from the mother cell at cytokinesis in yeast. Cytokinesis in filamentous fungi results in partitioning of hyphal compartments by septa, a process which still takes place in the Δ*aspA*, Δ*aspC*, and Δ*aspA* Δ*aspC* mutants, although it is delayed or reduced. This is, to our knowledge, the first report of an increase in the number of new growth foci associated with loss of septin function in any or-

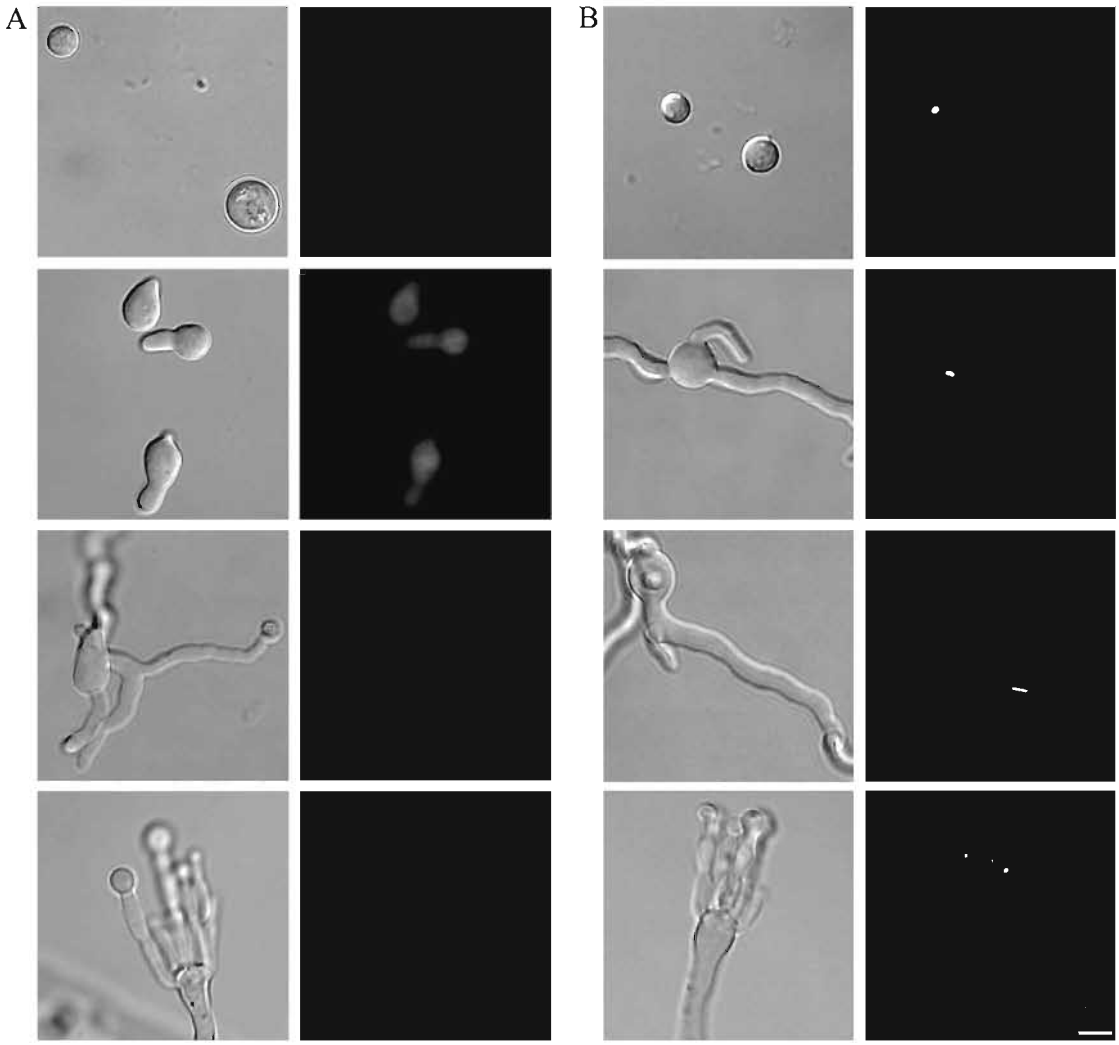

FIG. 6. AspC fails to localize in Δ*aspA* cells, and AspA localizes abnormally in Δ*aspC* cells. (A) An AspC-GFP, Δ*aspA* strain was incubated, and live cells were photographed using fluorescence microscopy. (B) An AspA-GFP, Δ*aspC* strain was incubated, and live cells were photographed using fluorescence microscopy. Scale bar, 5 μm.

ganism and raises the intriguing possibility that septins might limit new growth foci in other multicellular organisms.

ACKNOWLEDGMENT

This work was supported by National Science Foundation grant MCB-0211787 to M.M.

REFERENCES

1. **An, H., J. Morrell, J. Jennings, A. Link, and K. Gould.** 2004. Requirements of fission yeast septins for complex formation, localization, and function. Mol. Biol. Cell **15**:5551–5564.
2. **Beites, C. L., H. Xie, R. Bowser, and W. S. Trimble.** 1999. The septin CDCrel-1 binds syntaxin and inhibits exocytosis. Nat. Neurosci. **2**:434–439.
3. **Bertin, A., M. McMurray, P. Grob, S. Park, G. Garcia, I. Patanwala, H. Ng, T. Alber, J. Thorner, and E. Nogales.** 2008. Saccharomyces cerevisiae septins: supramolecular organization of heterooligomers and the mechanism of filament assembly. Proc. Natl. Acad. Sci. U. S. A. **105**:8274–8279.
4. **Caviston, J. P., M. Longtine, J. R. Pringle, and E. Bi.** 2003. The role of Cdc42p GTPase-activating proteins in assembly of the septin ring in yeast. Mol. Biol. Cell **14**:4051–4066.
5. **DeMay, B. S., R. A. Meseroll, P. Occhipinti, and A. S. Gladfelter.** 2009. Regulation of distinct septin rings in a single cell by Elm1p and Gin4p kinases. Mol. Biol. Cell **20**:2311–2326.
6. **Dietrich, F. S., S. Voegeli, S. Brachat, A. Lerch, K. Gates, S. Steiner, C. Mohr, R. Pohlmann, P. Luedi, S. Choi, R. A. Wing, A. Flavier, T. D. Gaffney, and P. Philippsen.** 2004. The Ashbya gossypii genome as a tool for mapping the ancient Saccharomyces cerevisiae genome. Science **304**:304–307.
7. **Frazier, J. A., M. L. Wong, M. S. Longtine, J. R. Pringle, M. Mann, T. J. Mitchison, and C. Field.** 1998. Polymerization of purified yeast septins: evidence that organized filament arrays may not be required for septin function. J. Cell Biol. **143**:737–749.
8. **Gladfelter, A., J. Pringle, and D. Lew.** 2001. The septin cortex at the yeast mother-bud neck. Curr. Opin. Microbiol. **4**:681–689.
9. **Gladfelter, A. S.** 2006. Control of filamentous fungal cell shape by septins and formins. Nat. Rev. Microbiol. **4**:223–229.
10. **Gladfelter, A. S., L. Kozubowski, T. R. Zyla, and D. J. Lew.** 2005. Interplay between septin organization, cell cycle and cell shape in yeast. J. Cell Sci. **118**:1617–1628.
11. **Harris, S. D.** 1999. Morphogenesis is coordinated with nuclear division in germinating *Aspergillus nidulans* conidiospores. Microbiology **145**:2747–2756.
12. **Harris, S. D.** 2001. Genetic analysis of ascomycete fungi, p. 56–57. *In* N. J. Talbot (ed.), Molecular and cellular biology of filamentous fungi. Oxford University Press, New York, NY.

13. **Harris, S. D., J. L. Morrell, and J. E. Hamer.** 1994. Identification and characterization of Aspergillus nidulans mutants defective in cytokinesis. Genetics **136:**517–532.
14. **Hartwell, L. H.** 1971. Genetic control of the cell division cycle in yeast. IV. Genes controlling bud emergence and cytokinesis. Exp. Cell Res. **69:**265–276.
15. **Ihara, M., A. Kinoshita, S. Yamada, H. Tanaka, A. Tanigaki, A. Kitano, M. Goto, K. Okubo, H. Nishiyama, and O. Ogawa.** 2005. Cortical organization by the septin cytoskeleton is essential for structural and mechanical integrity of mammalian spermatozoa. Dev. Cell **8:**343–352.
16. **Iwase, M., J. Luo, E. Bi, and A. Toh-e.** 2007. Shs1 plays separable roles in septin organization and cytokinesis in Saccharomyces cerevisiae. Genetics **177:**215–229.
17. **Kafer, E.** 1977. Meiotic and mitotic recombination in *Aspergillus* and its chromosomal aberrations. Adv. Genet. **19:**33–131.
18. **Kartmann, B., and D. Roth.** 2001. Novel roles for mammalian septins: from vesicle trafficking to oncogenesis. J. Cell Sci. **114:**839–844.
19. **Kinoshita, M., C. Field, M. Coughlin, A. Straight, and T. Mitchison.** 2002. Self- and actin-templated assembly of mammalian septins. Dev. Cell **3:**791–802.
20. **Lin, X., and M. Momany.** 2003. The Aspergillus nidulans swoC1 mutant shows defects in growth and development. Genetics **165:**543–554.
21. **Lin, X., and M. Momany.** 2004. Identification and complementation of abnormal hyphal branch mutants ahbA1 and ahbB1 in Aspergillus nidulans. Fungal Genet. Biol. **41:**998–1006.
22. **Lindsey, R., and M. Momany.** 2006. Septin localization across kingdoms: three themes with variations. Curr. Opin. Microbiol. **9:**559–565.
23. **Lougtine, M., and E. Bi.** 2003. Regulation of septin organization and function in yeast. Trends Cell Biol. **13:**403–409.
24. **Longtine, M., D. DeMarini, M. Valencik, O. Al-Awar, H. Fares, C. De Virgilio, and J. Pringle.** 1996. The septins: roles in cytokinesis and other processes. Curr. Opin. Cell Biol. **8:**106–119.
25. **Longtine, M., C. Theesfeld, J. McMillan, E. Weaver, J. Pringle, and D. Lew.** 2000. Septin-dependent assembly of a cell cycle-regulatory module in Saccharomyces cerevisiae. Mol. Cell. Biol. **20:**4049–4061.
26. **Madden, K., and M. Snyder.** 1998. Cell polarity and morphogenesis in budding yeast. Annu. Rev. Microbiol. **52:**687–744.
27. **Momany, M., and I. Taylor.** 2000. Landmarks in the early duplication cycles of Aspergillus fumigatus and Aspergillus nidulans: polarity, germ tube emergence and septation. Microbiology **146:**3279–3284.
28. **Momany, M., P. J. Westfall, and G. Abramowsky.** 1999. Aspergillus nidulans swo mutants show defects in polarity establishment, polarity maintenance and hyphal morphogenesis. Genetics **151:**557–567.
29. **Momany, M., J. Zhao, R. Lindsey, and P. J. Westfall.** 2001. Characterization of the Aspergillus nidulans septin (asp) gene family. Genetics **157:**969–977.
30. **Pan, F., R. L. Malmberg, and M. Momany.** 2007. Analysis of septins across kingdoms reveals orthology and new motifs. BMC Evol. Biol. **7:**103.
31. **Spiliotis, E., and W. Nelson.** 2006. Here come the septins: novel polymers that coordinate intracellular functions and organization. J. Cell Sci. **119:**4–10.
32. **Spiliotis, E. T., M. Kinoshita, and W. J. Nelson.** 2005. A mitotic septin scaffold required for mammalian chromosome congression and segregation. Science **307:**1781–1785.
33. **Sudbery, P. E.** 2001. The germ tubes of Candida albicans hyphae and pseudohyphae show different patterns of septin ring localization. Mol. Microbiol. **41:**19–31.
34. **Sudbery, P. E., and A. S. Gladfelter.** 2008. Pathocycles. Fungal Genet. Biol. **45:**1–5.
35. **Surka, M., C. Tsang, and W. Trimble.** 2002. The mammalian septin MSF localizes with microtubules and is required for completion of cytokinesis. Mol. Biol. Cell **13:**3532–3545.
36. **Timberlake, W.** 1991. Temporal and spatial controls of Aspergillus development. Curr. Opin. Genet. Dev. **1:**351–357.
37. **Versele, M., B. Gullbrand, M. Shulewitz, V. Cid, S. Bahmanyar, R. Chen, P. Barth, T. Alber, and J. Thorner.** 2004. Protein-protein interactions governing septin heteropentamer assembly and septin filament organization in Saccharomyces cerevisiae. Mol. Biol. Cell **15:**4568–4583.
38. **Versele, M., and J. Thorner.** 2004. Septin collar formation in budding yeast requires GTP binding and direct phosphorylation by the PAK, Cla4. J. Cell Biol. **164:**701–715.
39. **Warenda, A. J., and J. B. Konopka.** 2002. Septin function in Candida albicans morphogenesis. Mol. Biol. Cell **13:**2732–2746.
40. **Westfall, P. J., and M. Momany.** 2002. Aspergillus nidulans septin AspB plays pre- and postmitotic roles in septum, branch, and conidiophore development. Mol. Biol. Cell **13:**110–118.
41. **Wolkow, T. D., S. D. Harris, and J. E. Hamer.** 1996. Cytokinesis in *Aspergillus nidulans* is controlled by cell size, nuclear positioning, and mitosis. J. Cell Sci. **109:**2179–2188.
42. **Xie, H., M. Surka, J. Howard, and W. Trimble.** 1999. Characterization of the mammalian septin H5: distinct patterns of cytoskeletal and membrane association from other septin proteins. Cell Motil. Cytoskeleton **43:**52–62.
43. **Xue, J., C. Tsang, W. Gai, C. Malladi, W. Trimble, J. Rostas, and P. Robinson.** 2004. Septin 3 (G-septin) is a developmentally regulated phosphoprotein enriched in presynaptic nerve terminals. J. Neurochem. **91:**579–590.
44. **Yang, L., L. Ukil, A. Osmani, F. Nahm, J. Davies, C. P. De Souza, X. Dou, A. Perez-Balaguer, and S. A. Osmani.** 2004. Rapid production of gene replacement constructs and generation of a green fluorescent protein-tagged centromeric marker in Aspergillus nidulans. Eukaryot. Cell **3:**1359–1362.

Aspergillus terreus accessory conidia are multinucleated, hyperpolarizing structures that display differential dectin staining and can induce heightened inflammatory responses in a pulmonary model of aspergillosis

Eszter Deak,[1] Michael Nelson,[2] Yainitza Hernández-Rodríguez,[3] Lalitha Gade,[1] John Baddley,[2] Michelle Momany,[3] Chad Steele[2] and S. Arunmozhi Balajee[1,*]

[1]Mycotic Diseases Branch; Centers for Disease Control and Prevention; Atlanta, GA USA; [2]Department of Medicine; University of Alabama-Birmingham; Birmingham, AL USA; [3]Department of Plant Biology; University of Georgia; Athens, GA USA

Key words: *Aspergillus terreus*, accessory conidia characterization, β-glucan, aspergillosis, pathogenesis

In addition to phialidic conidia (PC), *A. terreus* produces accessory conidia (AC) both in vitro and in vivo. AC are distinct from PC in cell surface architecture, with the AC surfaces displaying more β-glucan, a molecule that can be a trigger for the induction of inflammatory responses. The present study follows β-glucan cell surface presentation throughout the course of germination of both types of conidia, and analyzes the differential capacity of AC and PC to elicit immune responses. Results show that AC display early, increased dectin-1 labeling on their cell surfaces compared to PC, and this differential dectin-1 labeling is sustained on the cell surface from the time of breaking dormancy through early germ tube emergence. Mouse alveolar macrophages showed a stronger inflammatory cytokine/chemokine response when challenged with AC than with PC in both ex vivo and in vivo experiments, correlating with the greater exposure of β-glucan exhibited by AC. Further, histopathologic staining of the lungs from mice challenged with AC demonstrated heightened cell recruitment and increased inflammatory response compared to the lungs of mice challenged with PC. Our study also demonstrates that AC are multinucleate structures with the ability to germinate rapidly, polarizing in multiple directions and producing several hyphal extensions. We present evidence that *A. terreus* AC are phenotypically distinct from PC and can be potent activators of the innate immune mechanism thus possibly playing a role in this organism's pathogenesis.

Introduction

Aspergillus terreus produces two types of asexual conidia: accessory conidia (AC, asexual conidia formed directly on hyphae) and phialidic conidia (PC, asexual conidia arising from conidiophores generated on hyphae).[1] Accessory conidia are produced both in vitro and in vivo, and a recent study from our laboratory indicated that AC were morphologically distinct from PC in that they lacked a pigment-like outer layer and were larger than PC.[1] We demonstrated other phenotypic differences between these two conidial forms including the ability of AC to germinate more rapidly, enhanced adherence of AC to microspheres, heightened AC metabolic activity, less cell membrane ergosterol and lower susceptibility of AC to the antifungal drug amphotericin B.[1,27] Additionally, our study showed that dormant AC displayed uniform β-glucan staining, with enhanced staining in a ring pattern suggesrive of a bud scar, in contrast to PC, for which β-glucan staining demonstrated a non-uniform staining pattern.[1]

β-glucan recognition has been shown to be important in innate immune defenses against many pathogenic fungi, including *Pneumocystis carinii*, *Coccidioides posadasii*, *Histoplasma capsulatum* and *Aspergillus fumigatus*.[2-13] In the yeast *Candida albicans*, exposure of β-glucan patches at budding and cell separation has been shown to elicit inflammatory responses in macrophages through Dectin-1 mediated β-glucan recognition.[14-16] In *A. fumigatus*, the β-glucan moieties are concealed in dormant conidia by surface hydrophobins or rodlet layers.[17] Over the course of germination surface β-glucans are unmasked, becoming most evident during spore swelling and early germ tube formation, and are again veiled in the early stages of hyphal growth.[3,5,11,18] Exposed β-glucans are recognized by Dectin-1 receptors on alveolar macrophages, and thus induce stage specific inflammatory responses against fungal morphological forms undergoing rapid

*Correspondence to: S. Arunmozhi Balajee; Email: fir3@cdc.gov
Submitted: 01/14/11; Revised: 04/11/11; Accepted: 04/12/11
DOI:

cell cycle processes, indicative of the potential for invasion or early infection.[2,5,6,11,13] Blockage of Dectin-1 recognition of β-glucans substantially increases susceptibility to infection through down-regulation of chemokine/cytokine production.[3]

Phenotypic differences and unique germination and metabolic rates between Aspergillus species conidia may account for differences in invasiveness and dissemination.[19] The same may be true of AC compared to PC. Given our recent findings of differential labeling of β-glucan on AC compared to PC, the present study was designed with the following objectives: (1) to compare β-glucan labeling over time on *A. fumigatus* conidia and *A. terreus* AC and PC, (2) to measure cytokine/chemokine production by macrophages exposed to AC versus PC ex vivo and (3) to compare inflammatory responses to AC and PC in an in vivo pulmonary mouse model of aspergillosis. Additionally, we explored other phenotypic features of AC including number of nuclei and polarization of these structures.

Results

Species-specific differences in β-glucan display on phialidic conidia. Staining with soluble dectin-1 was performed on *A. fumigatus* and *A. terreus* PC to demonstrate surface β-glucan display. As described previously in reference 20, no β-glucan label was observed on the surface of dormant *A. fumigatus* PC (**Fig. 1A**). In contrast, dormant *A. terreus* PC exhibited irregular staining around the conidia. During germination, PC from both species displayed uniform binding of dectin-1 to the cell surface (**Fig. 1B**). Early germlings of *A. fumigatus* displayed staining over the entire conidial and hyphal surface, with concentrated staining at the tips, whereas *A. terreus* germlings displayed uniform dectin-1 staining on both the conidia and the germ tube, without enhanced tip staining (**Fig. 1C**). Dectin-1 labeling was apparent on mature *A. fumigatus* hyphae, but low. Meanwhile, the *A. terreus* hyphae demonstrated intense punctuate (spotted) staining, and the emergence of AC that displayed dectin-1 staining (Fig. 1D).

Staining with soluble dectin-1 is heightened on *Aspergillus terreus* accessory conidia. Given the differences observed in *A. terreus* PC and AC β-glucan labeling in our previous study,[1] we were also interested in looking at stage specific β-glucan display between these conidial forms. We therefore examined the ability of dectin-1 to recognize *A. terreus* AC at different stages of maturation (Fig. 2). Fluorescence microscopy revealed that, in contrast to the irregular staining of *A. terreus* dormant PC (Fig. 1A), the entire surface of freshly harvested AC bound s-dectin-mFc, with a heightened patch of detection evident on one side of the AC (Fig. 2A). *A. terreus* PC exhibited uniform dectin-1 labeling as swelling occurred (Fig. 1B), while the pattern of swollen AC continued to have uniform staining with enhanced "ring-shaped" staining (Fig. 2B). Early germ tubes emerging from *A. terreus* PC stained homogenously (Fig. 1C), whereas the AC germlings maintained very strong dectin-1 recognition on the originating conidial surface, with concentrated ring-shaped patch staining similar to that seen in the dormant and swollen stages, in addition to uniform staining of the entire germ tube (Fig. 2C). During hyphal extension, dectin-1 labeling became more irregular for *A. terreus* PC (Fig. 1D) and AC (Fig. 2D) hyphae. At this stage, the two conidial forms looked identical, as both were producing AC on their hyphae, and the attached AC were clearly recognized and stained with soluble dectin-1. Accessory conidia that were attached to hyphae did not have the heightened ring-shaped staining observed on harvested AC.

***Aspergillus terreus* conidia are multinucleate structures.** The DNA intercalating Hoechst dye was employed to ascertain nuclear content within freshly harvested AC (Fig. 3B) and PC (Fig. 3C). Accessory conidia were found to be multinucleated, with the nuclear number varying considerably. On average, AC contained three to four nuclei, but as many as seven could be distinguished in some AC. Nuclear staining was absent in several AC, possibly due to inefficient incorporation of the Hoechst dye into the cells or nonviability of the conidia. Hoechst staining was also performed on AC still attached to the hyphae (Fig. 3A). Again, the AC were found to contain multiple nuclei. Furthermore, AC were found to produce multiple germ tubes in early germ tube formation (Fig. 4). Dormant *A. terreus* PC were found to contain, on average, two, with as many as three nuclei (Fig. 3C), whereas dormant *A. fumigatus* PC contained only one nucleus (Fig. 3D).

***Aspergillus terreus* accessory conidia, but not phialidic conidia, elicit a heightened inflammatory response.** Given that β-glucan displayed different patterns of expression in AC and PC, we hypothesized that inflammatory responses to the two conidial forms would also differ. Initial examination of the inflammatory response utilized mouse alveolar macrophages exposed to either AC or PC ex vivo. The results showed that, consistent with the pattern of β-glucan display, co-culture of AC with alveolar macrophages elicited a heightened inflammatory response, with significantly increased production of MCP-1, IL-6, IL-1β, G-CSF, TNFα, CXCL2/MIP-2, KC, CCL4/MIP-1β, CCL3/MIP-1α and IL-1α compared to PC elicited responses after only 2 h (data not shown). Differences in chemokine/cytokine production proved more profound after 6 (Fig. 5A) and 20 (Fig. 5B) h. Production of chemokines and cytokines was not appreciably altered by heat killing the conidia (data not shown). Negligible levels of chemokine and cytokine production were observed for unstimulated alveolar macrophages (controls).

Further investigations assessed chemokine and cytokine production in the lungs after intratracheal challenge with *A. terreus* AC or PC. In vivo and ex vivo experiments demonstrated a similar trend of increased chemokine/cytokine production elicited by AC compared to PC, albeit with more G-CSF, MCP-1, IL-6 and IL-1β production observed in vivo (Fig. 6A). Additionally, hematoxylin and eosin staining, also performed on the lungs of these intratracheally challenged mice, indicated infiltration of cells into the site of infection (Fig. 6B), in support of the chemokine and cytokine data. Little inflammatory response was observed in PBS challenged mice (controls).

Discussion

The extent of differences inherent amongst the aspergilli is often underappreciated, but is evidenced by phenotypic features such

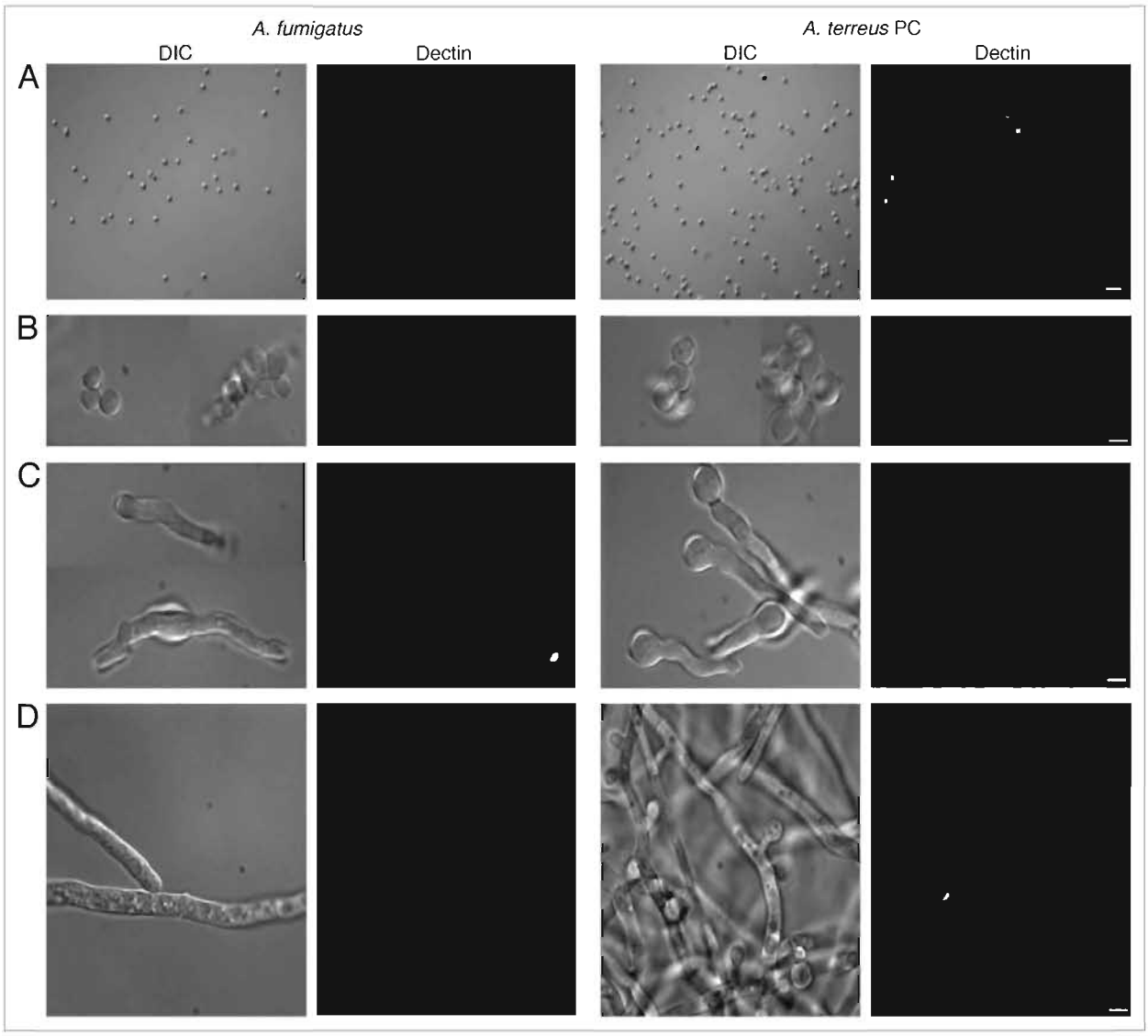

Figure 1. Differential dectin-1 binding on *Aspergillus fumigatus* and *Aspergillus terreus* phialidic conidia. Soluble dectin-1 binding *A. fumigatus* and *A. terreus* phialidic conidia at various stages of germination (A) dormant conidia (B) swollen condia (C) early germ tube formation and (D) late germination. Differential interference microscopy (DIC) and fluorescence images were captured by microscopy at 40x (A) and 100x (B–D), and are representative of 3 experiments. Scale bars denote 5 μm and 10 μm for 40x and 100x magnification, respectively.

as color, hydrophobicity, rate of germination, cell size and surface structure. For instance, although both *A. fumigatus* and *A. nidulans* conidia contain two hydrophobins, RodAp and RodBp (*A. fumigatus*), RodAp and DewAp (*A. nidulans*), and the *rodA* gene of *A. fumigatus* has been shown to complement homologous RodAp mutations in *A. nidulans*, the *rodB* gene is unable to complement *A. nidulans* DewAp mutations in spite of having the same molecular mass and similar signal sequence.[21] Analysis of physicochemical properties in the RodAp knockouts of the two species also suggests that there may be other differences in the composition of their outer cell walls, i.e., lipid and glycoprotein content, that are unmasked by disruption of the rodlets upon germination.[22]

Similarly, the asexual conidia of *A. fumigatus* and *A. terreus* are distinct in color and cell size and recent studies in our laboratory indicate differential rates of germination and hydrophobicity between these conidia.[1] In this study, we further demonstrate that *A. terreus* PC have an average of two nuclei compared to *A. fumigatus* conidia, which often contains one nucleus. Additionally, PC of both species exhibit distinct cell surface characteristics including β-glucan expression. Specifically, there was no β-glucan staining on the surface of dormant *A. fumigatus*

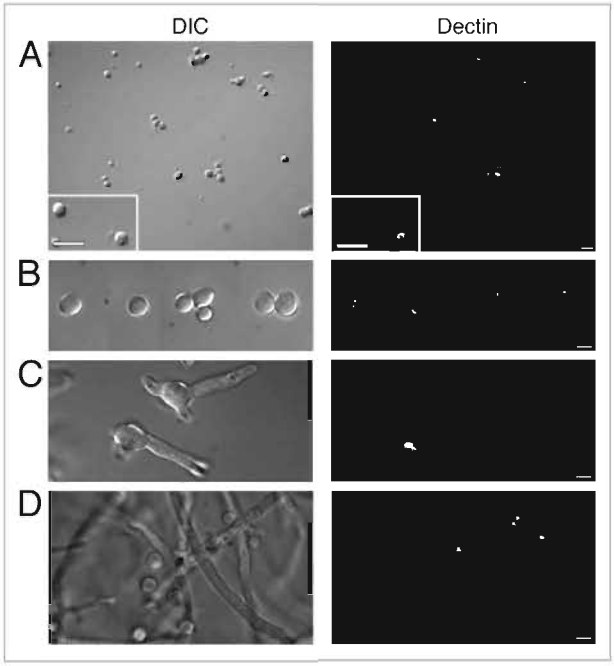

Figure 2. Dectin-1 binding on phialidic conidia and accessory conidia at different germination stages. Soluble dectin-1 binding on *A. terreus* phialidic and accessory conidia at (A) dormant conidia (B) swollen conidia, (C) early germ tube formation and (D) late germination. DIC and fluorescence images were captured by microscopy at 40x (A) and 100x (B–D), and are representative of 3 experiments. Within windows, arrows depict the ring-like staining pattern on AC at 100x (A). Scale bars denote 5 μm and 10 μm for 40x and 100x magnification, respectively.

PC, in contrast to the irregular staining apparent on dormant *A. terreus* PC. Furthermore, early germlings of *A. fumigatus* displayed concentrated β-glucan staining at the tips while this was not observed on the tips of *A. terreus* germlings. Finally, in late polar growth, dectin-1 labeling was uniform throughout the surface but considerably diminished in *A. fumigatus*, while staining of *A. terreus* hyphae was punctuate and intense. No significant differences were observed between the clinical and environmental isolate tested. These species specific characteristics hold the potential to elicit differential immune responses to these organisms and will need to be tested in future experiments.

Our previous study indicated that *A. terreus* AC have enhanced β-glucan display compared to dormant *A. terreus* PC,[1] suggesting that these conidia differ markedly as well. In the present study, β-glucan display was continuous on the surface of AC throughout the stages of germination. In contrast, β-glucan display showed an irregular staining pattern on dormant *A. terreus* PC. β-glucan display was enhanced during swelling and early germ tube formation, and subsequently diminished. In *A. fumigatus*, conidia swell upon induction of germination, in the process losing a hydrophobin or rodlet layer, as well as pigments such as melanin. These surface molecules conceal β-glucans that serve as binding sites for Dectin-1, as well as other Pathogen-associated molecular patterns (PAMPs) that can be recognized by immune cells, i.e., Toll-like receptor 4 (TLR4) and mannose receptors, thus modulating stage specific immune responses.[17,20,21,23] Here, we show that the two different conidial types of *A. terreus* have differential β-glucan display and accordingly are recognized differently by immune cells. The influence of differential patterns of β-glucan presentation on pathogenicity for AC versus PC, and the consequences of altering these patterns, requires deeper investigation.

Phenotypically, *A. terreus* AC are lighter in color compared to PC. Previous SEM and TEM studies from our laboratory demonstrated that the cell surface of AC appear to be devoid of a yet to be characterized fungal pigment in contrast to the PC surface.[1] *A. fumigatus* conidia lacking the pigment melanin are white in color and a recent study demonstrated that albino *A. fumigatus* conidia induced significantly more proinflammatory cytokines in human peripheral blood mononuclear cells (PBMC), as compared to melanized wild-type conidia.[23] Similarly, in the present study, we found that production of cytokines/chemokines elicited by AC was greater than that elicited by PC, both ex vivo and in vivo in a mouse model. This heightened proinflammatory response could be attributed to "albino" AC (lacking pigment) that display strong cell surface β-glucan. Since we only inactivated the conidia by heat killing and did not perform additional blocking experiments with Laminarin (for β-glucan), we cannot at this time rule out the presence of other stimulatory PAMPs like mannan derivatives on the AC surface. However we did use *A. fumigatus* as a control since staining of *A. fumigatus* with Dectin-1 has been well characterized in previous studies. An additional limitation of this study was that we did not elucidate fungal burden or survival and thus mice were sacrificed at 18 h post-challenge. Future studies, powered to understand survival after challenge with PC and AC need to be performed.

Our studies show that *A. terreus* AC are multinucleate and may contain as many as seven nuclei. To ensure that the AC were not breaking "dormancy" upon detachment from the hyphae, thus inducing cell cycle stages to progress within the conidial structures and the multiple nuclei observed, Hoechst staining was performed on AC still attached to the hyphae. These AC were also found to contain multiple nuclei, again varying in number. In *A. oryzae*, multi-nucleation of conidia conferred greater viability and resistance to UV radiation and freeze-thaw treatment, thus resulting in better adaptation to adverse environmental conditions and could ensure conidial preservation.[24] Although such viability experiments were not performed in the present study, there is some evidence that AC are at least more resistant to antifungal drugs than PC. If indeed multinucleation imparted viabiliry benefirs to AC, this would be a significant virulence factor for *A. terreus* as it would allow the organism to survive the harsh environment of the host during infection.

Alternatively, multinucleation could suggesr a rudimentary form of conidia that have not yet evolved cell cycle control mechanisms, the evolutionary benefit of which might be rapid germ tube emergence. In fact, our previous studies demonstrated that AC germinated much more rapidly than either *A. fumigatus* or *A. terreus* PC, and this study found that the AC formed multiple

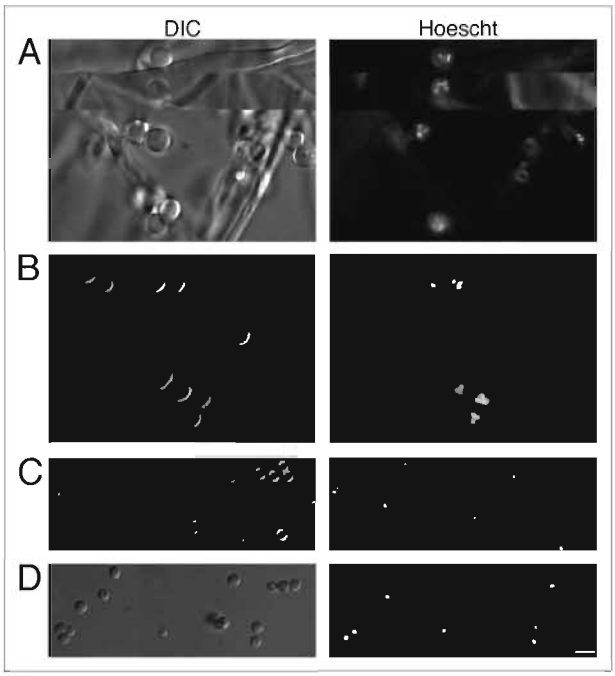

Figure 3. Accessory conidia are multinucleated prior to germination. Hoechst staining was performed on *A. terreus* accessory conidia, both attached (A) and detached (B) from the hyphae, and *A. terreus* PC (C) and *A. fumigatus* PC (D). DIC and UV images were captured by microscopy at 100x, and are representative of 3 experiments. Scale bars denote 10 μm.

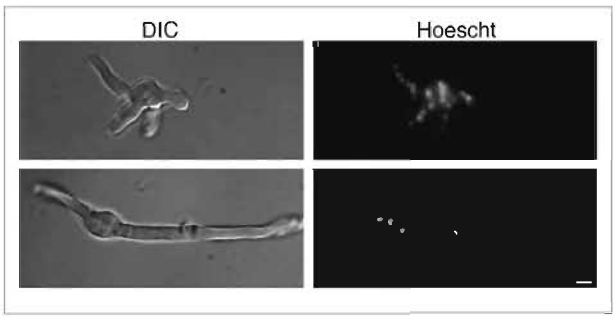

Figure 4. Accessory conidia undergo hyperpolarization during germination. Early germ tube formation and Hoechst nuclei staining was assessed for *A. terreus* accessory conidia. DIC and UV images were captured by microscopy at 100x, and are representative of 3 experiments. Scale bars denote 10 μm.

germ tubes (Fig. 4). Similar to our study, in *A. oryzae*, multinucleate conidia had a higher germination efficiency than uninucleate conidia.[24] Additionally, late stage germination of both *A. terreus* PC and AC culminates in production of hyphae on which grow more AC, which in turn polarize in multiple directions to quickly form several more hyphal extensions. In spite of differences in germination porential between the two conidial forms, once both conidia achieved germination, the ensuing developmental stages appear to proceed comparably resulting in similar mycelial masses as assessed visually under a microscope (data not shown). The ability for each AC to produce multiple hyphae and subsequently more AC and ultimately more hyphae in a very short period of time perhaps sets the stage for rapid invasion and dissemination during infection in spite of inducing strong immune responses.

In summary, our study demonstrates phenotypic differences between *A. fumigatus* and *A. terreus*, specifically β-glucan display. Additionally, we demonstrate differences in cell surface β-glucan between the two *A. terreus* asexual conidia, elucidate the role of AC in inducing inflammatory responses in a mouse model of aspergillosis, and demonstrare multinucleation and hyperpolorization in these structures, all of which may contribute towards the pathogenicity of this organism.

Materials and Methods

Isolation of *A. terreus* phialidic and accessory conidia. To assess surface β-glucan exposure and nuclear staining for both conidial forms, *A. terreus* AC and PC from isolates CLF 29 and CLF 52, recovered from an environmental and a clinical sample respectively, were harvested along with *A. fumigatus* (ATCC1022) conidia as control. Since no significant differences were observed between the two *A. terreus* isolates, all following ex vivo and in vivo studies were performed with *A. terreus* AC and PC from isolate CLF 52. *A. terreus* isolates were cultured on Sabouraud dextrose agar plates (SDA) and incubated at 37°C for three days. To prepare PC inocula, colonies were gently probed with a loop and the resultant conidia were suspended in Sabouraud dextrose broth (SDB) and counted on a hemocytometer. For AC harvest, PC were collected in phosphate-buffered saline (PBS), and 5 x 10^5 cells/ml transferred to Sabouraud dextrose broth (SDB) with 0.1% Tween 20 (SDB Tween) and incubated for 7 days, after which AC were harvested as described previously in reference 25.

β-glucan exposure studies. Conidia were adhered to cover slips and allowed to incubate at 0, 5, 10 and 20 h for *A. fumigatus*, 0, 8, 11 and 20 h for *A. terreus* PC and 0, 4, 7 and 12 h for *A. terreus* AC to induce swollen conidia, early and late germ tubes respectively. Conidia were incubated with s-dectin-mFc (Chad Steele),[26] on ice for 45 minutes, washed with 1x PBS (plus 0.01% Tween), resuspended in Alexa Fluor 594 conjugared chicken anti-mouse antibody (Molecular Probes) diluted 1:250 in 1x PBS/plus 0.01% Tween, and incubated on ice for 45 minutes. Conidia were washed with 1x PBS/0.01% Tween, resuspended in Fluoromount G (Electron Microscopy Sciences), mounted onto slides and examined under a fluorescenr microscope (Zeiss Axiovert 25).

Animal experiments. Male C57BL/6 mice, 6–8 weeks of age, were purchased from the National Cancer Institute, National Institutes of Health (Bethesda, Maryland United States). All mice were maintained in a specific pathogen free environment in microisolator cages within an American Association for Laboratory Animal Science certified animal facility at the University of Alabama at Birmingham. Animal studies

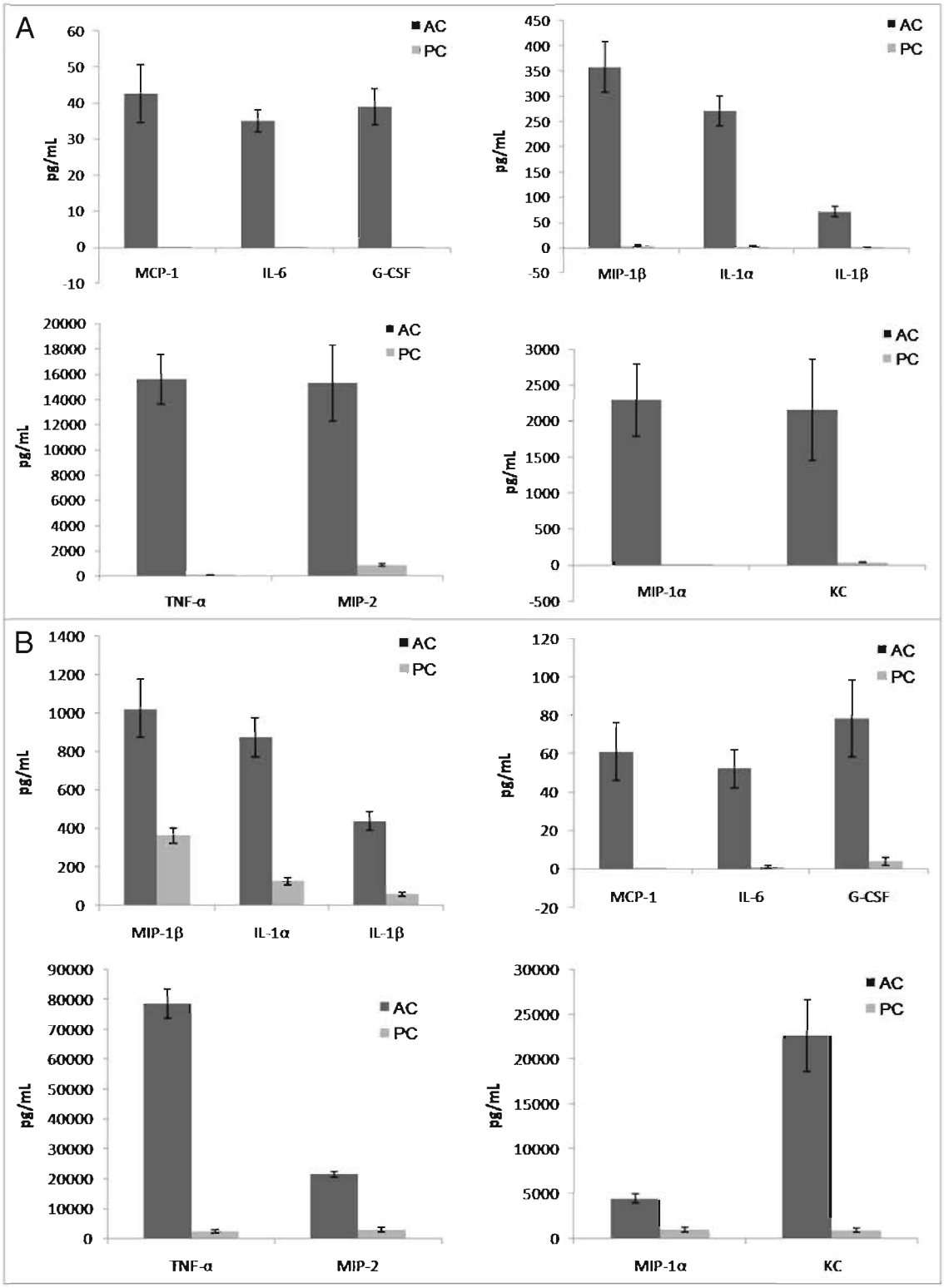

Figure 5. *Aspergillus terreus* accessory conidia elicit a heightened inflammatory response by alveolar macrophages. Alveolar macrophages were co-cultured with *A. terreus* AC or PC. Supernatants were collected at (A) 6 or (B) 20 h and assayed for chemokine/cytokine levels by Bio-Plex or ELISA. Experiments were performed 3 times.

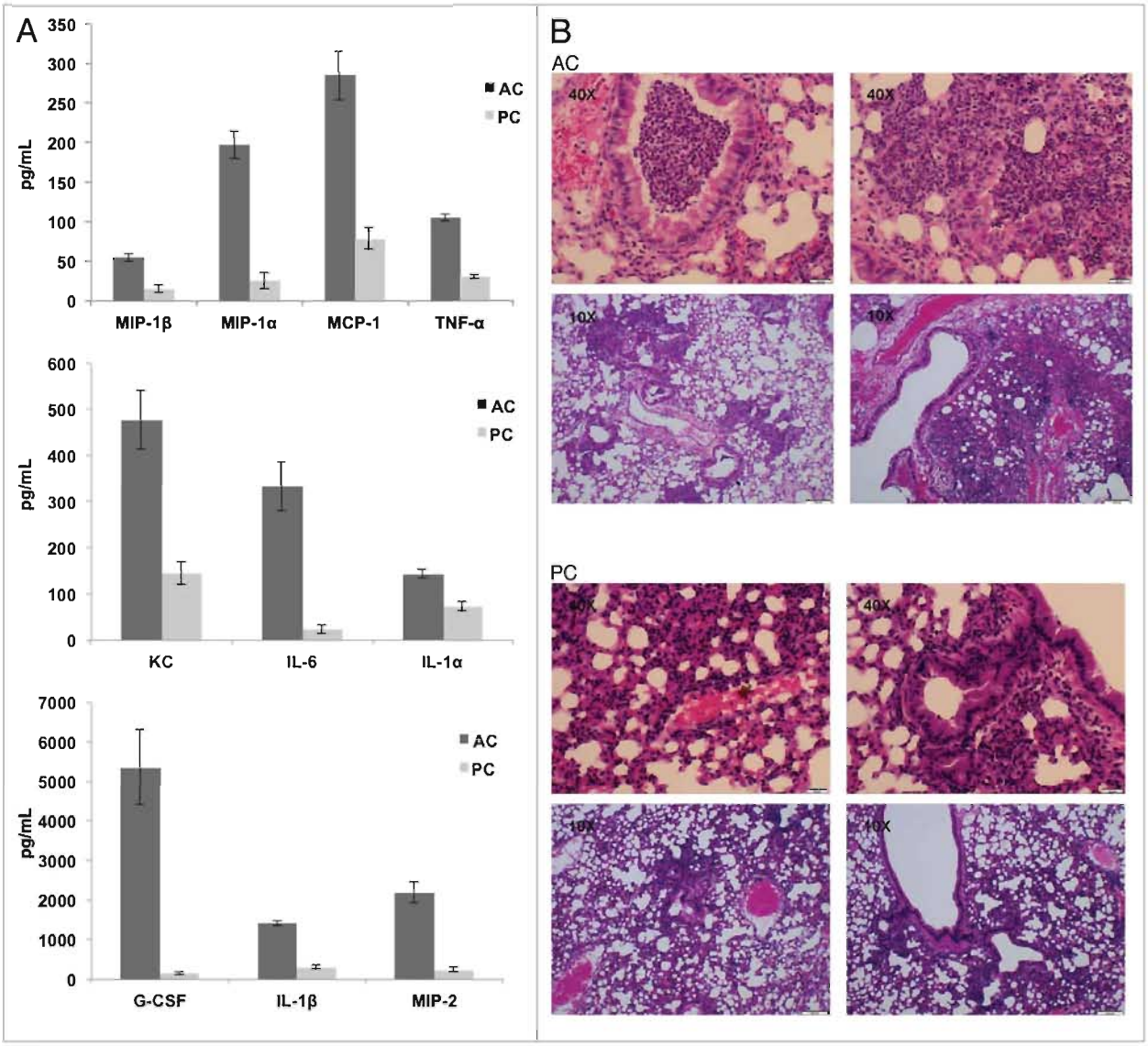

Figure 6. Mice intratracheally challenged with *Aspergillus terreus* accessory conidia exhibit enhanced chemokine/cytokine production and cell recruitment in lungs. C57BL/6 mice were intratracheally challenged with AC or PC. (A) Chemokine/cytokine levels in the supernatants of homogenized lungs collected at 18 h post-challenge with AC or PC (need to indicate from figure). (B) Hematoxylin and eosin staining of sections of lungs post-challenge with AC or PC (also denote figure labels). All experiments were performed 3 times.

were reviewed and approved by the University of Alabama at Birmingham Institutional Animal Care and Use Committee (IACUC).

For ex vivo studies, ten to fifteen healthy mice were anesthetized with isoflurane intraperitoneally and sacrificed by exsanguination. Lungs were subsequently lavaged with PBS, lavage fluids pooled and alveolar macrophages collected as previously described in reference 11. Harvested alveolar macrophages were co-cultured with live PC or AC at MOI of 1:1 ratio for 2, 6 or 20 h in a 96-well plate at 37°C, 5% CO_2 in RPMI 1640 with 10% heat inactivated fetal calf serum. Controls included alveolar macrophages cultured in medium alone. Cytokine and chemokine levels were assessed in the supernatants using the Bio-Plex Protein Array System (Bio-Rad, Hercules, California United States) as per the manufacturer's instructions. MIP-2 concentrations were also determined using a commercially available ELISA kit (R&D Systems, Minneapolis, Minnesota, United States) as per manufacturer's instructions. In another set of experiments, harvested mouse alveolar macrophages were challenged with heat killed PC or AC at MOI of 1:1 for 6 h, and supernatants were assessed for cytokines/chemokines. Both conidia types were heat killed by incubation at 100°C for 10 minutes prior to co-culture

with alveolar macrophages and efficacy of heat killing confirmed by plating on SDA.

For in vivo studies, eight mice were anesthetized and 7.5 x 10^6 conidia in 50 μl AC or PC administered intratracheally. At 18 h post-challenge, one lung was collected from each mouse for hematoxylin and eosin (H&E) and Gomori methenamine silver (GMS) staining, and the second lung homogenized and cytokine/chemokine levels measured as above.

Nuclear staining of PC and AC. Nuclear staining of PC and AC was accomplished by fixing (3.7% formaldehyde, 0.2% Triton X-100, 50 mM phosphate buffer, pH 7) cells for 30 minutes, followed by incubation with Hoechst dye (1 mg/ml) for 5 minutes. Conidia were washed with distilled water, resuspended in Fluoromount G (Electron Microscopy Sciences), mounted onto slides and examined by UV detection under a fluorescent microscope (Zeiss Axiovert 25).

Disclaimer

The findings and conclusions in this article are those of the author(s) and do not necessarily represent the views of the CDC.

References

1. Deak E, Wilson SD, White E, Carr JH, Balajee SA. *Aspergillus terreus* accessory conidia are unique in surface architecture, cell wall composition and germination kinetics. PLoS One 2009; 4:7673.
2. Balloy V, Huerre M, Latge JP, Chignard M. Differences in patterns of infection and inflammation for corticosteroid treatment and chemotherapy in experimental invasive pulmonary aspergillosis. Infect Immun 2005; 73:494-503.
3. Gersuk GM, Underhill DM, Zhu L, Marr KA. Dectin-1 and TLRs permit macrophages to distinguish between different *Aspergillus fumigatus* cellular states. J Immunol 2006; 176:3717-24.
4. Gomez BL, Nosanchuk JD. Melanin and fungi. Curr Opin Infect Dis 2003; 16:91-6.
5. Hohl TM, Van Epps HL, Rivera A, Morgan LA, Chen PL, Feldmesser M, et al. *Aspergillus fumigatus* triggers inflammatory responses by stage-specific beta-glucan display. PLoS Pathog 2005; 1:30.
6. Luther K, Torosantucci A, Brakhage AA, Heesemann J, Ebel F. Phagocytosis of *Aspergillus fumigatus* conidia by murine macrophages involves recognition by the dectin-1 beta-glucan receptor and Toll-like receptor 2. Cell Microbiol 2007; 9:368-81.
7. Overland G, Stuestol JF, Dahle MK, Myhre AE, Netea MG, Verweij P, et al. Cytokine responses to fungal pathogens in Kupffer Cells are Toll-like receptor 4 independent and mediated by tyrosine kinases. Scand J Immunol 2005; 62:148-54.
8. Rapaka RR, Goetzman ES, Zheng M, Vockley J, McKinley L, Kolls JK, et al. Enhanced defense against *Pneumocystis carinii* mediated by a novel dectin-1 receptor Fc fusion protein. J Immunol 2007; 178:3702-12.
9. Rappleye CA, Eissenberg LG, Goldman WE. *Histoplasma capsulatum* alpha-(1,3)-glucan blocks innate immune recognition by the beta-glucan receptor. Proc Natl Acad Sci USA 2007; 104:1366-70.
10. Segal BH. Role of macrophages in host defense against aspergillosis and strategies for immune augmentation. Oncologist 2007; 12:7-13.
11. Steele C, Rapaka RR, Metz A, Pop SM, Williams DL, Gordon S, et al. The beta-glucan receptor dectin-1 recognizes specific morphologies of *Aspergillus fumigatus*. PLoS Pathog 2005; 1:42.
12. Viriyakosol S, Fierer J, Brown GD, Kirkland TN. Innate immunity to the pathogenic fungus *Coccidioides posadasii* is dependent on Toll-like receptor 2 and Dectin-1. Infect Immun 2005; 73:1553-60.
13. Werner JL, Metz AE, Horn D, Schoeb TR, Hewitt MM, Schwiebert LM, et al. Requisite role for the dectin-1 beta-glucan receptor in pulmonary defense against *Aspergillus fumigatus*. J Immunol 2009; 182:4938-46.
14. Gantner BN, Simmons RM, Underhill DM. Dectin-1 mediates macrophage recognition of *Candida albicans* yeast but not filaments. EMBO J 2005; 24:1277-86.
15. Greene RE, Schlamm HT, Oestmann JW, Stark P, Durand C, Lortholary O, et al. Imaging findings in acute invasive pulmonary aspergillosis: clinical significance of the halo sign. Clin Infect Dis 2007; 44:373-9.
16. Wheeler RT, Kombe D, Agarwala SD, Fink GR. Dynamic, morphotype-specific *Candida albicans* beta-glucan exposure during infection and drug treatment. PLoS Pathog 2008; 4:1000227.
17. Aimanianda V, Bayry J, Bozza S, Kniemeyer O, Perruccio K, Elluru SR, et al. Surface hydrophobin prevents immune recognition of airborne fungal spores. Nature 2009; 460:1117-21.
18. Hohl TM, Feldmesser M, Perlin DS, Pamer EG. Caspofungin modulates inflammatory responses to *Aspergillus fumigatus* through stage-specific effects on fungal beta-glucan exposure. J Infect Dis 2008; 198:176-85.
19. Walsh TJ, Petraitis V, Petraitiene R, Field-Ridley A, Sutton D, Ghannoum M, et al. Experimental pulmonary aspergillosis due to *Aspergillus terreus*: pathogenesis and treatment of an emerging fungal pathogen resistant to amphotericin B. J Infect Dis 2003; 188:305-19.
20. Paris S, Debeaupuis JP, Crameri R, Carey M, Charles F, Prevost MC, et al. Conidial hydrophobins of *Aspergillus fumigatus*. Appl Environ Microbiol 2003; 69:1581-8.
21. Flori P, Bellete B, Durand F, Raberin H, Cazorla C, Hafid J, et al. Comparison between real-time PCR, conventional PCR and different staining techniques for diagnosing *Pneumocystis jiroveci* pneumonia from bronchoalveolar lavage specimens. J Med Microbiol 2004; 53:603-7.
22. Girardin H, Paris S, Rault J, Bellon-Fontaine MN, Latge JP. The role of the rodlet structure on the physicochemical properties of *Aspergillus conidia*. Lett Appl Microbiol 1999; 29:364-9.
23. Antonopoulou S, Aoun M, Alexopoulos EC, Baka S, Logothetis E, Kalambokas T, et al. Fenticonazole activity measured by the methods of the European Committee on Antimicrobial Susceptibility Testing and CLSI against 260 *Candida vulvovaginitis* isolates from two European regions and annotations on the prevalent genotypes. Antimicrob Agents Chemother 2009; 53:2181-4.
24. Ishi K, Maruyama J, Juvvadi PR, Nakajima H, Kitamoto K. Visualizing nuclear migration during conidiophore development in *Aspergillus nidulans* and *Aspergillus oryzae*: multinucleation of conidia occurs through direct migration of plural nuclei from phialides and confers greater viability and early germination in *Aspergillus oryzae*. Biosci Biotechnol Biochem 2005; 69:747-54.
25. Dornbusch HJ, Buzina W, Summerbell RC, Lass-Florl C, Lackner H, Schwinger W, et al. Fusarium verticillioides abscess of the nasal septum in an immunosuppressed child: case report and identification of the morphologically atypical fungal strain. J Clin Microbiol 2005; 43:1998-2001.
26. Mattila PE, Metz AE, Rapaka RR, Bauer LD, Steele C. Dectin-1 Fc targeting of *Aspergillus fumigatus* beta-glucans augments innate defense against invasive pulmonary aspergillosis. Antimicrob Agents Chemother 2008; 52:1171-2.
27. Lass-Florl C, Rief A, Leitner S, Speth C, Wurzner R, Dierich M. In vitro activities of amphotericin B and voriconazole against aleurioconidia from *Aspergillus terreus*. Antimicrob Agents Chemother 2005; 49:2539-40.